

Modeling of Adsorption – Reaction Phenomenon on Activated Carbon

by

Ekhator Emmanuel Osagie

A Thesis Presented to the

FACULTY OF THE COLLEGE OF GRADUATE STUDIES

KING FAHD UNIVERSITY OF PETROLEUM & MINERALS

DHAHRAN, SAUDI ARABIA

In Partial Fulfillment of the
Requirements for the Degree of

MASTER OF SCIENCE

In

CHEMICAL ENGINEERING

July, 1995

INFORMATION TO USERS

This manuscript has been reproduced from the microfilm master. UMI films the text directly from the original or copy submitted. Thus, some thesis and dissertation copies are in typewriter face, while others may be from any type of computer printer.

The quality of this reproduction is dependent upon the quality of the copy submitted. Broken or indistinct print, colored or poor quality illustrations and photographs, print bleedthrough, substandard margins, and improper alignment can adversely affect reproduction.

In the unlikely event that the author did not send UMI a complete manuscript and there are missing pages, these will be noted. Also, if unauthorized copyright material had to be removed, a note will indicate the deletion.

Oversize materials (e.g., maps, drawings, charts) are reproduced by sectioning the original, beginning at the upper left-hand corner and continuing from left to right in equal sections with small overlaps. Each original is also photographed in one exposure and is included in reduced form at the back of the book.

Photographs included in the original manuscript have been reproduced xerographically in this copy. Higher quality 6" x 9" black and white photographic prints are available for any photographs or illustrations appearing in this copy for an additional charge. Contact UMI directly to order.

UMI

A Bell & Howell Information Company
300 North Zeeb Road, Ann Arbor MI 48106-1346 USA
313/761-4700 800/521-0600

**MODELING OF ADSORPTION - REACTION PHENOMENA ON
ACTIVATED CARBON**

by

EKHATOR EMMANUEL OSAGIE

A Thesis Presented to the
FACULTY OF COLLEGE OF GRADUATE STUDIES

In Partial Fulfillment of the Requirements
for the degree
MASTER OF SCIENCE

IN

CHEMICAL ENGINEERING

KING FAHD UNIVERSITY
OF PETROLEUM & MINERALS

Dhahran, Saudi Arabia.

JULY 1995.

UMI Number: 1381994

UMI Microform 1381994
Copyright 1996, by UMI Company. All rights reserved.

**This microform edition is protected against unauthorized
copying under Title 17, United States Code.**

UMI
300 North Zeeb Road
Ann Arbor, MI 48103

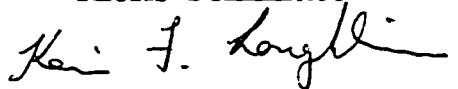
**KING FAHD UNIVERSITY OF PETROLEUM & MINERALS
DHAHRAN 31261, SAUDI ARABIA**

COLLEGE OF GRADUATE STUDIES

This thesis, written by **EKHATOR EMMANUEL OSAGIE** under the direction of his Thesis Committee , has been presented to and accepted by the Dean of the College of Graduate Studies, in partial fulfillment of the requirement for the degree of

MASTER OF SCIENCE IN CHEMICAL ENGINEERING

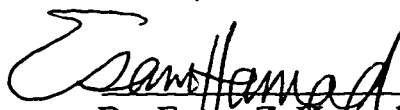
Thesis Committee



Dr. Kevin F. Loughlin



Dr. Ashraf I. Fatehi




Dr. Ezam Z. Hamad



Dr. Abdulla A. Shaikh

Chairman

Department of Chemical Engineering



Dr. Abdullah M. Al-Shehri

Dean

College of Graduate Studies



Date 14-9-96

CONTENTS

	PAGE
THESIS ABSTRACT	VI
ARABIC ABSTRACT	VII
LIST OF FIGURES	VIII
LIST OF TABLES	X
Chapter 1 Introduction	1
1.1 Introduction	1
1.2 Status of Adsorption in Pollution removal	3
1.3 Detailed background on Granular Activated Carbon	4
1.4 Scope of this thesis	5
1.5 Literature Cited	6
Chapter 2 Diffusion Models in Batch Systems.	7
2.1 Introduction	7
2.2 Literature Survey	8
2.3 Theoretical Model	14
2.4 Results and Discussion	28
2.5 Conclusions and Recommendations	55
2.6 Literature Cited	57

2.7 Nomenclature	63
Chapter 3 Diffusion and Reaction in Batch Systems.	66
3.1 Introduction	66
3.2 Literature Survey	66
3.3 Theoretical Model	72
3.4 Results and Discussion	76
3.5 Conclusions and Recommendations	87
3.6 Literature Cited	89
3.7 Nomenclature	92
Chapter 4 Combined Pore and Surface Diffusion in Packed Beds.	95
4.1 Introduction	95
4.2 Literature Survey	96
4.3 Theoretical Model	98
4.4 Results and Discussion	116
4.5 Conclusions and Recommendations	117
4.6 Literature Cited	120
4.7 Nomenclature	122
Chapter 5 Combined Pore and Surface Diffusion with Reaction in Packed Beds.	126

5.1 Introduction	126
5.2 Literature Survey	126
5.3 Theoretical Model	127
5.4 Results and Discussion	131
5.5 Conclusions and Recommendations	132
5.6 Literature Cited	137
Chapter 6 Conclusions and Recommendations	138
Appendices	140
A1 Program for pore and surface diffusion in batch systems	141
A2 Optimization program to evaluate parameters for batch systems	150
A3 Program for pore and surface diffusion with reaction in batch systems	160
A4 Optimization program to calculate parameters for pore and surface diffusion with reaction in batch systems	170
A5 Program to calculate breakthrough curves for pore and surface diffusion in packed bed systems.	181
A6 Program to calculate breakthrough curves for pore and surface diffusion with reaction in packed bed systems	188
VITAE	195

THESIS ABSTRACT

NAME OF STUDENT : EKHATOR EMMANUEL OSAGIE
TITLE OF THESIS : MODELING OF ADSORPTION REACTION
PHENOMENA ON ACTIVATED CARBON
MAJOR FIELD : CHEMICAL ENGINEERING
DATE OF DEGREE : JULY 1995

The adsorption of phenol and its reaction with oxygen on granular activated carbon is modeled using a dual mechanism pore and surface diffusion model and the homogeneous surface diffusion model in both batch and column systems combined with a reaction term involving phenol and oxygen adsorbate concentration.

The dependence of surface diffusivity coefficient on adsorbed phase concentration is accounted for by the use of Darken's relation. From experimental studies, the rate and extent of reaction is established as dependent on oxygen availability in the system. Hence, a rate of reaction expression is incorporated in the model based on the assumption that the rate is proportional to the oxygen imbalance and the adsorbed phase concentration.

The adsorption and reaction models are tested by fitting the experimental data generated by Abuzaid(1993). The models parameters are optimized. The resulting model is in good agreement with the experimental data. Generally, the model fits obtained from the batch studies are better than those obtained from the column studies.

MASTER OF SCIENCE DEGREE

KING FAHD UNIVERSITY OF PETROLEUM & MINERALS

Dhahran, Saudi Arabia

Date : July 1995

ملخص الرسالة

- اسم الطالب : إختور إيمانويل أوساجي
عنوان الرسالة : إيجاد صيغة لظواهر التفاعل الإمتزاجي على الكربون المنشط .
التخصص : هندسة كيميائية .
تاريخ الرسالة : يوليو ١٩٩٦ م .

امتزاج الفينول وتفاعله مع الاكسجين على حبيبات الكربون المنشط تمت صياغته باستعمال ميكانيكية مزدوجة لصورة الانتشار المسامي والسطحي وصورة الانتشار السطحي المتماثل في كل من نظامي (البرجي & batch) مع حد للتفاعل بين الفينول والاكسجين المتمز على السطح .

اعتماد معامل قابلية الانتشار السطحي على تركيز الطور الامتزاجي تم احتسابه باستعمال علاقة داركن . أثبتت الدراسات التجريبية أن معدل وحجم التفاعل يعتمد على وجود الاكسجين في المفاعل.

بناءً على ذلك فإن صيغة معدل التفاعل ادخلت في الصيغة بناءً على الافتراض بأن المعدل يتناسب مع اختلال توازن الاكسجين وتركيز الطور الامتزاجي .

صيغ الامتزاج والتفاعل تم اختبارها بإخضاعها إلى نتائج التجارب التي توصل إليها أبوزيد (١٩٩٣) حدود الصيغة وضعت في أفضل صورة الصيغة الناتجة على إتفاق طيب مع نتائج التجارب. بصورة عامة ، مطابقات الصيغة التي تم الحصول عليها من دراسات (batch) كانت أفضل من تلك التي تم الحصول عليها من دراسات المفاعل البرجي .

درجة الماجستير في العلوم

جامعة الملك فهد للبترول والمعادن

الظهران ، المملكة العربية السعودية

يوليو ١٩٩٦ م

LIST OF FIGURES

Figure	Page No.
2.1 Langmuir-Freundlich fit of phenol adsorption on GAC	29
2.2 Langmuir-Freundlich fit of o-cresol adsorption on GAC	30
2.3 Reproducibility of Program to Produce data of Suzuki(1990, pp 9)	33
2.4 Predicted and Experimental Fractional Uptakes at 308 K. Adsorption of phenol. Comparison between 71 and 21 nodes.	34
2.5 Predicted and Experimental Fractional Uptakes at 281 K. Adsorption of phenol.	36
2.5 Predicted and Experimental Fractional Uptakes at 281 K. Adsorption of phenol.	36
2.6 Predicted and Experimental Fractional Uptakes at 294 K. Adsorption of phenol.	37
2.7 Predicted and Experimental Fractional Uptakes at 308 K. Adsorption of phenol.	38
2.8 Predicted and Experimental Fractional Uptakes at 281 K. Adsorption of phenol.	39
2.9 Predicted and Experimental Fractional Uptakes at 294 K. Adsorption of phenol.	40
2.10 Predicted and Experimental Fractional Uptakes at 308 K. Adsorption of phenol.	41
2.11 Plot of D_s vs. Dimensionless Time at 281 K. Adsorption of phenol. Comparison between models 2 and 3.	45
2.12 Plot of D_s vs. Dimensionless Time at 294 K. Adsorption of phenol. Comparison between models 4 and 5..	47
2.13 Plot of $\ln D_s$ vs. $1/T$ for HSDM-Models 2 and 3. Adsorption of phenol	48
2.14 Plot of $\ln D_s$ vs. $1/T$ for PSDM-Models 4 and 5. Adsorption of phenol	49
2.15 Plot of $\ln D_s$ vs. $1/T$ for HSDM-Model 3. Adsorption of o-cresol	50
2.16 Plot of $\ln D_s$ vs. $1/T$ for PSDM-Model 5. Adsorption of o-cresol	51
2.17 Plot of Pore Diffusion Flux/Surface Diffusion Flux vs. Bulk Phase Concentration. Adsorption of phenol.	54

3.1	Predicted and Experimental Fractional Uptakes at 281 K. Adsorption with Reaction of o-cresol.	79
3.2	Predicted and Experimental Fractional Uptakes at 294 K. Adsorption with Reaction of o-cresol.	80
3.3	Predicted and Experimental Fractional Uptakes at 308 K. Adsorption with Reaction of o-cresol.	81
3.4	Predicted and Experimental Fractional Uptakes at 281 K. Adsorption with Reaction of phenol.	82
3.5	Predicted and Experimental Fractional Uptakes at 294 K. Adsorption with Reaction of phenol.	83
3.6	Predicted and Experimental Fractional Uptakes at 308 K. Adsorption with Reaction of phenol.	84
3.7	Plot of $\ln K$ vs. $1/T$. Adsorption with Reaction of o-cresol.	85
4.1	Predicted and Experimental Breakthrough Curves. Adsorption of o-cresol in column at 294 K	118
4.2	Predicted and Experimental Breakthrough Curves. Adsorption of phenol in column at 294 K	119
5.1	Predicted and Experimental Breakthrough curves. Adsorption with reaction of phenol in column at 294 K(1st order)	133
5.2	Predicted and Experimental Breakthrough curves. Adsorption with reaction of phenol in column at 294 K(2nd order)	134
5.3	Predicted and Experimental Breakthrough curves. Adsorption with reaction of o-cresol in column at 294 K(1st order)	135
5.4	Predicted and Experimental Breakthrough curves. Adsorption with reaction of o-cresol in column at 294 K(2nd order)	136

LIST OF TABLES

Table	Page No.
1.1 Typical values of GAC physical properties	5
2.1 Normalized values of $d\ln C/d\ln q$	25
2.2 Program input for batch systems	31
2.3 Diffusivity coefficient and rms. values for various models	42
2.4 Surface diffusivity coefficients from literature for batch data using HSDM model	43
2.5 Temperature Dependence of Surface Diffusivity Coefficient	53
3.1 Reaction orders and overall constants in batch system.	78
4.1 Dimensionless groups in column	103
4.2 Column parameters	116
4.3 Program input for column systems	116
5.1 Reaction orders and overall constants for column systems	132

CHAPTER ONE

INTRODUCTION

1.1 Introduction

A large number of synthetic organic chemicals are currently produced in the process industries, and several of these are introduced into the environment by accident or through poor design. Many of these compounds are of toxicological importance, causing carcinogenic, teratogenic, and mutagenic effects when ingested as part of drinking water over a long period of time.

Adsorption is the selective collection and concentration onto solid surfaces of particular types of molecules contained in a liquid or a gas. Adsorption offers an effective means of selectively separating mixtures of gases or liquids even at very low concentration. The molecules are removed from the liquid or gas stream by attachment to a variety of specific materials known as adsorbents. The material which is adsorbed onto the adsorbent is called the adsorbate.

Adsorption on granular activated carbon (GAC), is one of the most dependable and effective technologies currently available for the treatment of drinking water and wastewater's contaminated with low concentrations of hazardous compounds. Activated carbon is commonly utilised in environmental engineering due to its good adsorption characteristics for the removal of organic compounds. The removal of pollutants by adsorption onto activated carbon involves transport of an adsorbate molecule to the exterior surface of an adsorbent particle, pore diffusion and surface

diffusion, and adsorption of the adsorbate onto the interior surfaces of the adsorbent. Normally, one or more of these steps controls the process.

Activated carbon is used in various water treatment reactors. These include the fixed bed reactor, fluidized bed anaerobic reactor, and activated sludge systems. The design of contact systems and the prediction of their performance have been dependent on laboratory equilibrium data. The need for a better understanding of the nature of granular activated carbon (GAC) and its capacity for the retention of various compounds necessitated the extensive research efforts that have been channelled in this direction.

The adsorption capacity of an adsorbent is the amount of solute it can adsorb per unit mass. It is a key component needed for the prediction of adsorber performance and it is given by an adsorption isotherm which represents the equilibrium between the quantity of adsorbate retained per unit mass of adsorbent, and the concentration of adsorbate in solution at constant temperature.

The adsorption uptake is the amount of solute adsorbed from the bulk phase as a fraction of that present initially. It is dependent on some variables that includes the size of the particle, the initial solute concentration in the bulk phase, the amount of adsorbent used, maybe the presence of dissolved oxygen and the equilibration time allowed. All but one of these variables are well known and have received adequate attention. The elusive variable, whose influence on adsorption capacity of GAC is obfuscated by its seeming indirect involvement in the phenomenon is the level of dissolved oxygen. In the involvement of dissolved oxygen lies the solution to the conundrum that has baffled many researchers. Only recently has there been a conscientious and systematic study designed to elucidate the effects of the presence of dissolved oxygen on adsorption equilibrium. The puzzling discrepancies in

the various adsorption isotherms reported is now linked to the different amounts of dissolved oxygen in the experimental set-ups. It is an established fact that oxygen adsorbed on GAC forms surface acidic oxides. These oxides are responsible for the oxidative coupling reactions occurring presumably on the surface of the carbon. This reaction is promoted by oxygen. The paramount effect of this is manifested in a change in the adsorption capacity of GAC.

Various models have been used to predict the adsorption process. In most of these models the effective diffusivity coefficient is assumed constant. However, diffusivity coefficients have been found to be concentration dependent.

1.2 Status of Adsorption in Pollution Removal

The findings of various independent researches corroborates the fact that adsorption by granular activated carbon is one of the most effective water treatment units process to remove many different types of trace organics found in drinking water (Symons, 1978).

McGuire et al. (1991) conducted a detailed evaluative study on the use of GAC for trihalomethane (THM) in water control. One of the objectives of the study was the estimation of the costs associated with optimised GAC treatment for the Metropolitan Water District of southern California (MWD) and for six other water utilities across the United States of America. GAC adsorption was found to be an expensive means of THM control. The capital costs of implementing GAC adsorption as a unit process for THM precursor removal range from \$730 to \$3,900 million (based on a capacity of 2,970 mgd), depending on whether the upcoming regulations are set at 50 or 5 μ g/L.

1.3 Detailed Background On Granular Activated Carbon

Activated carbon can be made from a number of raw materials having a high carbonaceous content. The principal raw materials for commercially available carbons are sawdust, lignite, wood charcoal, peat, bituminous coal, and petroleum coke.

There are two principal methods for making activated carbons. In each of these methods, the starting materials is heated in the absence of air. The two principal methods are :

1. High - temperature oxidation with steam of a previously charred carbonaceous substance(coal, char, charcoal)
2. Lower temperature chemical dehydration and/or chemical reaction of a carbonaceous raw material (Perrich, 1981)

Much of the substances devolatilize leaving behind a porous structure of carbon that usually contains some hydrogen. Activation of the carbon is done by controlled oxidation with steam or carbon dioxide to further open up the pores and increase the total surface area. Precise control of both reaction temperature and time is very important in steam activation processes to impart desired properties. Temperatures usually range upwards from $800^{\circ}C$.

The activated carbon may contain up to about 10 wt % oxygen, which may cover a large fraction of the surface as chemisorbed oxygen in the form of ketones, hydroxyls, or carboxylic acids. The surface area can range up to about $1200 \text{ m}^2/\text{gm}$ (Satterfield, 1991).Granular Activated carbons generally have particle sizes larger than 20 mesh. They are widely used in liquid phase operations.

A cross section of a portion of an activated carbon particles might look like a maze of inter connecting channels, quite large at the surface and terminating in small channels in the interior. The distribution of the pores is

basically trimodal. The actual distribution and the total pore volume associated with each pore size range are however sensitive to the conditions of the initial pyrolysis and activation procedures. Typical ranges are given in Table 1.1. However, activated carbons with desired porosity, surface area, and adsorptive capacity can be tailored by special procedure.

When prepared and stored under inert environment, the surface of carbon is essentially non-polar. However, surface oxidation does occur when the surrounding atmosphere is non-inert. As a result, carbon adsorbents tends to be hydrophobic and organophilic.

Table 1.1 : Typical values of GAC physical properties.

	Micropore	Mesopore or Transitional pores	Macropore
Diameter (°A)	< 20	20 - 500	0.2 - 0.5
Pore volume (cm ³ / g)	0.15 - 0.5	0.02 - 0.1	0.2 - 0.5
Surface area (m ² / g)	100 - 1000	10 - 100	0.5 - 2

The particle density in the range of 0.6 - 0.9 g/cm³ and the porosity is in the range of 0.4 - 0.6.

1.4 Scope Of This Thesis

In this study three specific areas are treated. First is the modelling of the adsorption occurring in GAC. The pore and surface diffusion model (PSDM)

and the homogeneous diffusion model (HSDM) will be used. Two cases will be considered. Case one treats the surface diffusivity as constant. In case two, the concentration dependence of surface diffusivity using Darken's relation is incorporated in the model.

The second area is concerned with adsorption with reaction on GAC in batch systems. Here, it is desired to fit our model results to experimental data where reaction has occurred. To this end, a reaction model is postulated. The attendant objective is to ascertain the optimum values of the reaction order with respect to phenol and oxygen and the reaction rate constant by minimising the root mean square deviation between experimental and model results.

The third is simply an extrapolation of the batch results to the fixed bed reactor. The kinetic parameters determined in the batch system are directly utilised here.

1.5 Literature Cited

(1) McGuire, M. J., Davis, M. K., Tate, C. H., Aieta, E. M., Howe, E. M., and Crittenden, J. C. "Evaluating GAC for Trihalomethane control", J. American Water. Works Assoc., 83, 1, 1991.

(2) Perrich, J.R., "Activated Carbon Adsorption for Wastewater Treatment", CRC press Inc., 1981.

(3) Satterfield, C.N., "Heterogeneous Catalysis in Industrial Practice", 2nd ed., McGraw Hill, Inc., 1991.

(4) Symons, J.M., "Interim Treatment Guide For Controlling Organic Contaminants in Drinking Water using Granular Activated Carbon", U.S. EPA, MERL, Cincinnati, OH, 1978.

CHAPTER TWO

DIFFUSION MODELS IN BATCH SYSTEMS.

2.1 Introduction :

The diffusion of adsorbate onto activated carbon involves a number of steps, each offering its own resistance. First we have diffusion through the film layer surrounding the activated carbon onto its exterior surface. This is film diffusion. Secondly, there is intraparticle diffusion which involves the transport of molecules through the solution in the adsorbent macropores (macropore diffusion), and micropores (micropore diffusion). Micropore and macropore diffusion are normally classed together as pore diffusion. Thirdly, there is diffusion of adsorbed molecules along the surface of the adsorbent. This is called surface diffusion.

External mass transfer or film diffusion is usually the rate-limiting step in systems that have poor mixing, dilute adsorbate concentrations, small adsorbent particle sizes and high adsorbate affinity for adsorbent. In contrast, the intraparticle step limits the overall transport for those systems that have good mixing, large adsorbent particle sizes, high adsorbate concentrations and low adsorbate affinity for the adsorbent. The adsorption step in physical adsorption processes is generally accepted to be very rapid (Weber and Morris, 1964). Consequently, the rate of adsorption is controlled by one of the preceding diffusional steps.

When adsorption takes place in a large vessel, the concentration of the fluid in the vessel is regarded as being constant throughout the process of

adsorption. Such a vessel is called an infinite bath and the adsorption process is conceptualized as occurring at constant boundary condition.

When adsorption takes place in a bath of finite volume, concentration of the fluid in the vessel decreases with progress of the process. Such a vessel is called a finite bath and the adsorption process is conceptualized as occurring with an unsteady state boundary condition. The diffusion in an infinite bath or a finite bath may be pore diffusion controlled, surface diffusion controlled, external mass transfer controlled, or all of these steps could play a significant role.

2.2 Literature survey :

Adsorption capacity is expressed by an adsorption isotherm which represents the equilibrium between the quantity of adsorbate retained per unit mass of adsorbent, and the concentration of adsorbate in solution at constant temperature. Isotherm data are most commonly obtained using the so called bottle-point technique. Unfortunately, a unified experimental procedure has not yet been established. The experimental approach of most researchers differ. These procedural differences reflect in the carbon preparation, particle size, and volume of container used in the experiment, volume of adsorbate solution added, buffer application and, equilibration time allowed. Consequently, a myriad of different isotherms are reported in the literature for the same combination of chemical compound and granular activated carbon (GAC). Isotherm data can also be obtained using batch reactor and column methods.

Theoretically, equilibrium data are independent of the way they are obtained and GAC capacities must be in agreement irrespective of the experimental procedure adopted. However, many researchers report that such

was not always the case (Crittenden and Weber, 1985; Van Vliet et al., 1980; Yonge et al., 1985; Liu and Weber, 1981; Reschke et al., 1986). The following explanations for the discrepancies have been suggested :

- (1) continuously decreasing liquid phase adsorbate concentration during the equilibration period (Yonge et al., 1985)
- (2) irreversible adsorption (Yonge et al., 1985)
- (3) decline in intraparticle diffusion rate during the later part of breakthrough, as saturation is approached (Van Vliet et al., 1980)
- (4) difference in diffusion processes into macropores and micropores (Peel and Benedek, 1981; Seidel and Gelbin, 1986; Seidel et al., 1985).

Adsorption isotherms assume various forms. Some are accurate only within a limited concentration range. The Freundlich isotherm falls into this category (Hand et al., 1983; Seidel et al., 1983; Chatzopoulos et al., 1994). Thus the form of the isotherm used can affect the accuracy of predictions when modeling the adsorption process. Most researchers in the past fitted phenol adsorption data by the Freundlich isotherm. The commonly used adsorption isotherms are Langmuir, Freundlich, Redlich-Peterson, (Seidel et al., 1985, Hand et al., 1983), Radke- Prausnitz, and Fritz- Schlunder (Chatzopoulos et al., 1994).

Adsorption onto activated carbon is usually an unsteady state process. The rate of adsorption is influenced by a number of parameters. The most important include the pH of the solution, temperature, initial concentration of the adsorbates, particle size, flow rate (in column) of adsorbate solution and competitive adsorption in multi-component systems.

The adsorption uptake of carbon increases with increased mass of the adsorbent (McKay and Bino, 1988) and the size of the particle used.

(Wilmanski and Lipinski, 1989; Mathews and Zayas, 1989; Cooney and Xi, 1992).

Physical adsorption is an exothermic phenomenon. Consequently, the extent of adsorption generally increases with decreasing temperature. Alben et al. (1978) observed gradual diminution of GAC adsorption capacity of trihalomethanes on granular activated carbon with increasing temperature in the range of 4 to 45 degree celsius. This trend is supported by the work of Abuzaid (1993) for the adsorption of phenol and o-cresol on GAC.

In general, adsorption of typical organic pollutants from water increases with decreasing pH. Alhert and Gorgol (1983), investigated the adsorption of the supernatant of two landfill leachates on GAC for total organic carbon with the adsorptive capacity at pH 7 greater than that at pH 2.

The adsorption process has been represented in the past by a variety of models. In the homogeneous surface diffusion model (HSDM), first used by Rosen (1952) to describe adsorption kinetics from aqueous solutions, an isotropic adsorbent particle with a narrow pore-size distribution is assumed. Rosen (1952) used a linear isotherm. The HSDM has been successfully applied for non-linear isotherms (Fritz et al. 1983; Hand et al., 1983). Also, adsorbate molecules are assumed to creep along the abundant inner surfaces of the adsorbent in the adsorbed state. In the pore diffusion model (PDM), first used by Edeskuty and Amundson (1952), transport of molecules is assumed to take place in the liquid phase of the adsorbent pores. The pore and surface diffusion model (PSDM) was proposed by Weber and Chakrovorti (1974), and Fritz and Schluender (1974) in which simultaneous occurrence of surface and pore transports in significant amounts are assumed. GAC however, contains a wide range of pore sizes (Famularo et al., 1980; Peel and Benedek, 1981). Adsorption rates in most modeling studies have

been described using the "homogeneous" particle models. This is primarily because of the small number of solute transport parameters involved and the low computational effort required for the solution of these models. Previous studies showed that the dominant mechanism of intraparticle solute transport for activated carbon adsorption of organics from aqueous solutions is by surface diffusion (Neretnieks, 1976; Fritz et al.; 1981; Hand et al.; 1983).

Until recently, activated carbon adsorption of organics from aqueous solutions was most commonly described by the homogeneous surface diffusion model (HSDM). The HSDM is also called the solid diffusion model (Hand et al., 1983; Al-Duri and McKay, 1991, Vidic et al., 1994; Chatzopoulos et al., 1994). In most cases, the surface diffusion coefficient D_s was assumed to remain constant throughout the adsorption process. However, there has been considerable evidence that D_s increases with surface loading both in single component and multicomponent solutions (Sudo et al., 1978; Al-Duri and McKay; 1991, Vidic et al., 1994). This phenomenon has been well established for the diffusion of gases on solid surfaces and can be explained by the energetic heterogeneity of the surface, the increase in the mean free path of surface diffusion with surface loading and the lateral interactions among the adsorbed molecules at high surface coverages (Sudo et al., 1978; Kapoor et al., 1989, Chatzopoulos et al., 1994; Vidic and Suidan, 1994). In addition, a $D_s(q)$ dependence also arises when the solute diffusion flux is represented in terms of the chemical potential gradient rather than the concentration gradient on the surface (Sudo et al., 1978; Ruthven, 1984).

Kapoor et al. (1989) presented a review of existing models for the concentration dependence of the surface diffusion coefficient in gas solid systems. Among these models, the one proposed by Gilliland et al. (1974) has been widely used to describe the dynamics of adsorption from dilute aqueous

solutions (Neretnieks, 1976; Muraki et al.; 1982; Seidel and Carl, 1989). This model assumes an implicit exponential dependence of D_s on the surface concentration. A correlation similar to this form was used by some researchers to account for the concentration dependent D_s . (Chatzopoulos et al., 1994).

Some researchers fitted adsorption rates in finite bath batch systems with the assumption that D_s remains constant throughout the course of the adsorption and observed that the resulting D_s values increased with initial solute concentration in the solution. (Neretnieks, 1976; Sudo et al. 1978; Fritz et al. 1981; Itaya et al., 1987; Al-Duri and McKay, 1991; Chatzopoulos et al., 1994, Vidic et al., 1994).

McKay and Bino (1985), fitted the adsorption data by a model based on external mass transfer and pore diffusion. They observed a deviation from theory which they attributed to a probable change in D_s with varying extents of adsorption in line with Peel and Benedek's (1981) branched pore theory. The extent of adsorption is noted to be a function of pore size distribution within the particle and the relative size of the solute molecules.

Wilmanski and Lipinski (1989) after a study of the activated carbon adsorption kinetics of total organic carbon from water in a batch reactor reported that the effective pore diffusion coefficient continuously decreases as the total organic carbon removal on activated carbon proceeds. They claimed that this phenomenon can be substantially limited after reducing the carbon particle diameter to a value of about 0.1 mm. The effective pore diffusivity is reported to have an inverse relationship with the diameter to the particles used in the adsorption process. This is in agreement with the work of Randtke and Snoeyink (1983) and Crittenden et al. (1984).

Vidic et al. (1994) reported a variation of D_s in a closed batch kinetic experiment with initial adsorbate concentration in the liquid phase and this is in accordance with the findings of Komiyama and Smith (1974) and Gilliland et al. (1974). They showed that there is a linear relationship between the equal surface loading and the best fit D_s value when different initial adsorbate concentrations are used. Sladek et al. (1974) observed that for both physically and chemically adsorbed species, the activation energy for the formation of a vacant site adjacent to the adsorbed molecule decreases with an increase in surface coverage. This is a direct consequence of a decrease in the bonding energy of adsorption, which represents a fraction of the heat of adsorption, for higher concentration of adsorbate molecules on the carbon surface. As a result, the movement of adsorbate molecules intensifies and, consequently the surface diffusion coefficient increases.

Hu et al. (1993b) investigated the effect of the concentration dependence of surface diffusivity in binary adsorption, desorption and displacement kinetics under various conditions. They used the macropore, surface and micropore diffusion (MSMD) and the constant surface diffusivity macropore, surface and micropore diffusion (CMSMD). Of these two, the results given by the MSMD model were superior since it accounted for the concentration dependence of surface diffusivity. However, the CMSMD fitted single component system very well by using different bulk concentrations (Hu et al., 1993a). The effect of concentration dependent surface diffusion was noted to be most significant at low temperatures and with small particles. The high dependent level at low temperatures is a result of the great contribution of diffusion to the transport process.

Various attempts of theoretical work to quantitatively predict the concentration dependence of surface diffusivity have been devoid of promise

(Higashi et al., 1963; Yang et al., 1973; Chen and Yang, 1991; Do et al., 1992). Noting this, Hu et al. (1994) devised a new experimental procedure to be used with the differential adsorption bed to determine the intrinsic concentration dependence of the surface diffusivity of hydrocarbons in activated carbon. They employed the pore and surface diffusion model. Ethane and propane were used in the experimental work. The pore diffusivities used in the model were calculated from standard correlations. Along with the experimental work, a theoretically based investigation was conducted solely for the purpose of comparison. The theoretical prediction was based on the chemical potential gradient as the driving force. This reduces to the Darken's relation. Juxtaposed with the experimental results, the Darken's relation gave a very poor prediction of the concentration dependence of the surface diffusivity. This has also been reported by Gutsche and Yoshida (1994). The experimentally determined surface diffusivity roughly follows Darken relation if the amount adsorbed is less than 1 mmol/g. However, when the amount adsorbed is more than 1 mmol/g, the increase of surface diffusivity with loading is much faster than that calculated by the Darken's relation. The failure of Darken's relation is most pronounced along the non-linear part of the isotherm. The intrinsic surface diffusivity determined increases with both temperature and surface loading.

2.3 Theoretical Model.

2.3.1 Model Development For A Batch System

Consider a finite bath loaded with GAC particles of constant size-that is sieved to a homogeneous size of 0.156 cm. The particles may be freely suspended in the liquid phase or fixed in a wire mesh container to reduce the

film mass transfer limitation. The liquid phase generally consists of water plus the dissolved organic with or without oxygen. The bath contains an impeller and baffles. The rate of rotation of the impeller influences the mass transfer.

The following assumptions are made :

- (i) the bath is finite,
- (ii) the system is at constant temperature,
- (iii) the adsorbent particles are isotropic with uniform pores and no preferential pore direction,
- (iv) the solution is dilute so that the molecular diffusivity and the mass transfer coefficient are constant

Consider a general model incorporating all of the various adsorption resistances and steps. The first step of the overall transport process is the transfer of the solute from the bulk phase at concentration C to the surface of the particle at concentration C_s . The transport occurs by convective mass transfer and the describing equation is :

$$N = k(C - C_s) \quad 2.1$$

where k is the convective mass transfer coefficient and N , the mass flux, is based on the total external area (solid plus pore mouth) of the particle.

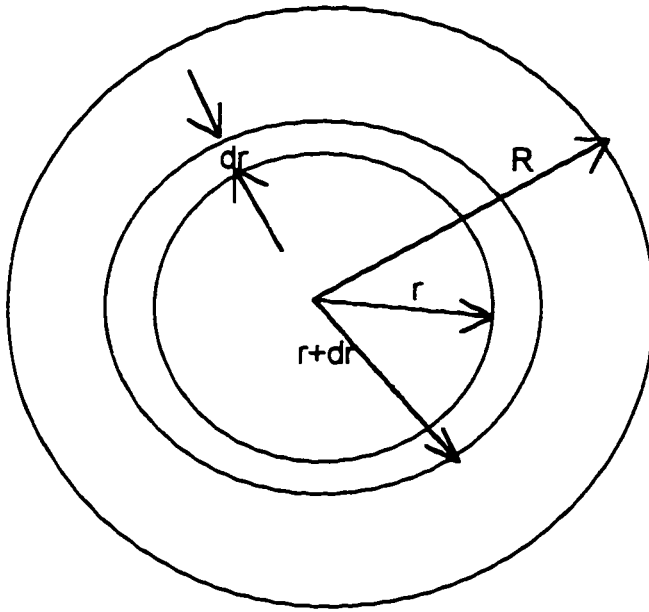
Step two is the molecular diffusion of the solute in the liquid in the pores of the particle (pore volume diffusion). This step which is in series with the first step is described by the following equation :

$$N_p = -\left(\frac{\varepsilon D_{AB}}{\tau}\right) \frac{\partial C_p}{\partial r} = -D_{e,p} \frac{\partial C_p}{\partial r} \quad 2.2$$

where D_{AB} and $D_{e,p}$ are respectively the effective molecular and pore diffusivities.

The adsorption of the solute on the surface of the pore constitutes step three. Here, it is assumed that the concentration C_p in the pore liquid is in local equilibrium with the amount adsorbed, q at the given position, i.e., the rate of step three is reversible and fast (Furusawa and Smith, 1974). Various isotherm forms are normally used in relating q and C_p

Performing a mass balance on the shell of the particle gives



Accumulation = Input - Output + Generation - Consumption

$$4\pi r^2 \Delta r \left[\epsilon \frac{\partial C_p}{\partial t} + \rho_p \frac{\partial q}{\partial t} \right] = \left[4\pi r^2 N \right]_r - \left[4\pi r^2 N \right]_{r+\Delta r} \quad 2.3$$

$$\begin{aligned}
 \varepsilon \frac{\partial C_p}{\partial t} + \rho_p \frac{\partial q}{\partial t} &= -\frac{1}{4\pi r^2} \left(\frac{[4\pi r^2 N]_{r+\Delta r} - [4\pi r^2 N]_r}{\Delta r} \right) \\
 &= -\frac{1}{4\pi r^2} \frac{\partial [4\pi r^2 N]}{\partial r}
 \end{aligned}
 \tag{2.4}$$

Assume the combined pore and surface flux to be :

$$N = -\left(\varepsilon D_p \frac{\partial C_p}{\partial r} + \rho_p D_s \frac{\partial q}{\partial r} \right) \tag{2.5}$$

$$\varepsilon \frac{\partial C_p}{\partial t} + \rho_p \frac{\partial q}{\partial t} = \frac{1}{r^2} \frac{\partial}{\partial r} \left\{ r^2 \left[\varepsilon D_p \frac{\partial C_p}{\partial r} + \rho_p D_s \frac{\partial q}{\partial r} \right] \right\} \tag{2.6}$$

Now

$$\frac{\partial C_p}{\partial r} = \frac{\partial C_p}{\partial q} \frac{\partial q}{\partial r} \tag{2.7}$$

$$\varepsilon \frac{\partial C_p}{\partial t} + \rho_p \frac{\partial q}{\partial t} = \frac{1}{r^2} \frac{\partial}{\partial r} \left\{ r^2 \left[\varepsilon D_p \frac{\partial C_p}{\partial q} + \rho_p D_s \right] \frac{\partial q}{\partial r} \right\} \tag{2.8}$$

$\frac{\partial C_p}{\partial q}$ is obtained from the isotherm equation used.

Initial conditions :

$$\begin{aligned}
C &= C_o; & r=0 \\
C_p &= C_p(\tau,0) = 0; & 0 \leq r \leq r_s \\
q(r,0) &= 0; & 0 \leq r \leq r_s
\end{aligned} \tag{2.9}$$

Boundary conditions :

BC.1

$$\left. \frac{\partial q(0,t)}{\partial r} \right|_{r=0} = 0 \tag{2.10}$$

$$\left. \frac{\partial C_p}{\partial r} \right|_{r=0} = 0 \tag{2.11}$$

BC 2(A) : At the surface :

Abuzaid (1993) calculated the value of the film resistance for this system to be $1.8E-3 \text{ cm}^2 / \text{sec}$. As this value may be considered miniscule, the film resistance contribution may be neglected.

$$-V \frac{dC}{dt} = 4\pi r^2 n \rho_p D_{\text{eff}} \left. \frac{\partial q}{\partial r} \right|_{r=r_s} \tag{2.12}$$

where

$$D_{\text{eff}} = \varepsilon \frac{D_p}{\rho_p} \frac{\partial C_p}{\partial q} + D_s \tag{2.13}$$

As

$$\frac{3V_s}{r_s} = 4\pi r_s^2 n \tag{2.14}$$

Therefore

$$V \frac{dC}{dt} = \frac{3V_S}{r_S} \rho_p D_{eff} \left. \frac{\partial q}{\partial r} \right|_{r=r_S} \quad 2.15$$

BC 2(B)

$$V \frac{dC}{dt} = -W_S \frac{d\bar{q}}{dt} - \epsilon V_p \frac{d\bar{C}_p}{dt} \quad 2.16$$

where \bar{q} and \bar{C}_p are average values.

$$V \frac{dC}{dt} = -W_S \frac{d\bar{q}}{dt} \left\{ 1 + \frac{\epsilon}{\rho_p} \frac{d\bar{C}_p}{d\bar{q}} \right\} \quad 2.17$$

$$\bar{q} = \frac{\int_0^{r_s} (4\pi r^2 q) dr}{4\pi r_s^3 / 3} \quad 2.18$$

$$\bar{C}_p = \frac{\int_0^{r_s} (4\pi r^2 C_p) dr}{4\pi r_s^3 / 3} \quad 2.18b$$

Dimensionless Form

Defining dimensionless variables as :

$$Q = \frac{q}{q_{os}} : \quad \eta = \frac{r}{r_s} : \quad \tau = \frac{D_p t}{r_s^2} \quad 2.19$$

$$\frac{\partial q}{\partial Q} = q_{os} : \frac{\partial \tau}{\partial t} = \frac{D_p}{r_s^2} : \frac{\partial \eta}{\partial r} = \frac{1}{r_s} \quad 2.20$$

$$\frac{\partial q}{\partial t} = \frac{\partial q}{\partial Q} \cdot \frac{\partial Q}{\partial \tau} \cdot \frac{\partial \tau}{\partial t} = q_{os} \frac{D_p}{r_s^2} \frac{\partial Q}{\partial \tau} \quad 2.21$$

$$\frac{\partial q}{\partial r} = \frac{\partial q}{\partial Q} \cdot \frac{\partial Q}{\partial \eta} \cdot \frac{\partial \eta}{\partial r} = \frac{q_{os}}{r_s} \frac{\partial Q}{\partial \eta} \quad 2.22$$

$$\frac{\partial^2 q}{\partial r^2} = \frac{\partial}{\partial \eta} \cdot \frac{\partial \eta}{\partial r} \left(\frac{q_{os}}{r_s} \cdot \frac{\partial Q}{\partial \eta} \right) = \frac{q_{os}}{r_s^2} \frac{\partial^2 Q}{\partial \eta^2} \quad 2.23$$

$$\left[\frac{\varepsilon}{\rho_p} \frac{\partial C_p}{\partial q} + 1 \right] \frac{\partial Q}{\partial \tau} = \frac{1}{\eta^2} \frac{\partial}{\partial \eta} \left\{ \eta^2 \left[\frac{\varepsilon}{\rho_p} \frac{\partial C_p}{\partial q} + \frac{D_s}{D_p} \right] \frac{\partial Q}{\partial \eta} \right\} \quad 2.24$$

The initial condition becomes:

$$\overline{C}(0) = 1$$

$$Q(\eta, 0) = 0 \quad 2.25$$

The boundary conditions become:

B.C.1: At the center of the particle

$$\frac{\partial Q(0, t)}{\partial \eta} = 0 \quad 2.26$$

B.C.2(A) At the surface of the particle:

$$\frac{d\bar{C}}{d\tau} = 3\alpha \frac{D_{eff}}{D_p} \left[\frac{\partial Q}{\partial \eta} \right]_{\eta=1} \quad 2.27$$

Define :

$$\alpha = \frac{W_s q_{os}}{VC_o} \quad 2.28$$

$$\bar{C} = \frac{C(t)}{C_o} \quad 2.29$$

and

$$\bar{Q} = 3 \int_0^1 (Q \eta^2) d\eta = \frac{\bar{q}}{q_{os}} \quad 2.30$$

Also :

$$\frac{d\bar{q}}{dt} = \frac{d\bar{q}}{d\bar{Q}} \cdot \frac{d\bar{Q}}{d\tau} \cdot \frac{d\tau}{dt}$$

Therefore

$$\frac{d\bar{q}}{dt} = q_{os} \frac{D_p}{r_s^2} \cdot \frac{d\bar{Q}}{d\tau} \quad 2.31$$

$$\frac{VC_o D_p}{r_s^2} \frac{d\bar{C}}{d\tau} = - W_s \frac{d\bar{q}}{dt} \left\{ 1 + \frac{\epsilon}{\rho p} \frac{d\bar{C}_p}{dq} \right\}_{avg} \quad 2.32$$

Neglecting :

$$\frac{\epsilon}{\rho p} \frac{d\bar{C}_p}{dq} \Big|_{avg} \ll 1 \quad 2.33$$

we obtain :

$$\frac{d\bar{C}}{d\tau} = - \left(\frac{q_{os} W_s}{VC_o} \right) \frac{d\bar{Q}}{d\tau} \quad 2.34$$

$$\frac{d\bar{C}}{d\tau} = -\alpha \frac{d\bar{Q}}{d\tau} \quad 2.35$$

Integrating this boundary conditions yields:

$$\bar{C}(\tau) = 1 - \alpha [\bar{Q}(\tau) - \bar{Q}(\tau = 0)] \quad 2.36$$

Conducting an adsorbate balance at any time t in the system yields

$$VC_o = VC_t + W_s \bar{q} \quad 2.37$$

$$\bar{q} = \frac{V}{W_s} (C_o - C_t) \quad 2.38$$

At equilibrium we have :

$$VC_o = VC_{\infty} + W_s \bar{q}_{\infty} \quad 2.39$$

$$\bar{q}_{\infty} = \frac{V}{W_s} (C_o - C_{\infty}) \quad 2.40$$

$$\frac{\bar{q}_{\infty}}{\bar{q}_o} = \frac{VC_o}{W_s q_{os}} \left(1 - \frac{C_{\infty}}{C_o} \right) ; \quad \bar{q}_o = q_{os} \quad 2.41$$

Hence :

$$\alpha = \frac{W_s q_{os}}{V C_o} = \left(1 - \frac{C_\infty}{C_o}\right) / \frac{\bar{q}_\infty}{\bar{q}_o} \quad 2.42$$

Also

$$\frac{\bar{q}}{\bar{q}_\infty} = \frac{M_t}{M_\infty} = \frac{[C_o - C_t]}{[C_o - C_\infty]} = \frac{[1 - C_t / C_o]}{[1 - C_\infty / C_o]} \quad 2.43$$

where $\frac{M_t}{M_\infty}$ is the fractional uptake at any time. It is an indication of the proximity to equilibrium.

$$1 - \frac{M_t}{M_\infty} = 1 - \frac{[1 - C_t / C_o]}{[1 - C_\infty / C_o]} \quad 2.44$$

2.3.2. Taking into Account the Concentration Dependence of Surface Diffusivity.

At high concentration levels in an adsorbent, the equilibrium isotherm becomes non-linear so that the gradient in concentration is no longer the same as the gradient in chemical potential. By considering the relationship between chemical potential and gradient one obtains Darken's relation.

$$D_s = D_{so} \left(\frac{d \ln C}{d \ln q} \right)_T \quad 2.45$$

Darken's relation can be derived for various isotherm models and this is done in Table 2.1. We observe, that except for the Freundlich isotherm, the diffusivity is strongly concentration dependent for all other isotherms. The

$$D_s = D_{so} \left(\frac{d \ln C}{d \ln q} \right)_T \quad 2.45$$

Darken's relation can be derived for various isotherm models and this is done in Table 2.1. We observe, that except for the Freundlich isotherm, the diffusivity is strongly concentration dependent for all other isotherms. The observation with regard to the Freundlich isotherm was recently reported by Gutsche and Yoshida (1994). They also reported that it was not able to reflect the concentration dependence of their data. Also Hu et al., (1994) corroborated this fact by their extensive theoretical and experimental studies of the intrinsic concentration dependence of surface diffusivity in hydrocarbons and granular activated carbon systems. Garg and Ruthven(1972) used the Darken relationship in explaining the concentration dependence of diffusivity in zeolites using the Langmuir and Volmer isotherms.

2.3.3 Effective Pore Volume Diffusivity Coefficient.

The effective pore volume diffusivity coefficient was estimated using the relation:

$$D_{e,p} = \frac{D_{AB}}{\tau_p} \quad 2.46$$

where D_{AB} , is the molecular diffusivity and τ_p is the tortuosity factor. The value of τ_p for activated carbon is reported to be 3.5 (Leyva-Ramos and Geankoplis, 1994) and this is in good agreement with the general values reported earlier in the literature (Komiya and Smith, 1974; Shibuya and Kawazoe, 1978). The value of D_{AB} predicted from correlations was reported

Table 2.1 : Normalized Values Of $d\ln C/d\ln q$ For Various Isotherms

ISOTHERM FORM		$\frac{d\ln C}{d\ln q}$	
NAME	EQUATION	θ - FORM	λ - FORM
Henry's Isotherm	$q = K_{\text{HT}} C$	1	1
Langmuir Isotherm	$\frac{q}{q_s} = \frac{K_L C}{1 + K_L C}$	$\frac{1}{1 - \theta}$	$\frac{1}{1 - \lambda Q}$
Toth Isotherm	$\frac{q}{q_s} = \frac{K_T C}{[1 + (K_T C)^n]^{\frac{1}{n}}}$	$\frac{1}{1 - \theta^n}$	$\frac{1}{1 - (\lambda Q)^n}$
Freundlich Isotherm	$q = K_F C^{\frac{1}{n}}$	n	n
Langmuir-Freundlich Isotherm	$\frac{q}{q_s} = \frac{K_{\text{LF}} C^{\frac{1}{n}}}{1 + K_{\text{LF}} C^{\frac{1}{n}}}$	$\frac{n}{1 - \theta}$	$\frac{n}{1 - \lambda Q}$
Volmer's Isotherm	$C = b \left(\frac{\theta}{1 - \theta} \right) \exp \left(\frac{\theta}{1 - \theta} \right)$	$\frac{1}{(1 - \theta)^2}$	$\frac{1}{(1 - \lambda Q)^2}$
Virial Isotherm	$C = \frac{q}{K} \exp(A_1 q + A_2 q^2 + A_3 q^3 + \dots)$	$1 + \sum_{i=1}^n A_i^* \theta^i$ Where $A_i^* = i A_i$	$1 + \sum_{i=1}^n A_i^* (\lambda Q)^i$ Where $A_i^* = i A_i$
Myer's Isotherm	$C = \frac{q}{K_H} \exp(K q^a)$	$1 + K^* Q^a$ where $k^* = a k q_s^a$	$1 + K^* \lambda^a Q^a$ where $k = a k q_s^a$

directly. from the Wilke-Chang equation (Reid et al., 1977). The molal volume of o-cresol (Hydroxymethylbenzene, $\text{CH}_3 - \text{C}_6\text{H}_4 - \text{OH}$) was estimated from the LeBas Atomic Volumes method (Reid et al., 1977).

$$D_{AB} = \frac{7.4E - 8 (\xi M_B)^{1/2} T}{\mu_B V_A^{0.6}} \quad 2.47$$

2.3.4 Langmuir Freundlich Isotherm.

The general form of Langmuir Freundlich isotherm is :

$$\theta = \frac{q}{q_s} = \frac{k_{LF} C^{1/n}}{1 + k_{LF} C^{1/n}} \quad 2.48$$

The following can readily be obtained by differentiation.

$$\frac{\partial C_p}{\partial q} = \frac{n}{k_{LF}^n q_s} \frac{(Q\lambda)^{n-1}}{(1 - Q\lambda)^{n+1}} \quad 2.49$$

Defining :

$$\lambda = \frac{q_o}{q_s} = \frac{k_{LF} C_o^{1/n}}{1 + k_{LF} C_o^{1/n}} \quad 2.50$$

In dimensionless form we have :

$$\lambda Q = \frac{q}{q_s} = \frac{k_{LF} (\bar{C} C_o)^{1/n}}{1 + k_{LF} (\bar{C} C_o)^{1/n}} \quad 2.51$$

$$\lambda Q_{\infty} = \frac{q_{\infty}}{q_s} = \frac{k_{LF} (\bar{C}_{\infty} C_o)^{1/n}}{1 + k_{LF} (\bar{C}_{\infty} C_o)^{1/n}} \quad 2.52$$

The overall equation (2.24) then becomes :

$$\left[\frac{\varepsilon}{\rho p k_{LF}^n} \frac{n}{q_s} \frac{(Q\lambda)^{n-1}}{(1-Q\lambda)^{n+1}} + 1 \right] \frac{\partial Q}{\partial \tau} = \quad 2.53$$

$$\frac{1}{\eta^2} \frac{\partial}{\partial \eta} \left\{ \eta^2 \left[\frac{\varepsilon}{\rho p k_{LF}^n} \frac{n}{q_s} \frac{(Q\lambda)^{n-1}}{(1-Q\lambda)^{n+1}} + \frac{D_s}{D_p} \frac{n}{(1-Q\lambda)} \right] \frac{\partial Q}{\partial \eta} \right\}$$

As

$$\frac{\varepsilon}{\rho p k_{LF}^n} \frac{n}{q_s} \frac{(Q\lambda)^{n-1}}{(1-Q\lambda)^{n+1}} \ll 1 \quad 2.54$$

The left hand bracketed side of equation (2.53) may be set equal to 1.

Therefore, the final equation becomes :

$$\frac{\partial Q}{\partial \tau} = \frac{1}{\eta^2} \frac{\partial}{\partial \eta} \left\{ \eta^2 \left[\frac{\varepsilon}{\rho p k_{LF}^n} \frac{n}{q_s} \frac{(Q\lambda)^{n-1}}{(1-Q\lambda)^{n+1}} + \frac{D_s}{D_p} \frac{n}{(1-Q\lambda)} \right] \frac{\partial Q}{\partial \eta} \right\} \quad 2.55$$

This must be solved numerically together with initial condition and the boundary conditions equations 2.25, 2.27, and 2.36.

2.4 Results And Discussion

In order to ascertain the most efficient mechanism for this work, five different models are examined, namely

Model 1 : The pore diffusion model,

Model 2 : The homogeneous surface diffusion model with constant surface diffusivity coefficient,

Model 3 : The homogeneous surface diffusion model with concentration dependent surface diffusivity coefficient,

Model 4 : The pore and surface diffusion model with constant surface diffusivity coefficient, and

Model 5 : The pore and surface diffusion model with concentration dependent surface diffusivity coefficient.

In models 3 and 5, the dependence of surface diffusivity on solid phase concentration was accounted for by taking chemical potential as the driving force using the Darken's relation. The equation data for phenol and o-cresol adsorption on GAC was fitted using a nonlinear regression program. The fit of the model to the data is illustrated in Figures 2.1 and 2.2, and the parameters of the isotherm are giving in Table 2.2. Abuzaid (1993) fitted the data using the Freundlich model but as this isotherm does not provide any indication of the saturation loading, the Langmuir Freundlich model was employed. The saturation concentration for phenol appears reasonable at 0.25 mg/mg but that for o-cresol appears high at 0.6 mg/mg.

The implicit Crank - Nicolson finite difference scheme was used to solve the resulting equations. This method averages the forward and backward

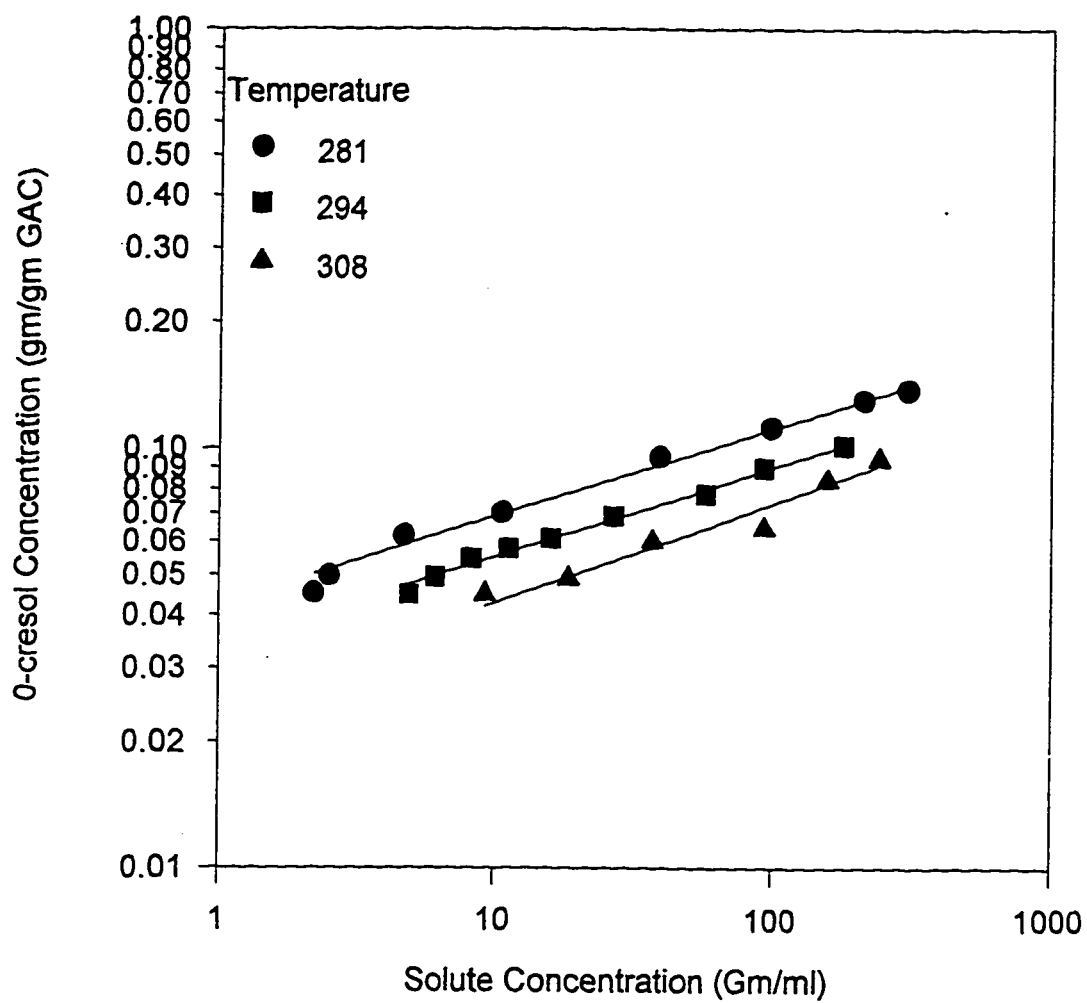


Figure 2.1. Langmuir-Freundlich fit of phenol adsorption on GAC

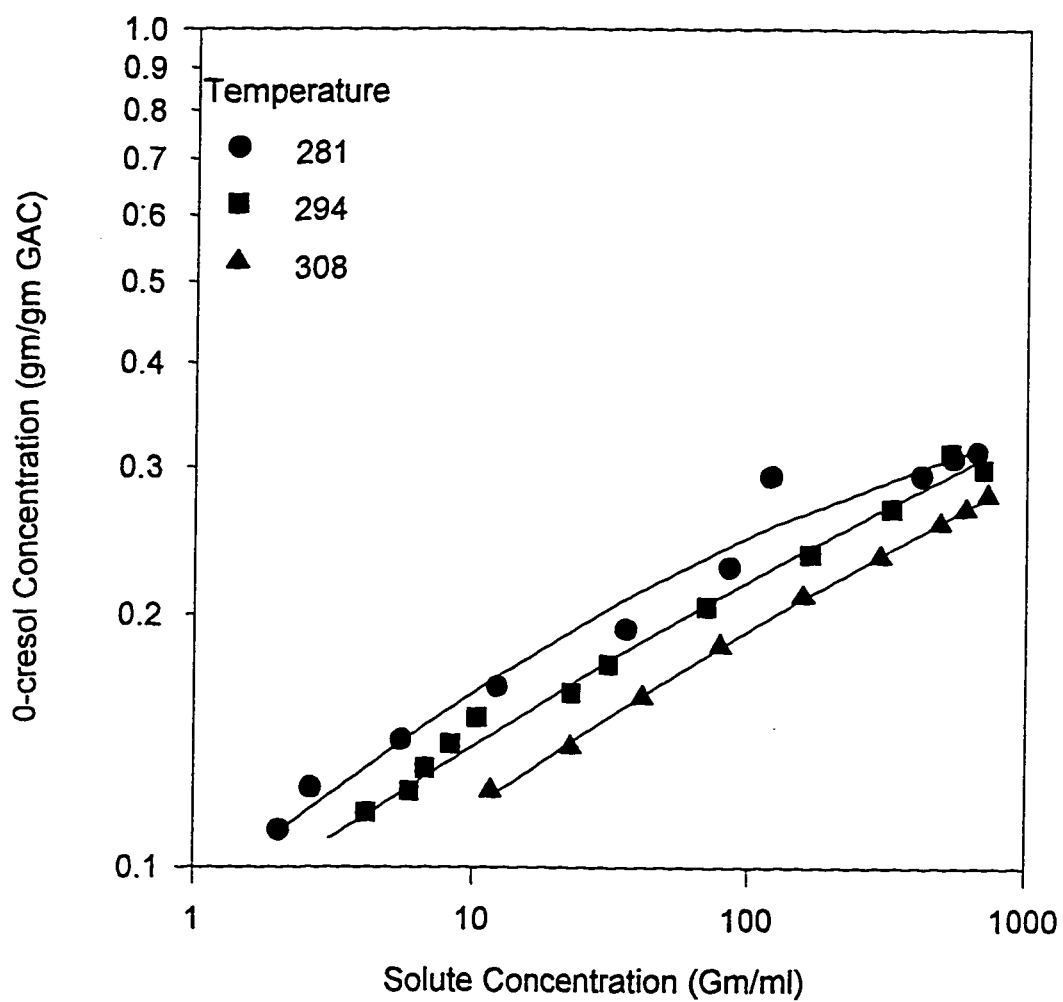


Figure 2.2. Langmuir-Freundlich fit of o-cresol adsorption on GAC

Table 2.2 : Input Parameters For Optimization of Surface Diffusivity

1	2	3	4	5		6	7
Temp, (K)	C_o , mg / L	C_∞ / C	Pore Fraction	Isotherm Constant		Pore Diffusi- -vity Coeff.	Particle Density, ρ_p , mg / cm ³
				k_{LF} , (mg / L)	n	q_s , mg / m	
For phenol.							
281	1000	0.213	0.63	0.1873	3.125	0.25	1.3957
294	1000	0.261	0.63	0.1345	3.125	0.25	2.0742
308	1000	0.463	0.63	0.0975	3.125	0.25	2.9610
For o-cresol							
281	1000	0.252	0.63	0.1842	3.448	0.60	1.6059
294	1000	0.301	0.63	0.1353	3.448	0.60	2.3865
308	1000	0.347	0.63	0.1230	3.448	0.60	3.4069

finite differences and is unconditionally stable. The resulting tridiagonal matrices were solved using Thomas algorithm. The applicability of the program was tested by reproducing the results of Suzuki (1980) for constant surface diffusivity and Freundlich isotherm (see Figure 2.3). The time step and number of nodes used are respectively 0.0005 and 51. A comparison of the results of the program for 21 nodes and 71 nodes is presented in Figure 2.4. The two results are indistinguishable. This is an attestation of the accuracy of the program used.

The IMSL library optimization program (BCPOL) was used in this work to minimize the sum of the root mean squares (rms.) of the residuals between predicted and experimental concentration values. The two forms of rms. equations commonly used are :

$$(i) \text{ The normalized RMS} = 100 * \sqrt{\frac{1}{N} \sum_{i=1}^N \left(\frac{C_{i,\text{exp}} - C_{i,\text{cal}}}{C_{i,\text{exp}}} \right)^2} \quad 2.56$$

$$(ii) \text{ The non-normalized RMS} = \sqrt{\frac{1}{N} \sum_{i=1}^N (C_{i,\text{exp}} - C_{i,\text{cal}})^2} \quad 2.57$$

The normalized RMS. was used in this work. The model parameter determined from the optimization program is the surface diffusivity coefficient at zero concentration.. The input parameters for the various models are given in Table 2.2. The parameters used by the various models are :

Model 1 input : Columns 2 - 7

Model 2 input : Columns 2, 3, and 5

Model 3 input : Columns 2, 3, and 5

Model 4 input : Columns 2 - 7

Model 5 input : Columns 2 - 7

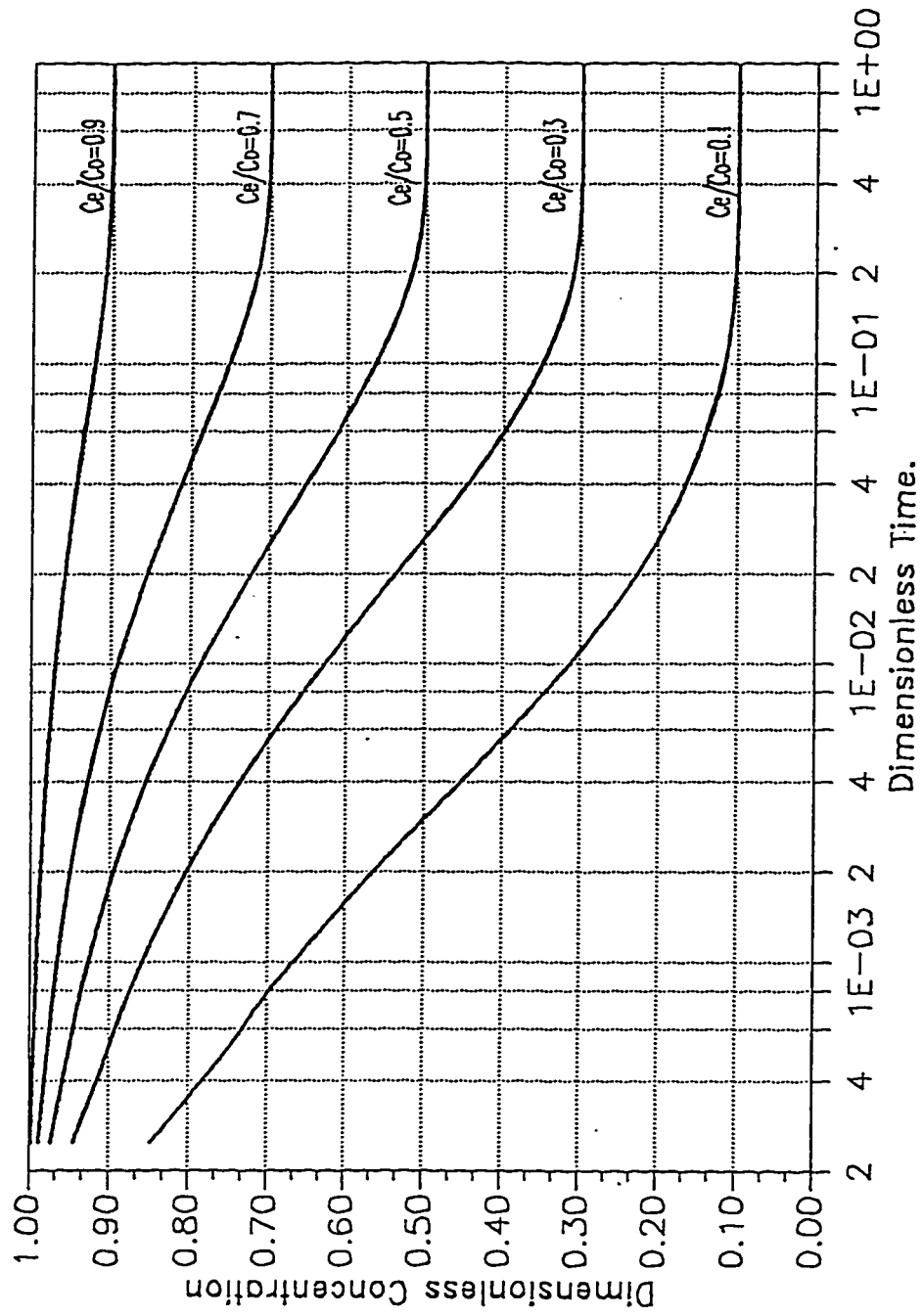


Fig 2.3: Reproducibility of Program to Produce data of Suzuki (1990), (Page 9).

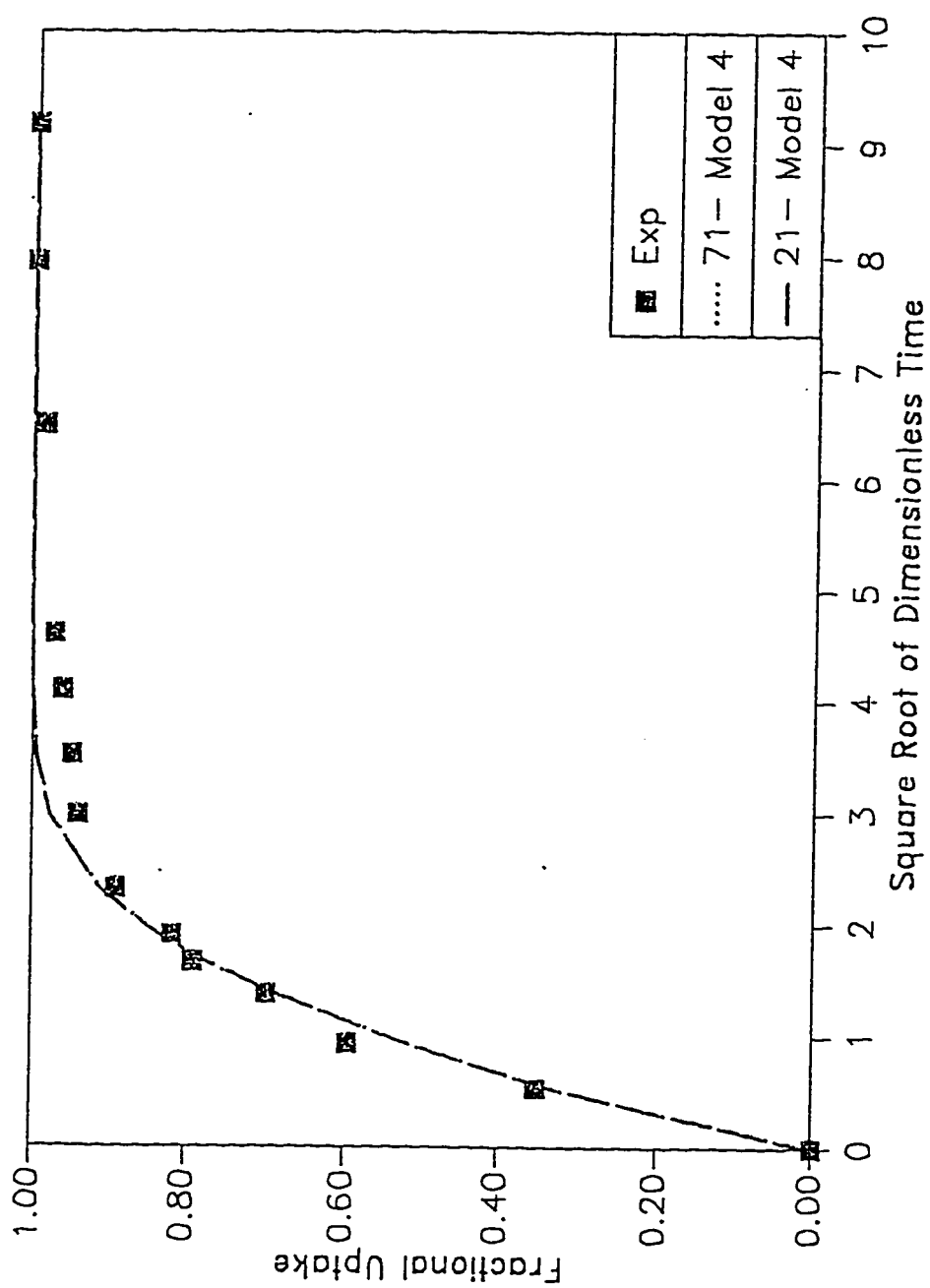


Fig 2.4: Predicted and Experimental Fractional Uptake at 308K. Adsorption of phenol. Comparison Between 71 and 21 nodes

To assess the effectiveness of each model, the root mean square deviations of the predicted concentration decay from the experimental values were computed. These are given in Table 2.2. The plots of the various models are presented in Figures 2.5 to 2.10. Note, $\epsilon = 0.64$ for the GAC used.

The pore diffusion model gave very poor fits with large rms. values. This indicates that the dominant mechanism in the adsorption process is not pore diffusion. Pore diffusion alone is inadequate in predicting the adsorption of phenol on granular activated carbon (GAC) when you have a high concentration data. However, Leyva and Geankoplis (1994) successfully fitted their data for phenol - GAC system using pore diffusion model. This is because their data is of very low concentration ($< 50 \text{ mg/L}$) which should be compared to the data used in this work which is at a high concentration (1000 mg/L). The poor fits of the pore diffusion model are shown in Figures 2.5 to 2.7.

The homogeneous surface diffusion model with constant D_s gives reasonably good fits as may be seen in Figures 2.5 to 2.7. This indicates that the surface diffusion model can be used in predicting the adsorption process. Abuzaid fitted this data using Freundlich isotherm and HSDM. and obtained reasonable fits at 281K, 294K and 308K. The difference in fits and resulting surface diffusivity coefficients values between this work and Abuzaid's may be partly attributed to the different isotherm forms used. The Freundlich isotherm gave a better fit than the Langmuir Freundlich isotherm. However, the surface diffusivity coefficients obtained are well within the range reported in literature as may be seen in Tables 2.3 and 2.4. The model which assumed a constant surface diffusivity coefficient exhibits a rather strong

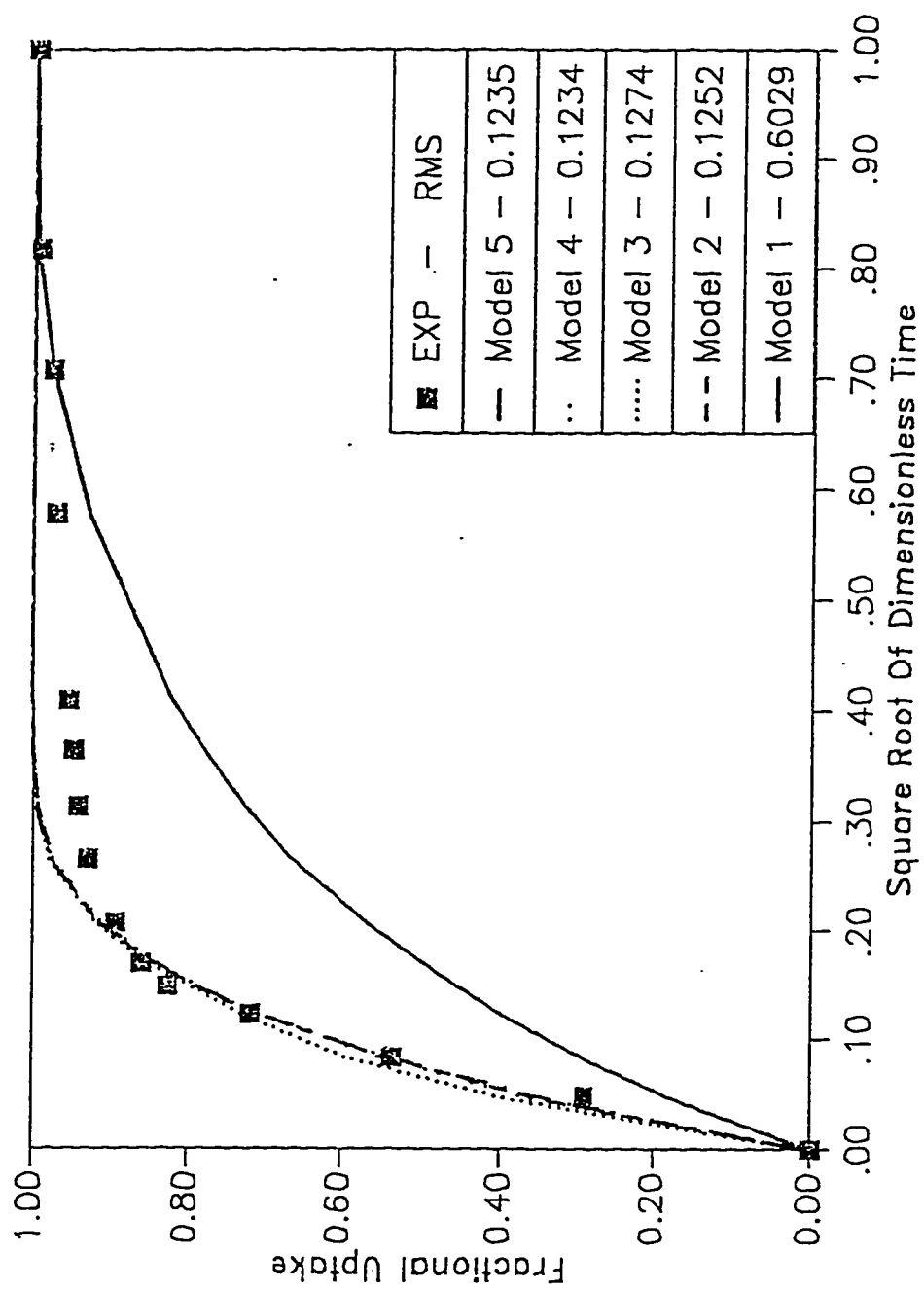


Fig. 2.5: Predicted and Experimental Uptake at 281K. Adsorption of phenol

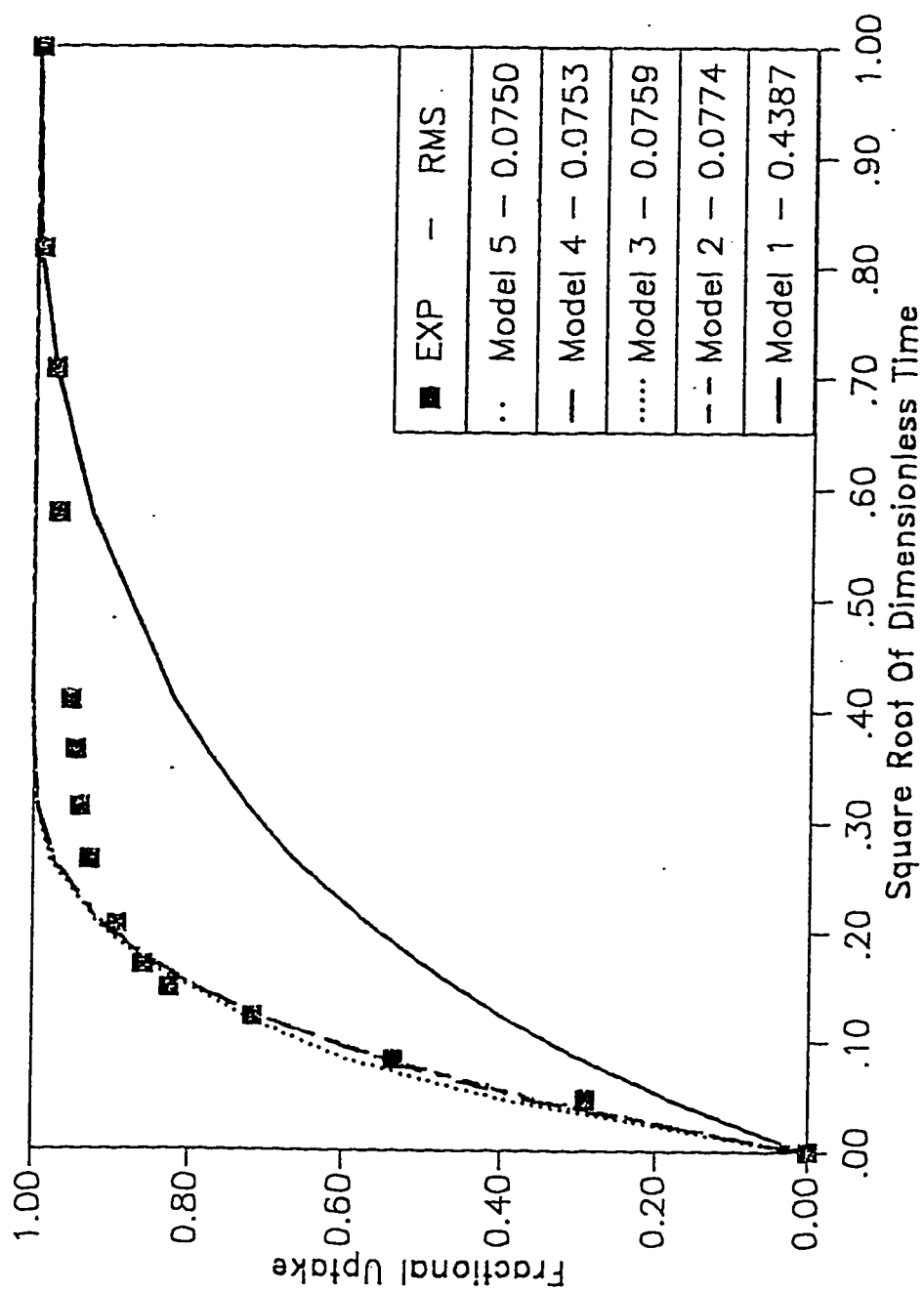


Fig. 2.6: Predicted and Experimental Uptake at 294K. Adsorption of phenol.

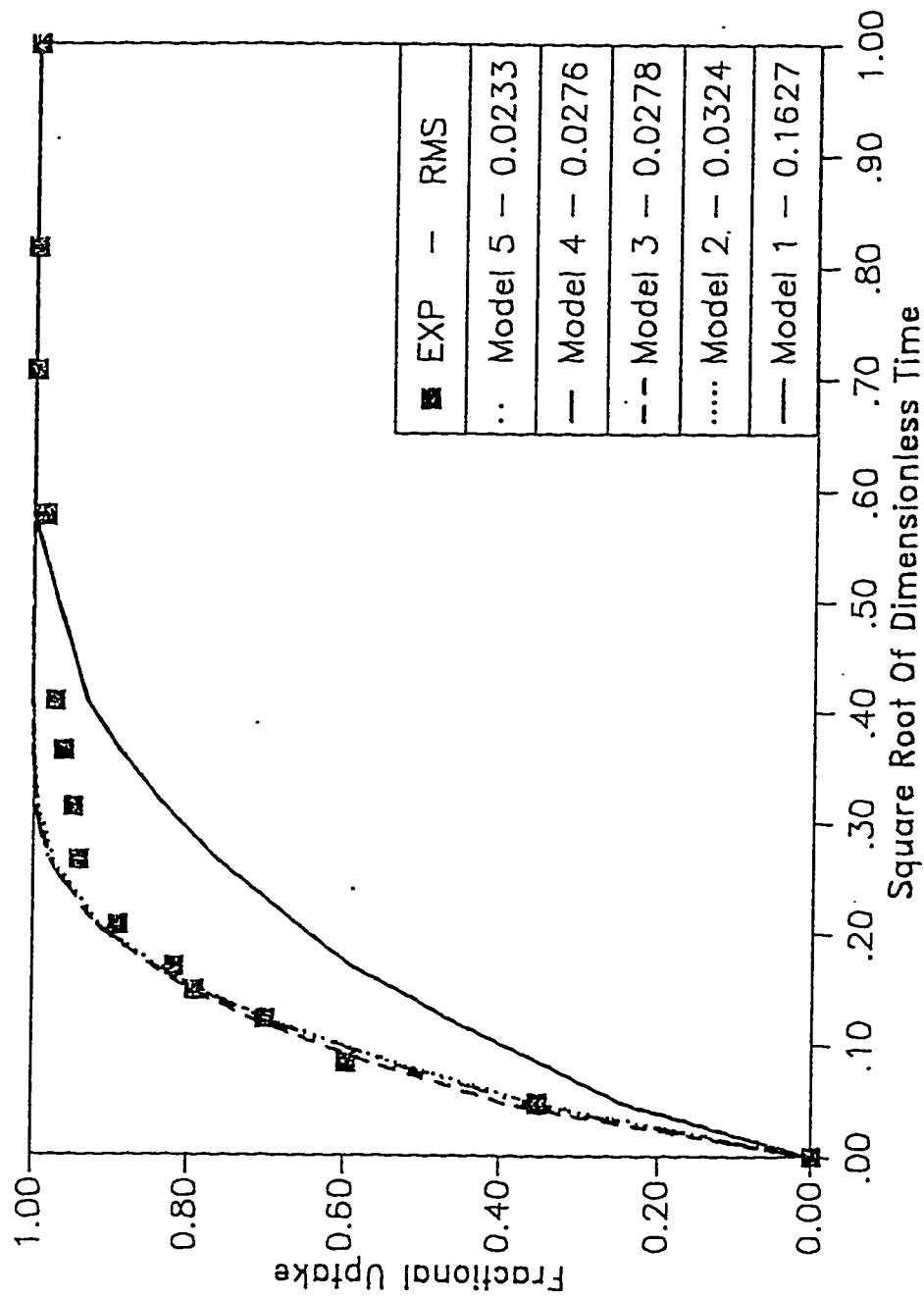


Fig 2.7: Predicted and Fractional Uptake
at 308K. Adsorption of phenol

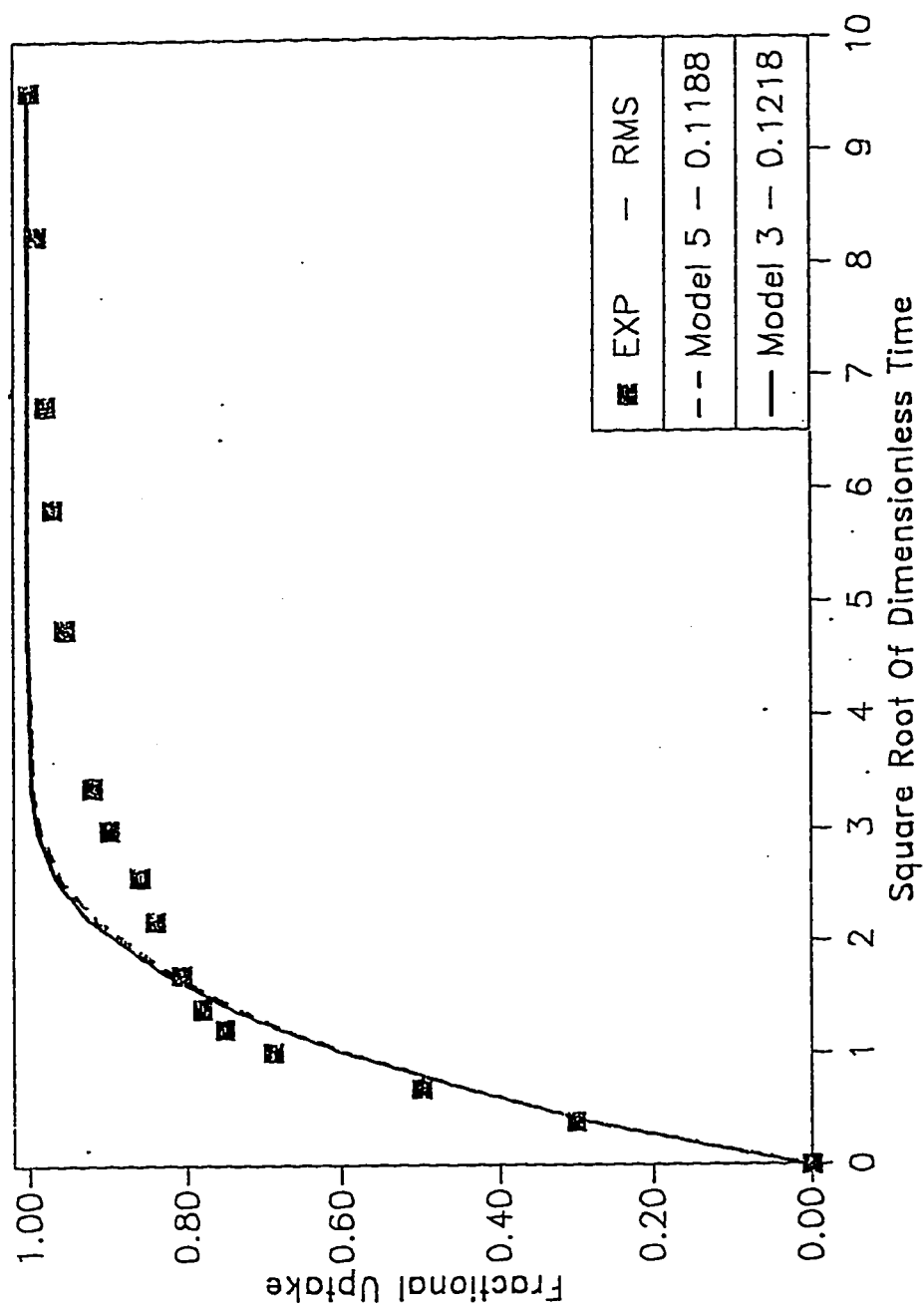


Fig. 2.8: Predicted and Experimental Fractional Uptake at 281K. Adsorption of o-Cresol

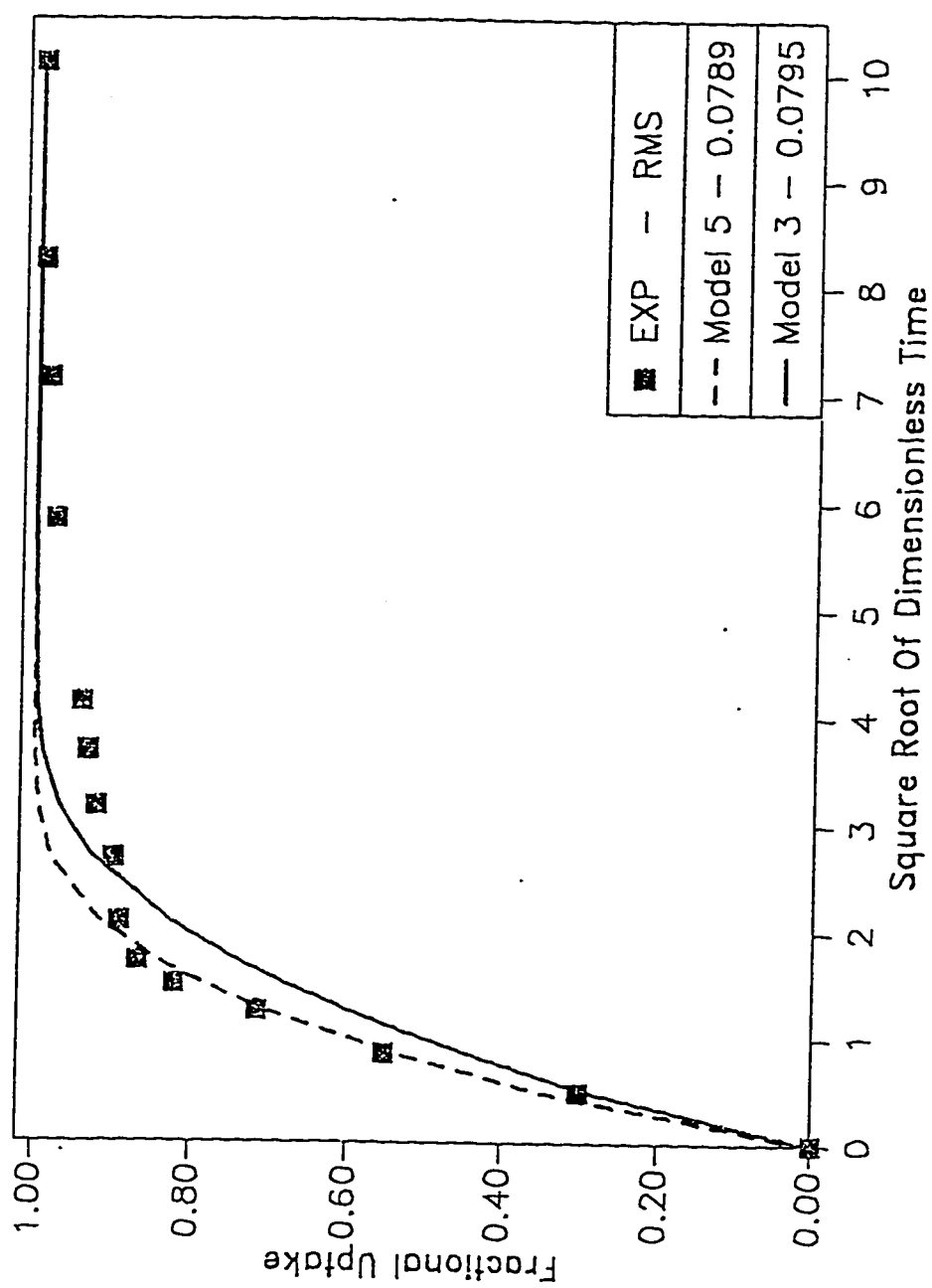


Fig. 2.9: Predicted and Experimental Fractional Uptake at 294K. Adsorption of o-Cresol

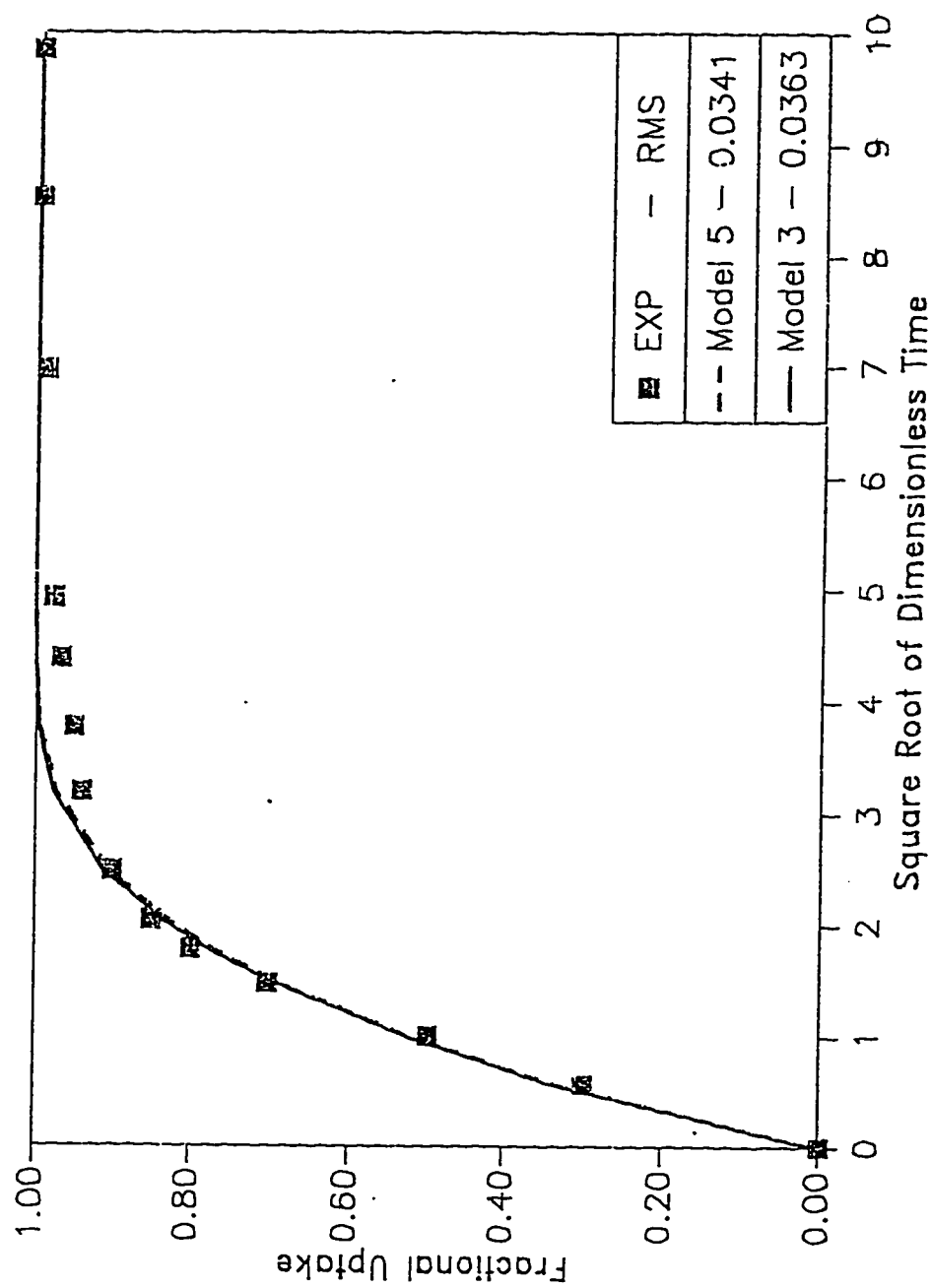


Fig 2.10: Predicted and Experimental Fractional Uptake at 308K. Adsorption of o-Cresol.

Table 2.3 : Diffusivity Coefficient And RMS values For The Various Models.

Temp (K)	Pore Diffusion Model (PD)		Homogeneous Surface Diffusion Model (HSDM) with constant surface Diffusivity		Homogeneous Surface Diffusion Model (HSDM) With concentration Dependent surface Diffusivity.		Pore And Surface Diffusion Model (PSD) with constant surface Diffusivity		Pore And Surface Diffusion Model (PSD) With concentration Dependent Surface Diffusivity	
	$D_p \cdot E/10$ (m^2 / s)	RMS.	$D_s \cdot E/2$ (m^2 / s)	RMS.	$D_{so} \cdot E/2$ (m^2 / s)	RMS.	$D_s \cdot E/2$ (m^2 / s)	RMS.	$D_{so} \cdot E/2$ (m^2 / s)	RMS.
For phenol										
281	1.396	60.29	6.16	12.52	1.12	12.74	5.17	12.34	0.82	12.35
294	2.074	43.87	7.97	7.74	1.61	7.59	6.29	7.53	1.33	7.50
308	2.961	16.27	9.05	3.24	1.95	2.78	5.92	2.76	1.30	2.33
For o-cresol										
281	1.606				1.0	12.18			0.803	11.88
294	2.387				1.735	7.96			1.468	7.90
308	3.407				1.745	3.63			1.346	3.65

Table 2.4 : Surface Diffusivity Coefficients from Literature for Batch Data and HSDM Model.

Researcher	Temp	Phenol D_s Values		o-cresol D_s Values	
		D_s^*E12 (m^2/s)	C_o , mg/L	D_s^*E12 (m^2/s)	C_o , mg/L
Suzuki and Kawazoe (1975)	room	4.3	-	-	-
Vidic and Suidan (1992)	308	-	-	2.406	1000.0
Vidic et al. (1994)	294	2.5893	100.0	-	-
		4.756	200.0		
		10.728	800.0		
Crittenden and Weber (1978)	room	3.53	465.0	-	-
Matthew and Su(1983)	297	3.75	100.0	-	-
Abuzaid (1993)	281	4.9	1000.0	8.3	1000.0
	294	6.3			
	308	8.8			

dependence of diffusivity on the solid surface concentration from point to point. Consequently, a substantial variation in the values of the surface diffusivity coefficient with time was observed suggesting the need to use a concentration dependent diffusivity model to account for this dependence. Hence Darken's relation was incorporated into the constant surface diffusivity coefficient model. The degree of fit obtained with the concentration dependent surface diffusivity model was slightly better than that obtained from its constant diffusivity counterpart. Moreover, this modification exerted a marked degree of influence on the variation of the surface diffusivity coefficient with time. There was a substantial reduction in variation but it was still not eliminated as may be observed in Figure 2.11. Darken's relation appreciably accounted for the concentration dependence of surface diffusivity coefficient with time. This observation is contrary to those of Hu et al. (1994), and Gutsche and Yoshida (1994). These researchers reported that the Darken's relation could only slightly account for the concentration dependence.

The dual mechanism pore and surface diffusion model (PSD) was used in order to assess the importance of pore diffusion contribution to the adsorption process. The PSD model was also used by Hu et al. (1994) and, Leyva and Geankoplis, (1994). The fits obtained from the PSD models were only slightly better than those obtained from the surface diffusion models as may be seen in Figure 2.5 to 2.10. Thus when high concentration data are fitted, the HSDM and the PSD model can predict the adsorption process equally well. The rms. values were in the range of 2.0 -13.5. Notably, the variation in the value of the surface diffusivity coefficient with time in the PSD model was markedly reduced when concentration dependence was accounted for as may be observed in Figure 2.12. Also, the fits from the

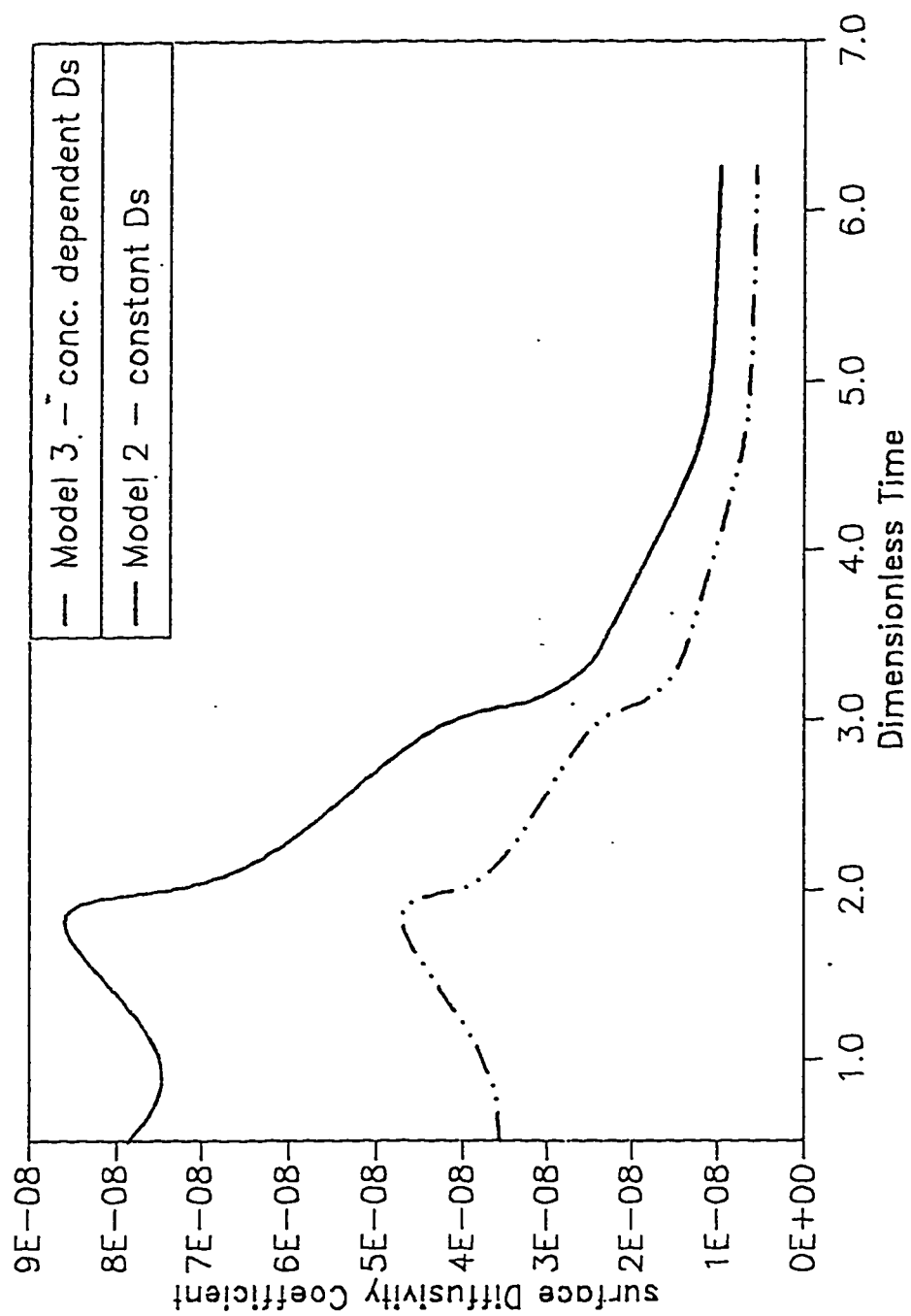


Fig 2.11 : Plot of D_s Vs Dimensionless Time at 281K.
Adsorption of phenol. Comparison between model 2 and 3

constant surface diffusivity coefficient model were almost identical to those from the concentration dependent diffusivity counterpart; the former being slightly better. The slight difference is attributed to noise in the program and to the fact that part of the resistance is being accounted for by pore diffusion.

The D_s values obtained are within the range of the values reported in the literature for both phenol and o-cresol as may be seen in Tables 2.3 and 2.4. The D_s values from the HSDM are higher than those from the PSD. This is expected as part of the diffusion flux is accounted for by pore diffusion in the PSD model. The D_s values increase with temperature continually in the case of the HSDM model. This is consistent with theory as physical adsorption is an exothermic phenomena. In the PSD model however, the D_s increases for the first two temperatures and then decreases at the third temperature. This seeming anomaly is accounted for by the rapid increase in the value of D_p with temperature. As temperature increases, the contribution of pore diffusion increases rapidly as the D_p value increases. Hence an increasing proportion of the diffusion flux is being accounted for by pore diffusion resulting in lower contribution by surface diffusion and as a result a decrease in D_s value. It worth noting that the variation in the D_s from the PSD model is very small compared to that from the HSDM. This observation is again attributed to the pore diffusion contribution which is not accounted for in the HSDM but is accounted for in the PSD model.

Surface adsorption is an activated process and hence D_s is a function of temperature. The D_{s0} values obtained in this study increase with temperature. This is a general observation. A plot of the logarithm of D_{s0} versus the inverse of temperature $1/T$ gives a straight line. These plots are shown for phenol and o-cresol in Figures 2.13 to 2.16. The temperature dependence of D_{s0} is expressed as

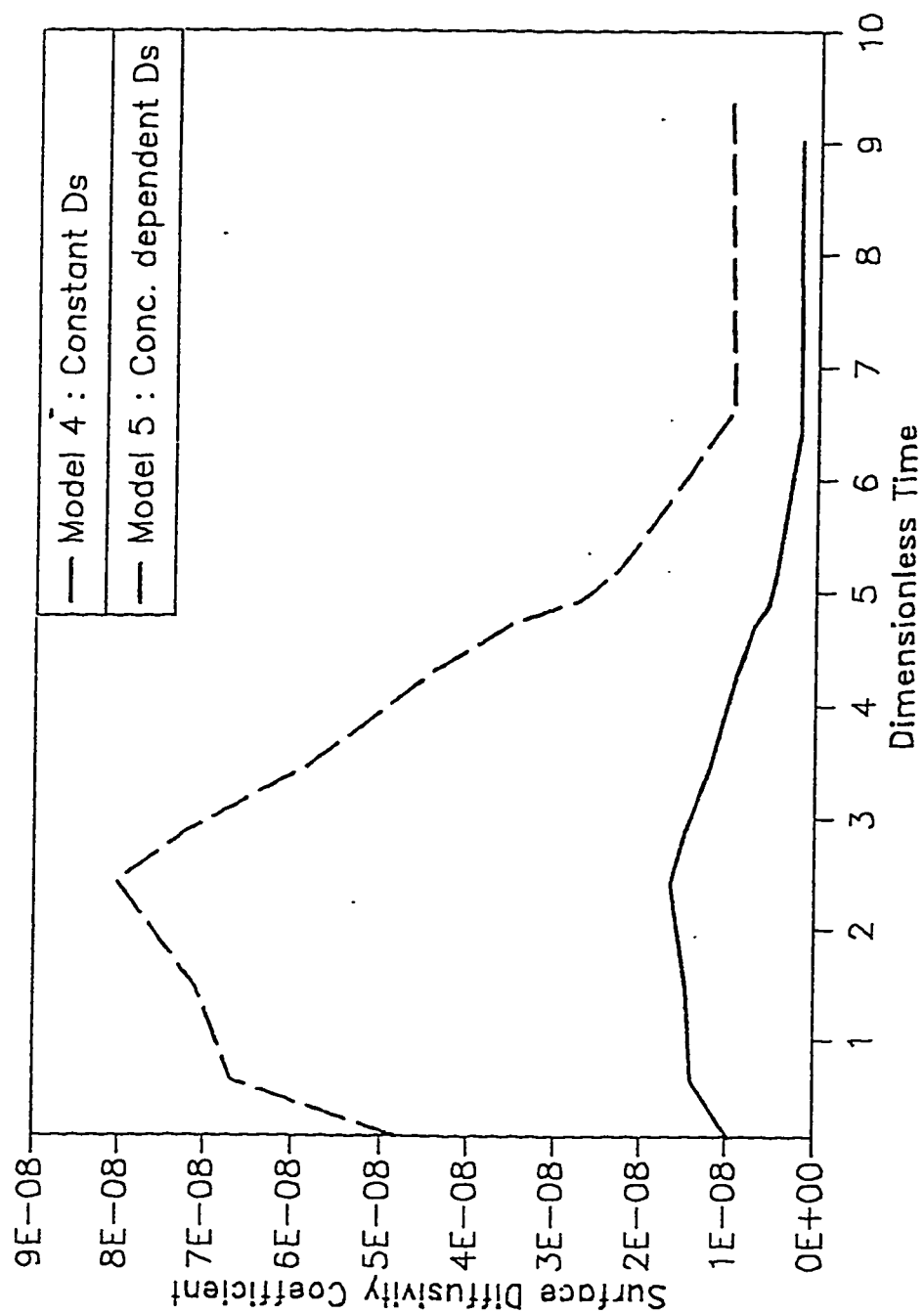


Fig. 2.12 Plot of D_s vs. Dimensionless Time at 294 K.
Adsorption of Phenol (Comparison between models 4 & 5)

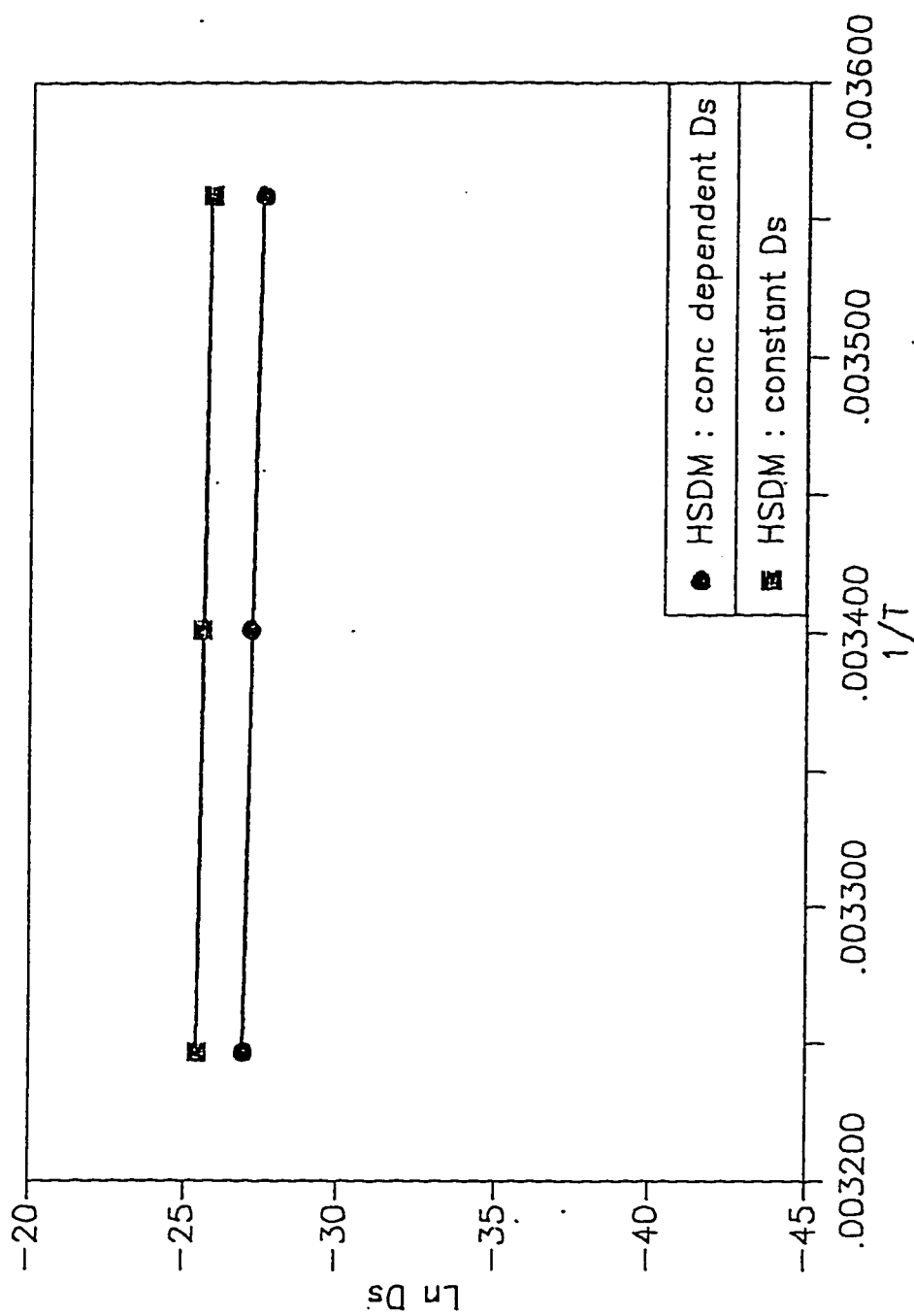


Fig 2.13: Plot of $\ln D_s$ Vs $1/T$
HSDM – Model 2 and 3. Adsorption of phenol

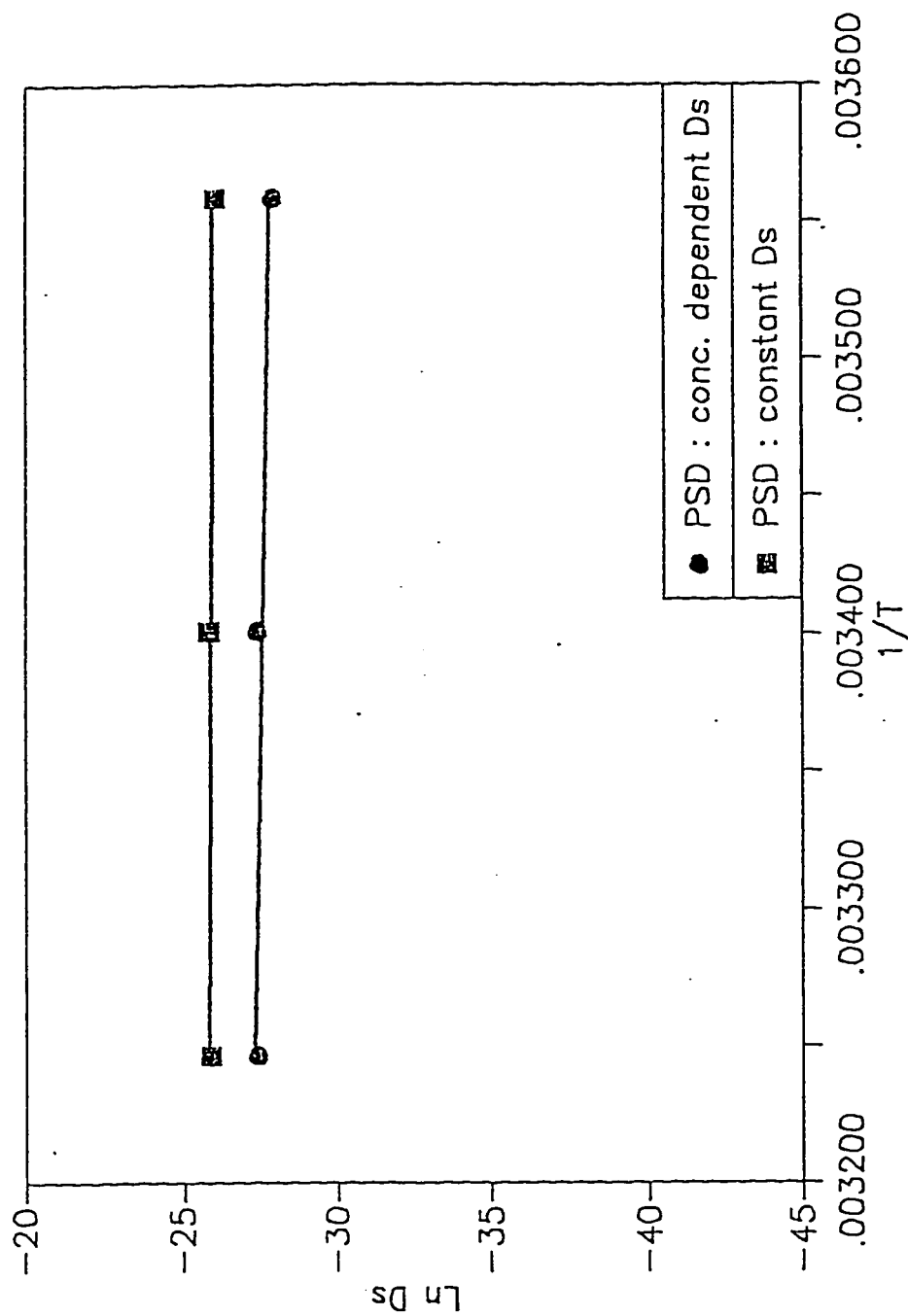


Fig 2.14: Plot of Ln Ds vs 1/T for
PSDM – Model 4 and 5. Adsorption of phenol

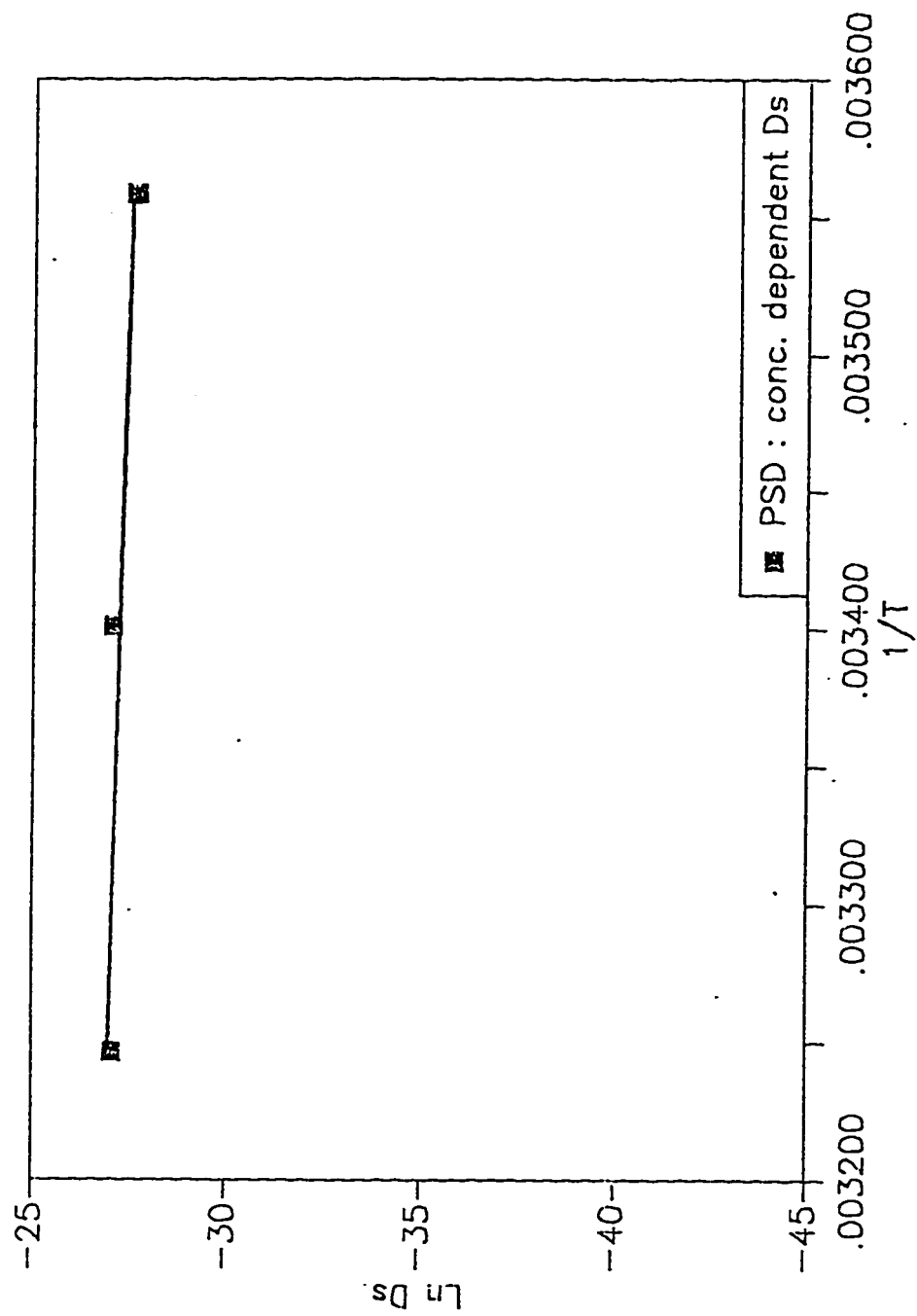


Fig 2.15: Plot of D_s vs $1/T$ for
HSDM – Model 3. Adsorption of o-cresol

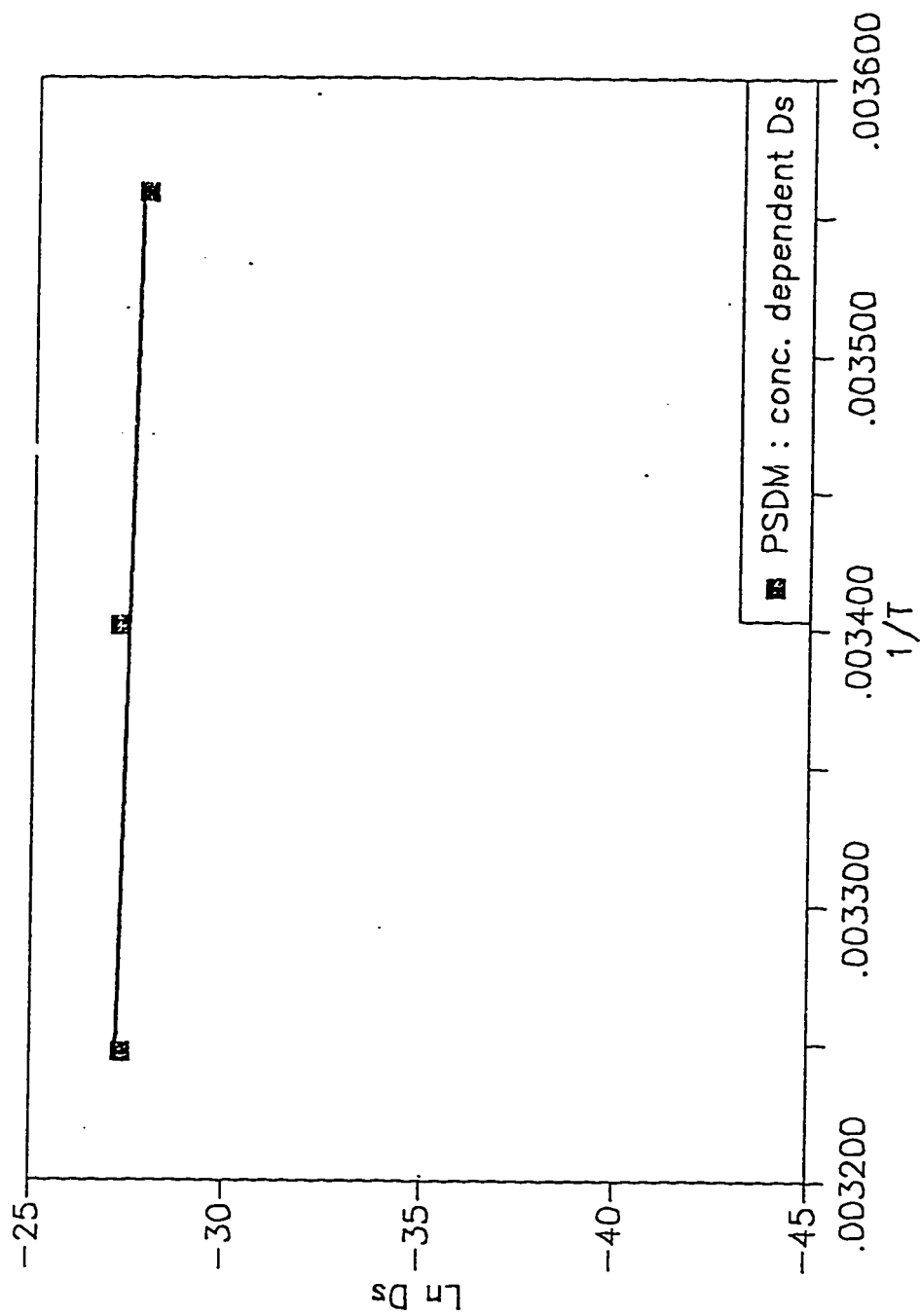


Fig. 2.16: Plot of Ln Ds vs $1/T$ for PSDM – model 5
Adsorption of o-cresol

$$D_{s0} = D_{s0}^* \exp(-E/RT) \quad (2.66)$$

where E is the diffusional activation energy and D_{s0}^* is the preexponential term. The values of E and D_{s0}^* for phenol and o-cresol for the various models are given in Table 2.5. It may be seen from Table 2.5 that both the preexponential term and the diffusional activation energies for the constant D_{s0}^* are lower than those for the of the concentration dependent D_{s0} processes. This results from the fact that the surface diffusivity coefficient of the constant D_{s0} process is higher than that of the concentration dependent D_{s0} process. The surface diffusivity used for the concentration dependent process is D_{s0} which represents the diffusivity at zero adsorbent concentration or when the chemical potential gradient is the same as the concentration gradient.

The literature D_s values indicates a dependence on initial adsorbate concentration as may be seen in Table 2.4. Moreover, the value of the initial adsorbate concentration determines the suitability of the pore diffusion model in predicted the adsorption process and also affects the advantage of the PSD model over the HSDM. To access the relative contributions and importance of pore diffusion to the surface diffusion the ratio of the pore diffusion flux in equilibrium with the bulk phase concentration at the surface of the particle to that of its surface diffusion counterpart was evaluated and plotted against the bulk phase concentration. This plot is presented in Figure 2.17. The flux ratio is found to vary with temperature and the bulk phase concentration. This indicates that pore diffusion is always present and is more important at high temperatures than at low temperatures. The values of D_s as seen in Table 2.3 are approximately constant in the PSD model but vary widely with temperature in the HSDM. for both the constant and

Table 2.5 Temperature Dependence of Surface Diffusivity Coefficient

Model No.	Preexponential Term $D_{s0}^* \cdot E10 \text{ (m}^2/\text{s)}$	Diffusional Activation Energy E (*E-4) (J/gmole)
Phenol		
2	5.1185	1.0279
3	6.4938	1.48
4	0.2558	0.364
5	1.7420	1.2330
o-cresol		
3	6.34	1.486
5	3.34	1.382

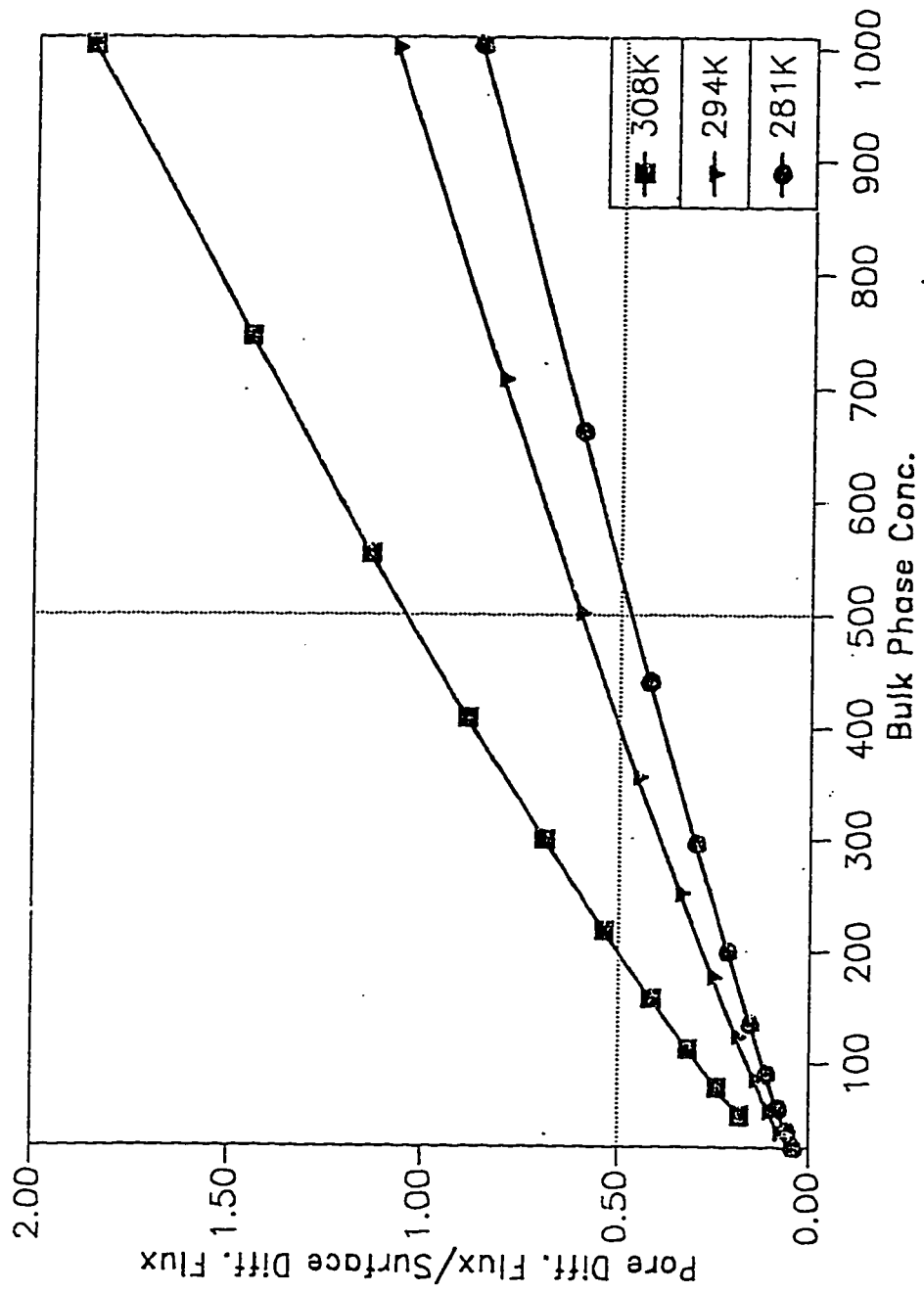


Fig.2.17: Plot of Pore Diffusion Flux/Surface Diffusion Flux Vs Bulk Phase Concentration. Adsorption of phenol

concentration dependent surface diffusivity models. The wide variation of D_s with initial adsorbate concentration that has been reported often times in literature in HSDM is due to the pore diffusion flux which increases with initial adsorbate concentration but is not accounted for.

2.5 Conclusions and Recommendations

The experimental data were fitted using five different models. These are

Model 1 : The pore diffusion model,

Model 2 : The homogeneous surface diffusion model with constant surface diffusivity coefficient,

Model 3 : The homogeneous surface diffusion model with concentration dependent surface diffusivity coefficient,

Model 4 : The pore and surface diffusion model with constant surface diffusivity coefficient, and

Model 5 : The pore and surface diffusion model with concentration dependent surface diffusivity coefficient.

Models 3 and 5, takes into account the surface energetic heterogeneity in the diffusion of adsorbed species. The Darken's relation, based theoretically on the chemical potential gradient driving force, is used to account for the dependence of surface diffusivity on solid phase concentration.

The values of the surface diffusivity coefficients were obtained by minimizing the rms. values of the normalized residuals between the experimental and predicted liquid concentrations. Relevant values are shown in Table 2.3.

The pore diffusion model gave a poor fit.

The fits of the HSDM and the PSD models with constant and concentration dependent surface diffusivity were equally good.

Recommendations

It is explicit from this study, that the PSD model is quite efficient in predicting batch adsorption process at all concentration levels. However, there is a slight degree of variation in the values of surface diffusivity coefficients with time. This needs to be accounted for by taking into consideration the surface energetic heterogeneity in the diffusion of adsorbed species. The Darken's relation, based on chemical potential gradient does not account for concentration dependence completely. This necessitates the need to investigate more fundamentally the dependence of surface diffusion coefficient on concentration and to contrive a more efficient correlation to account for it.

2.6 Literature Cited :

- (1) Alben, K. T., Shpirt, E., and Kaczmarczyc, J.H., "Temperature Dependence of Trihalomethane Adsorption on Activated Carbon : Implications for systems with seasonal variations in Temperature and Concentration", Water Sew. Works 125, 6, 1978.
- (2) Abuzaid, N.F. " Effect of Dissolved Oxygen on Activated Carbon Uptake" Ph.D. Dissertation. Civil Engineering Department, King Fahd University of Petroleum & Minerals, Saudi Arabia, 1993.
- (3) Al-Duri, B., and McKay, G., "Predictions of Binary System for Kinetics of Batch Adsorption using basic Dyes onto Activated Carbon", Chem. Eng. Sci., 46, 193, 1991.
- (4) Alhert, R.C and Gorgol, J.F., "Competitive Adsorption by Component of Landfill Leachate", Environ. Prog. 21, 1983.
- (5) Chen, Y.D., and Yang, R.T., "Concentration dependence of surface diffusion and zeolitic diffusion", AIChEJ, 37(10), 1579-1582, 1991.
- (6) Chatzopoulos, D., Varma, A., and Irvine R.I., "Activated Carbon Adsorption and Desorption of Toluene in the Aqueous Phase", AIChEJ., 39(12), 2027, 1993.
- (7) Cooney, D.O. and Xi, Z.P, "Activated Carbon can Catalyze Reactions of Phenolics during Liquid phase Adsorption", pub. in First Separation Division Topical Conference on Separation Technologies : New Developments and Opportunities,. AIChE Annual Conference, 415-418, 1992.
- (8) Crittenden, J. C., and Weber, W.J., Jr., "Predictive Model for design of Fixed - bed Adsorbers : Parameter estimation and Model development", J. Environ. Eng. Div., ASCE, 104(2), 185-197, 1978.

(9) Do, D.D, Jordi, R.G. and Ruthven, D.M., "Sorption Kinetics in Zeolite Crystals with Finite Intracrystal Mass Exchange : Isothermal Systems", J. Chem. Soc. Farad. Trans., 88(1), 121-131, 1992

(10). Edeskuty, F.J. and Amundson, N.R., "Mathematics for adsorption. for effects of intraparticle diffusion in agitated static systems", J. Phys. Chem. 56, 148, 1952.

(11) Famularo, J., Mueller, J. A., and Pannu, A. S., "Prediction of Carbon Column Performance from Pure - Solute Data", J. Water Pollut. Control Fed., 52, 2019, 1980

(12). Fritz, W., and Schluender, E.U., "Simultaneous adsorption equilibria of organic solutes in dilute aqueous solutions on activated carbon", Chem. Eng. Sci., 29, 1279, 1974.

(13). Fritz, W., Merk, W. and Schluender, E.U., "Competitive adsorption of two dissolved organics onto activated carbon -II. Adsorption kinetics in batch reactors", Chem. Eng. Sci. 36, 731, 1981.

(14) Garg, D.R. and Ruthven, D.M., "The effect of concentration dependence on zeolite sorption curves", Chem. Eng. Sci. 27, 417, 1972.

(15) Garten, V.A., Weiss, D.E, and Willis, J.B., Australian J. Chem., 10, 295, 1957.

(16). Gilliland, E.R., Baddour, R.F., Perkinson, G.P., and Sladek, K.J., "Diffusion on surfaces : I. Effect of concentration on the diffusivity of physically adsorbed gases", Ind. Eng. Chem. Fundam., 13, 95, 1974.

(17) Gordon, M. and Murad, J.B., "Adsorption of pollutants from wastewater onto activated carbon based on external mass transfer and pore diffusion", Wat. Res. 22(3),279, 1988.

(18) Goto, M., Goto, S., and Hayashi, N., "Adsorption and Desorption of Phenol on Anion-Exchange Resin and Activated Carbon", *Environ. Sci. Tech.*, 20, 463, 1986.

(19) Gutsche, R. and Yoshida, H., "Solid diffusion in the pores of cellulose membrane", *Chem. Eng. Sci.*, 49, 179, 1994.

(20) Hand, D.W., Crittenden, J.C., and Thacker, W.E., "Simplified models for design of fixed bed adsorption systems", *J. Environ. Eng.*, 110(2), 110, 1984.

(21) Higashi, K., Ito, H. and Oishi, J., "Surface diffusion phenomena in gaseous diffusion : I Surface diffusion of pure gas", *J. Atomic Energy Society Japan*, 5, 1963.

(22) Hu, X., Rao, G.N., and Do, D.D., "Effect of Energy Distribution on sorption kinetics in bidispersed particles", *AIChEJ*, 39, 249-261, 1993a.

(23) Hu, X., Rao, G.N., and Do, D.D., "A mathematical model for multicomponent adsorption, desorption and displacement kinetics of ethane, propane and n-butane on activated carbon", *Gas Sep. and Purification*, 7(4), 197-206, 1993b.

(24) Hu, X., Rao, G.N., and Do, D.D., "Experimental Concentration Dependence of surface diffusivity of Hydrocarbons in Activated Carbon", *Chem. Eng. Sci.* 49, 13, 1994.

(25). Itaya, A., Fujita, Y., Kato, N., and Okamoto, K., "Surface diffusion coefficient in aqueous phase adsorption on macroreticular adsorbents", *J. Chem. Eng. Japan*, 20, 638, 1987.

(26) Kapoor, A., Yang, R. T., and Wang, C., "Surface Diffusion", *Catal. Rev. Sci. Eng.*, 31, 129, 1989.

(27) Komiyama, H. and Smith, J. M., "Surface diffusion in liquid filled pores", *AIChEJ*, 20, 1110, 1974.

(28) Leyva-Ramos, R., "Surface Diffusion in Liquid - Filled Pores of Activated Carbon", Ph.D. Thesis, Ohio State University, Columbus, Ohio 1981.

(29) Leyva-Ramos, R. and Geankoplis C.J., "Diffusion in Liquid - Filled Pores of Activated Carbon. I. Pore Volume Diffusion", Can. Jour. Chem. Eng., 72,262-271,1994

(30) Liu, K. T., and Weber, W.J., Jr., "Characterization of mass transfer parameters for adsorber modeling and design", J. Wat. Pollut. Control Fed. 53, 1541, 1981.

(31) Magne, P., and Walker, P. Jr , "Phenol adsorption on activated carbon: Application to the regeneration of activated carbons polluted with Phenol",. Carbon 24,101, 1986

(32) Maqsood, R. and Benedek, A., "Low-Temperature Organic Removal and Denitrification in Activated Carbon Columns", Jour. Water Poll. Control Fed., 49, 2107, 1977.

(33). Mathews, A. P., and Zayas, I., "Particle Size And Shape Effects On Adsorption Rate Parameters.", J. Environ. Eng., 115,1, 1989.

(34) Mathews, A.P., and Weber, W.J., "Effect of external mass transfer and intraparticle diffusion on adsorption in slurry reactors", Symposium Series, AIChE, 73, 1977.

(35) Mathews, A.P., and Su, C.A., "Prediction of Competitive Adsorption Kinetics for Two Priority Pollutants", Environ. Prog., 2(4),257-261, 1983.

(36). Neretnieks, I., "Analysis of some Adsorption Experiments with Activated Carbon", Chem. Eng. Sci., 31, 1029, 1976

(37) Puri, B.R., "Carbon adsorption of Pure Compounds and Mixtures from Solution Phase. In Activated Carbon Adsorption of Organics from the

Aqueous Phase"; Suffet, I.H., McGuire, M.J., Eds.; Ann Arbor Science : Ann Arbor M.I., 1980.

(38) Randtke, S. J., and Snoeyink, V. L., "Evaluating GAC Adsorptive Capacity", J. Am. Water Works Assoc., 78(8), 406, 1983.

(39) Reid, R.C., Prausnitz, J.M., and Sherwood T.K., Properties of Gases and Liquids, 3rd edition, McGraw Hill, 1977.

(40). Rosen, J.B. "Kinetics Of A Fixed Bed System For Solid Diffusion Into Spherical Particles", J. Chem. Phys., 20., 377, 1952.

(41) Ruthven, D.M., Principles of Adsorption and Adsorption Processes, Wiley, New York, 1984

(42) Satterfield, C.N., Heterogeneous Catalysis In Industrial Practice., 2ed., McGraw Hill, pp122, 1991.

(43) Seidel, A. and Carl, P. S, "The concentration dependence of surface diffusion for adsorption on energetically heterogeneous adsorbents", Chem. Eng. Sci., 44(1), 189-194, 1989.

(44) Seidel, A. and Gelbin,.D., "Breakthrough Curves for single solutes in beds of Activated Carbon with a broad pore size distribution -I. Mathematical models of breakthrough curves in beds of Activated Carbon", Chem. Eng. Sci. 41, 3, 541, 1986.

(45) Seidel, A. and Gelbin, D., "Breakthrough curves for single solutes in beds of activated carbon with a broad pore- size distribution - II. Measuring and calculating breakthrough curves in of Phenol and Indole from aqueous solutions on activated carbon", Chem. Engng. Sci., 41, 549 ,1986

(46) Shibuya, A. and Kawazoe, K., "Diffusion of Heavy Water in Commercial Adsorbent Particles", J. Chem. Eng. Japan , 11, 1978.

(47) Sladek, K. J., Gilliland, E.-R., and Baddour, R.F., "Diffusion on Surfaces II. Correlation of diffusivities of physically and chemically adsorbed species", *Ind. Eng. Chem. Fundam.*, 13, 100, 1974.

(48) Snoeyink, V. L., Lai, H. T., Johnson, J. H., and Young J. F., "Active Carbon : Dechlorination and Adsorption of Organic compounds", *Chemistry of Water Supply Treatment and Distribution*, A. J., Rubin, ed; 232, Ann Arbor Science Publishers, Ann Arbor, Mich., 1974.

(49) Studebaker, M. L, Huffman, K. W. D., Wolfe, A.C., and Nabors, L.G.; *Ind. Eng. Chem.* 48, 162, 1956.

(50) Sudo, Y., Misic, D. and Suzuki, M. "Concentration dependence of effective surface diffusion coefficient in aqueous phase adsorption on activated carbon", *Chem. Eng. Sci.* 33, 1287, 1978

(51) Suzuki, M., Kawazoe, K.J., *Chem. Eng. Jpn.*, 8, 1975.

(52) Suzuki, M., *Adsorption Engineering*, Elsevier, Amsterdam, 9, 1990.

(53) Traegner, U.K., and Suidan, M.T., "Parameter Evaluation for Carbon Adsorption ", *J. Environ. Eng. ASCE*, 1, 109-128, 1989.

(54) Vidic, R.D., Suidan, M.T., "Selecting Batch Studies for Adsorber Design : Molecular Oxygen's Role", *Jour. AWWA*, 84(3), 101-109, 1992.

(55) Vidic, R.D., Suidan, M.T., and Brenner, R.C., "Impact of Oxygen Mediated Oxidative Coupling on Adsorption kinetics ", *Wat. Res.* 28(2), 263-268, 1994

(56) Weber, T.W. and Chakrovorti, R.K., "Pore and solid diffusion models for fixed bed adsorbers", *AIChEJ*, 20, 228, 1974.

(57) Weber, W.J., Jr., and Morris, J.C., "Equilibria and Capacities for adsorption on Carbon", *J. San. Engng. ASCE*, EE2, 185-197, 1964.

(58). Wilmanski, K., and Lipinski, K., "Adsorption Kinetics in GAC. systems for water treatment", *J. Environ. Eng.*, 115(1), 91-107, 1989.

(59) Yang, R.T., Fenn, J.B and Haller, G.L., "Modification to the Higashi model for surface diffusion", AIChE. J., 19(5), 1052-1053, 1973.

(60) Yonge, D.R., Keinath, T.M., Poznanska, K., Jiang, Z.P., "Single - Solute Irreversible Adsorption on Granular Activated Carbon", Environ. Sci. Technol., 19, 690, 1985

2.7 Nomenclature

a	constant in Myer's isotherm.
A_i	Virial coefficients.
B	equilibrium parameter.
C_o	initial liquid phase concentration
C_{p0}, \bar{C}_p, C_p	initial, dimensionless, and fluid pore concentrations
C_s	concentration at surface of the particle
C_∞	fluid phase equilibrium concentration
$C(t)$	fluid phase concentration as function of time.
$\bar{C}(\tau)$	dimensionless fluid phase concentration as function of dimensionless time.
C_{o_2}	fluid phase concentration of oxygen as a function of time.
$C_{o_2,0}$	initial fluid phase concentration of oxygen
$C_{o_2,\infty}$	fluid phase concentration of oxygen at equilibrium
D_{eff}	effective diffusivity coefficient
$D_{e,p}$	effective pore volume diffusivity coefficient
D_p	pore volume diffusivity coefficient
D_{AB}	mutual diffusion coefficient of solute A in a dilute concentration of solvent B
D_{so}	surface diffusivity at zero adsorbate loading,

D_s	surface diffusivity coefficient
D_{s0}^*	preexponential term in surface diffusivity coefficient temperature dependence expression
k_{LF}, K_i	Langmuir Freundlich isotherm constant, other isotherm constants
k	mass transfer coefficient
M_B	molecular weight of solvent B
M_t	total amount of adsorbate which diffuses from the bulk phase into the carbon particle at any time, t
M_∞	mass adsorbed at infinite time
n	Langmuir Freundlich isotherm constant
N	adsorbate flux into the particle,
q_{os}	adsorbate phase concentration in equilibrium with the initial fluid phase concentration ,
\bar{q}_∞	average adsorbate concentration at infinite time
$q(r, t)$	adsorbent phase concentration as a function of radial position and time
$\bar{q}(t)$	average adsorbate concentration on the particle as a time, t
$\bar{Q}(\tau)$	dimensionless average adsorbate concentration as a function of dimensionless time, $\bar{q}(t)/q_{os}$
$Q(\eta, \tau)$	dimensionless adsorbent phase concentration, $q(r, t)/q_{os}$
r	radial coordinate,
r_s	particle radius,
T	absolute temperature, K
t	time

u	uptake of adsorbent
V_A	molal volume
V_p	total volume of the particle
W_s	mass of the carbon particle

Greek alphabet

α	solute distribution parameter(dimensionless), $W_{q_{as}}/VC_o$,
ε_p	porosity of the particles
ρ_p	density of particle
η	dimensionless radius
η_B	viscosity of solvent B, cp
θ	loading, $\frac{q}{q_s}$
λ	loading, $\frac{q_o}{q_s}$
τ	dimensionless time
τ_p	tortuosity factor.

CHAPTER THREE

DIFFUSION AND REACTION IN BATCH SYSTEMS

3.1 Introduction

Activated carbons are known to have surface oxides groups (or oxygen complexes). These can arise from chemical adsorption of air or pure oxygen (oxidation) during the activation stage or during storage after activation. Also, the surface oxides can be produced by oxidation of carbon samples with aqueous solutions of oxidizing agents (Studebaker et al., 1956; Garten et al., 1957).

The oxide groups present on the surface of the GAC alters its adsorption characteristics and capacity. These oxides groups are directly responsible for the oxidative coupling reactions that occur on the surface of the GAC and are presumably catalyzed by it. The concentration of these oxides or else the degree of oxidation of the GAC is a determining factor of the magnitude of the reaction rate. The degree of oxidation, of course is directly related to the concentration of oxygen or oxidizing agent employed in the activation stage.

3.2 Literature Survey

The oxygen chemisorbed on carbon exists mainly in the form of four different acidic surface groups. These are :

- (i) strong carboxylic groups,
- (ii) weak carboxylic groups which exist as lactone groups

combined with the neighboring carbonyl groups,

- (iii) phenolic groups ,
- (iv) carbonyl groups which form lactone groups with carboxyl groups of type (ii) (Boehim et al., 1964).

Surface oxide groups can be removed by heat treatment of carbons in an inert atmosphere or under vacuum. The sorption characteristics and capacity of activated carbon is influenced by the surface functionality. Two different approaches have been followed in evaluating the influence of these surface oxide groups. The direction and magnitude of this influence with respect to the adsorption of phenol is directly dependent on the approach adopted. Past researchers oxidized the carbon prior to the adsorption process using various oxidizing agents, whereas recent researchers conducted the adsorption and oxidation processes simultaneously.

Coughlin (1970) reported that the oxidation of activated carbon by potassium permanganate solution increases the acidic oxides concentration on the surface. This lowered both the capacity and the rate of sorption of phenol. Snoeyink et al. (1974) found that oxidation with aqueous chlorine increased the acidic oxides concentration on activated carbon. This resulted in a decrease in sorption capacity for phenol and nitrophenol by about 50%. Subsequent to these findings, Prober et al. (1975) reported that sorption of nonpolar species should be impaired as a result of increasing surface oxides. Prober et al. further asserted that since carbon sorption of oxygen invariably increases the surface acidic oxides, a decrease in the sorption capacity for phenol is inevitable. However, his investigation showed that this decrease is

negligible in view of the small oxygen demand which would be exerted by activated carbon at normal dosages for wastewater treatment. Magne and Walker (1986), showed that chemisorption of oxygen on activated carbon at 573K prior to phenol adsorption reduces the initial capacity of the carbon for the retention of phenol.

Recent researchers ushered in an incisively different approach. The findings of previous researchers are diametrically opposed to that of the present ones. The formation of the surface oxides due to oxidation with dissolved oxygen is seen to have auspicious effects on phenolic adsorption by GAC. Vidic et al., (1990), investigated the influence of molecular oxygen on the adsorptive capacity of GAC. Their results showed a considerable increase in the GAC adsorptive capacity for various compounds under aerobic conditions. The adsorptive uptake of GAC under aerobic conditions increases for o-cresol by 22- 200% over that attainable under anaerobic conditions. The same trend was observed for 3- ethylphenol (18-92% increase) and phenol (42-85% increase). This increase was attributed to the chemical reaction between the adsorbed phenol and the oxygen adsorbed on the surface of the carbon. This reaction was presumably catalyzed by the carbon surface. The reaction occurs on a different (slower) time scale from physical adsorption. Similar results were reported by Vidic and Suidan (1992).

The work of Grant and King (1990) also showed that dissolved oxygen increases the adsorptive capacity of GAC. Their experiments showed that oxidative coupling of phenolic compounds on carbon surfaces was plausibly responsible for irreversible adsorption. The irreversible adsorption

on the carbon surface has been attributed to chemical reaction of sorbate molecules with oxygenated surface functional groups (Mattson et al.,1969; Modell et al.,1980; Puri , 1980; Chang et al., 1981; Yonge et al.,1985). This was supported by Grant and King (1990). Furthermore, Grant and King discovered that the presence of oxygen increases the total and irreversible adsorptive uptake of phenol by GAC. Their results showed that the chemical reaction is very slow compared to physisorption, and hence was rate limiting.

Cooney and Xi (1992) examined the kinetics of activated carbon catalyzed oxidative coupling reactions of phenolic compounds. They observed that after the initial rapid adsorption process had occurred, there was a slow but steady decline in solution concentration over a period of many days and weeks. They attributed these slow changes to oxidative coupling reactions. These reactions occurring on the carbon surface produces strongly adsorbed polymeric products. The coupling reactions reduces the phenol concentration creating free sites for phenol to be transferred from the solution. They concluded that although oxidative coupling reactions can occur in the absence of dissolved oxygen, its presence markedly accelerated them.

Abuzaid and Nakhla (1994) studied the effect of dissolved oxygen on activated carbon uptake. The influence of different dissolved oxygen levels at various temperatures and pHs were examined. Their results supported those of Vidic et al., Grant and King; and Cooney and Xi. The dissolved oxygen level definitely increases the adsorptive capacity of GAC. The uptake for phenol, o-cresol, and nitrophenol at 1mg/l under aerobic

conditions were respectively 163%, 114%, and 18% higher than the anaerobic uptakes. The increase in the GAC uptake was in direct proportion to the dissolved oxygen level. At constant temperature and pressure for a given adsorbate-adsorbent system, the increase in adsorption capacity was solely dependent on the mass of GAC and mass of dissolved oxygen. The increase in GAC uptake was shown to be the result of oxidative coupling reactions primarily occurring on the surface of the carbon. The reactions which are catalyzed by the carbon surface takes place plausibly between the physisorbed sorbate and chemisorbed oxygen molecules. The products of the oxidative coupling reactions were identified as 2,2-dihydroxy-1, 1'-biphenyl, 4-phenoxyphenol and a phenolic trimer.

Vidic and Suidan (1994) studied the impact of oxygen mediated oxidative coupling on adsorption kinetics of 2-methylphenol. They observed that for the initial phase of 12 hr., the aqueous phase concentration of the 2-methylphenol in anoxic bath rapidly reach equilibrium level, while it took almost 12 days in the oxic bath. It was noted that for the first 12 hr., the time dependent concentration profile of both the oxic and anoxic baths were indistinguishable. The adsorption capacity was clearly higher for the oxic case. Their attempt to evaluate the effect of GAC particle size on adsorption capacity was reportedly fruitless.

Grant and King (1990) found that the carbon surface catalyzed oxidative coupling reactions increases with temperature. Hence higher temperatures corresponds to higher GAC adsorption capacity. Also, the coupling reactions were promoted by high pH. and temperature.

Cooney and Xi (1992) studied the effect of pH on the adsorptive capacity of GAC in the presence of dissolved oxygen. They showed that at pH 2 and pH 7, the initial amount adsorbed was the same. At these pH values, phenol with a pka value of 9.99 was essentially 100% undissociated. At pH 12, however, the phenol totally dissociated. It is a known fact that ionized forms of species adsorb far less on activated carbon than do their undissociated forms. Thus, the initial amount of adsorbed phenol was less at pH 12 than at pH 7. However, the oxidative coupling reactions were reportedly promoted by high pH. At pH 2 the reactions were minimal. The reaction rate at pH 12 was faster than at pH 7. The pH of the solution and not the degree of dissociation is the important determinant of the reaction.

Abuzaid (1993) contended that the net effect of the pH and temperature on activated carbon adsorption is a combination of their influence on both physical adsorption and the coupling reactions. Physical adsorption was favored at 3, while the highest sorbate uptake occurred at pH 11. He quoted pH 7 as the optimum value for adsorption of phenolics by activated carbon under aerobic conditions. He observed that anaerobic adsorption of phenol and o-cresol increased with decreasing temperature and was highest at the lowest temperature studied (8C). The promotion of adsorption by the oxidative coupling reactions was greatest at 35C. The aerobic isotherms showed little dependence on temperature. This suggests that the positive and adverse influence of temperature on chemical reactions and physical adsorption respectively annuls each other.

3.3 Theoretical Model

The pore and surface diffusion model with concentration dependent surface diffusivity coefficient was used. The general assumptions made in formulating the model have been presented in chapter two of this work. The Darken's relation was used to account for the concentration dependence of diffusivity. This model can easily be converted to the homogenous surface diffusion model by setting the pore diffusion coefficient to zero.

The Darken's relation yields the following expression for the surface diffusivity coefficient.

$$D_s = D_{so} \frac{d \ln C_p}{d \ln q} \quad 3.1$$

The three possible ways of defining the reaction term, R are :

- (I) zero order in adsorbate, and proportional to the oxygen imbalance,
- (ii) first order in adsorbate, and proportional to the oxygen imbalance,
- (iii) m th order in adsorbate, and proportional to the oxygen imbalance to the n' order.

The general pore and surface diffusion model with reaction term added becomes :

$$\left[\frac{\epsilon}{\rho_p} \frac{\partial C_p}{\partial q} + 1 \right] \frac{\partial q}{\partial t} = \frac{1}{r} \frac{\partial}{\partial r} \left\{ r^2 \left[D_p \frac{\epsilon}{\rho_p} \frac{\partial C_p}{\partial q} + D_{so} \frac{d \ln C_p}{d \ln q} \right] \frac{\partial q}{\partial r} \right\} - R \quad 3.2$$

$$\text{As } \frac{\varepsilon}{\rho_p} \frac{\partial C_p}{\partial q} \ll$$

this term may be neglected since it is much less than one. The adsorption - reaction equation reduces to

$$\frac{\partial q}{\partial t} = \frac{1}{r} \frac{\partial}{\partial r} \left\{ r^2 \left[D_p \frac{\varepsilon}{\rho_p} \frac{\partial C_p}{\partial q} + D_{so} \frac{d \ln C_p}{d \ln q} \right] \frac{\partial q}{\partial r} \right\} - R \quad 3.3$$

where the first term on the right hand side is the pore diffusion term, the second term is the concentration dependent surface diffusivity term, and the third term, R is the reaction term. The reaction term R is defined as :

$$R = k_{o_2} k_{phe} q^m (q_{o_2} - q_{o_2, \infty})^{n'} \quad 3.4$$

where m and n' can take any value depending on the best fit of the experimental data.

Therefore the general adsorption - reaction equation becomes :

$$\frac{\partial q}{\partial t} = \frac{1}{r} \frac{\partial}{\partial r} \left\{ r^2 \left[\frac{D_p \varepsilon}{\rho_p} \frac{\partial C_p}{\partial q} + D_{so} \frac{d \ln C_p}{d \ln q} \right] \frac{\partial q}{\partial r} \right\} - k_{o_2} k_{phe} q^m (q_{o_2} - q_{o_2, \infty})^{n'} \quad 3.5$$

The initial conditions are clean adsorbent and the boundary conditions are those for a finite bath subject to nonlinear Langmuir - Freundlich adsorption .

Langmuir -Freundlich adsorption isotherm.

The Langmuir - Freundlich adsorption isotherm is :

$$\frac{q}{q_s} = \frac{k_{LF} C^{1/n}}{1 + k_{LF} C^{1/n}} \quad 3.6$$

Defining the following dimensionless groups:

$$\tau = \frac{D_{so} t}{r_s^2}; \eta = \frac{r}{r_s}; Q = \frac{q}{q_{os}}; \lambda = \frac{q_{os}}{q} = \frac{k_{LF} C_o^{1/n}}{1 + k_{LF} C_o^{1/n}}; X = \frac{\varepsilon n D_p}{\rho_p k_{LF}^n q_s D_{so}};$$

$$K = \Phi^2 \left(\frac{r_s^2}{D_{so}} \right)^{-n} (C_{o_2,0} - C_{o_2,\infty}) q_{os}^{m-1} H k'; \Phi = \sqrt{\frac{r_s^2 k_{o_2} k_{phe}}{D_{so}}}$$

The surface diffusivity and isotherm gradient in dimensionless form based on the Langmuir-Freundlich adsorption isotherm become:

$$D_s = D_{so} \frac{d \ln C_p}{d \ln q} = D_{so} \frac{n}{(1 - Q\lambda)}; \frac{\partial C_p}{\partial q} = \frac{n}{k_{LF}^n q_s} \frac{(Q\lambda)^{n-1}}{(1 - Q\lambda)^{n+1}} \quad 3.7$$

Assuming the bulk phase concentration of oxygen is linearly related to the adsorbed phase concentration, we have

$$q_{o_2} = H C_{o_2} \quad 3.8$$

Then :

$$\frac{q_{o_2} - q_{o_2,\infty}}{q_{o_2,0} - q_{o_2,\infty}} = \frac{C_{o_2} - C_{o_2,\infty}}{C_{o_2,0} - C_{o_2,\infty}} \quad 3.9$$

The data of Suidan and Vidic for oxygen in the reactor when plotted logarithmically versus time gave a straight line having the following relationship.

$$\frac{q_{o_2} - q_{o_2,\infty}}{q_{o_2,0} - q_{o_2,\infty}} = \frac{C_{o_2} - C_{o_2,\infty}}{C_{o_2,0} - C_{o_2,\infty}} = k' t^{-n''} \quad 3.10$$

where $-n''$ is the slope of the log - log plot of $\frac{C_{o_2} - C_{o_2,\infty}}{C_{o_2,0} - C_{o_2,\infty}}$ versus

time and the natural logarithm of k' is the abscissa intercept. Therefore we conclude that

$$q_{o_2} - q_{o_2,\infty} = H(C_{o_2,0} - C_{o_2,\infty}) k' t^{-n''} \quad 3.11$$

and R becomes

$$R = \left(\frac{r_s^2}{D_{so}} \right) k_{o_2} k_{phe} q_{os}^{m-1} Q^m \left[H(C_{o_2,0} - C_{o_2,\infty}) k' \left(\frac{r_s^2}{D_{so}} \right)^{-n''} \tau^{-n''} \right]^{n'} \quad 3.12$$

In this work, the value of n' was assumed to be one. The reaction term can be rearranged into the following :

$$R = \left(\frac{r_s^2}{D_{so}} \right) \left(\frac{r_s^2}{D_{so}} \right)^{-n''} (C_{o_2,0} - C_{o_2,\infty}) k_{o_2} k_{phe} q_{os}^{m-1} Q^m H k' \tau^{-n''} \quad 3.13$$

In dimensionless form the reaction term becomes :

$$R = \left(\frac{r_s^2}{D_{so}} \right) \left(\frac{r_s^2}{D_{so}} \right)^{-n''} (C_{o_2,0} - C_{o_2,\infty}) q_{os}^{m-1} Q^m k' k_{o_2} k_{phe} H \tau^{-n''} \quad 3.14$$

The reaction term simplifies to :

$$R = K Q^m \tau^{-n''} \quad 3.15$$

where K is the combined parameter.

The final adsorption - reaction equation becomes:

$$\frac{\partial Q}{\partial \eta} = \frac{1}{\eta} \frac{\partial}{\partial \eta} \left\{ \eta^2 \left[X \frac{(Q\lambda)^{n-1}}{(1-Q\lambda)^{n+1}} + \frac{n}{(1-Q\lambda)} \right] \frac{\partial Q}{\partial \eta} \right\} - KQ^m \tau^{-n''} \quad 3.16$$

In this work, the value of n is assumed first order due to lack of data to establish the order. The final adsorption -reaction equation (eqn 3.16) was solved for the initial and boundary conditions mentioned above using the Crank-Nicolson finite difference method.

3.4 Results and Discussion

The methodology of the modeling is as follows :

(i) The order of the reaction with respect to the adsorbed adsorbate, m (o-cresol and phenol) concentration was assumed. Specific values of m assumed are 0, 1, 2, and 3; but only 1 and 2 gave reasonable fits.

(ii) The IMSL optimization subroutine, BCPOL was used to obtain the best pair of values of n'' , the slope of the log-log plot of the oxygen imbalance and time; and K , the overall rate constant by minimizing the root mean square (RMS) of the residuals between predicted and experimental concentration values.

(iii) The IMSL optimization subroutine, BCPOL was used to obtain the best sets of values of m , n'' and K . No assumptions was made in this case..

Step (iii) gave the best value of n'' to be 0.6 and the best adsorbate concentration order to be first. Step (ii) also gave the value of n'' to be 0.6 with a variance with temperature. A fixed value of $n'' = 0.6$ was used for the

three different temperatures as this is consistent with the fixed initial oxygen concentration of 8mg / L which was used for all the runs.

The optimization results for K , n and RMS at the three different temperatures are presented in Table 3.1 and the fit of the model to the data is presented in Figures 3.1 to 3.6. Inspection of the root mean square (RMS) values in Table 3.1 reveals that the reaction order for the adsorbate favors first order. However, the differences in RMS values of the first order and second order plots are quite small. Consequently, an additional basis of judgment is needed to truly certify the order of the reaction.

The overall reaction rate constant, K increases with temperature as expected in the case of o-cresol. However, in the case of phenol, the value of K increases for the first two temperatures, (281K and 294K) but dropped at the last temperature (308K). A close scrutiny of the data at 308K, reveals a trend that is not quite the same as the trend observed in the data at 281K and 294K. The anomaly experienced at 308K could be attributed to errors in experimental readings. This point is excluded from the regression.

A plot of the natural logarithm of K versus inverse of temperature gives a straight line and is presented in Figure 3.7. The rate constant varies with temperature as follows:

$$K = K_0 \exp \left(\frac{-E_a}{RT} \right) \quad 3.17$$

Values of K_0 and E_0 are included in Table 3.1. The activation energies are a complex sum of rate, adsorption and diffusion activation energies and range from 322 to 1123 cal/mole.

Table 3.1: Reaction orders and overall constants for batch systems.

Temp	order = 1		order = 2	
K	n'' = 0.60		n'' = 0.60	
	K*E-3	RMS	K*E-3	RMS
Phenol				
281	32.0	.1336	57.0	.1424
294	36.0	.1662	58.0	.1974
308	38.0	.1686	60.0	.1803
	K _o * E - 2 = 1.89		K _o * E - 2 = 81.4	
	E _a = 755(cal / mole)		E _a = 1123(cal / mole)	
o-cresol				
281	48.0	.2904	106.	.3160
294	51.0	.2529	116.	.2789
308	48.0	.2730	90.	.2882
	K _o * E - 2 = 2.30		K _o * E - 2 = 1.02	
	E _a = 1080(cal / mole)		E _a = 322(cal / mole)	

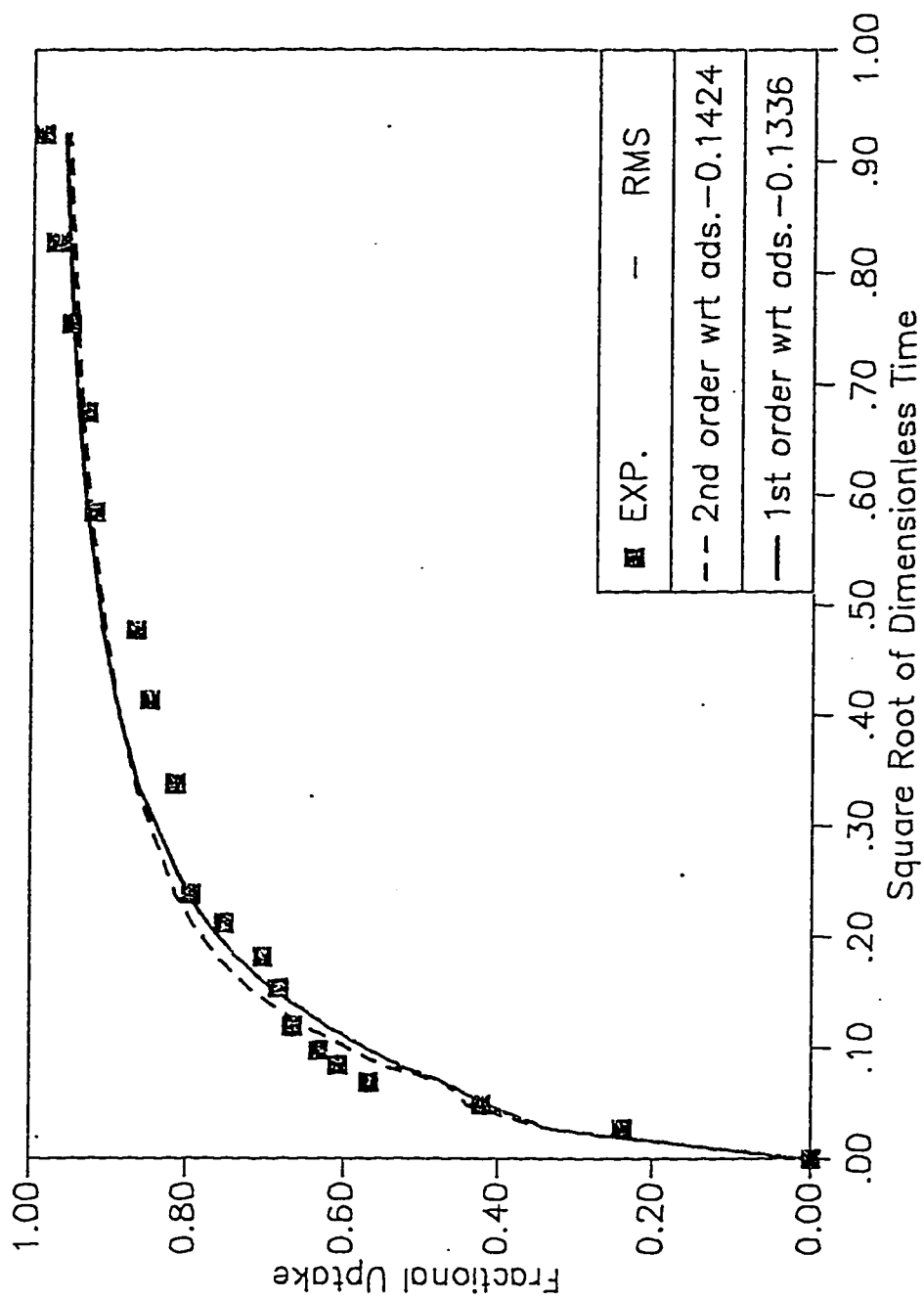


Fig 3.1: Predicted and Experimental Fractional Uptake at 281K. Adsorption with reaction of O-Cresol.

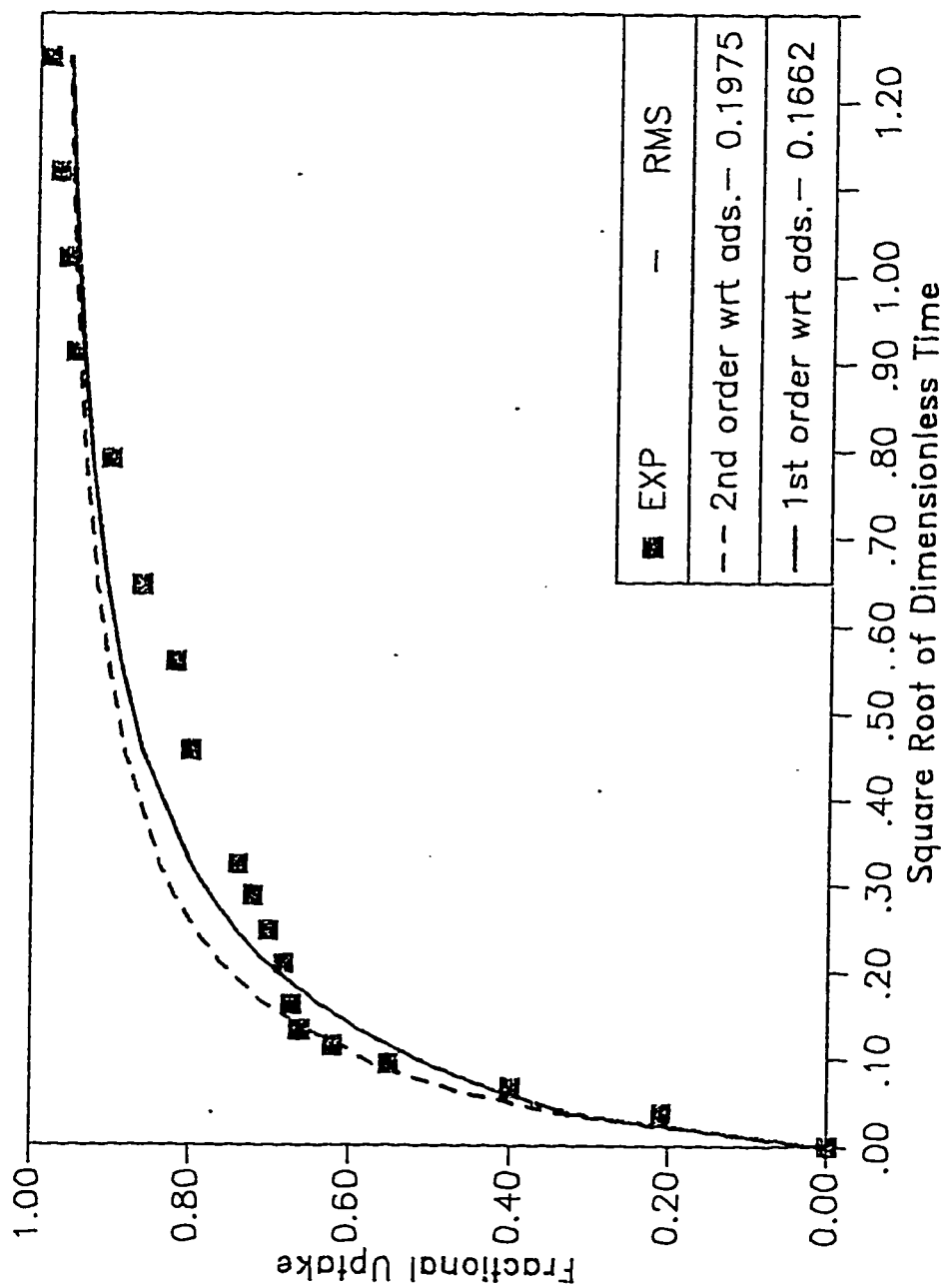


Fig 3.2: Predicted and Experimental Fractional Uptake at 294K. Adsorption with reaction of o-cresol

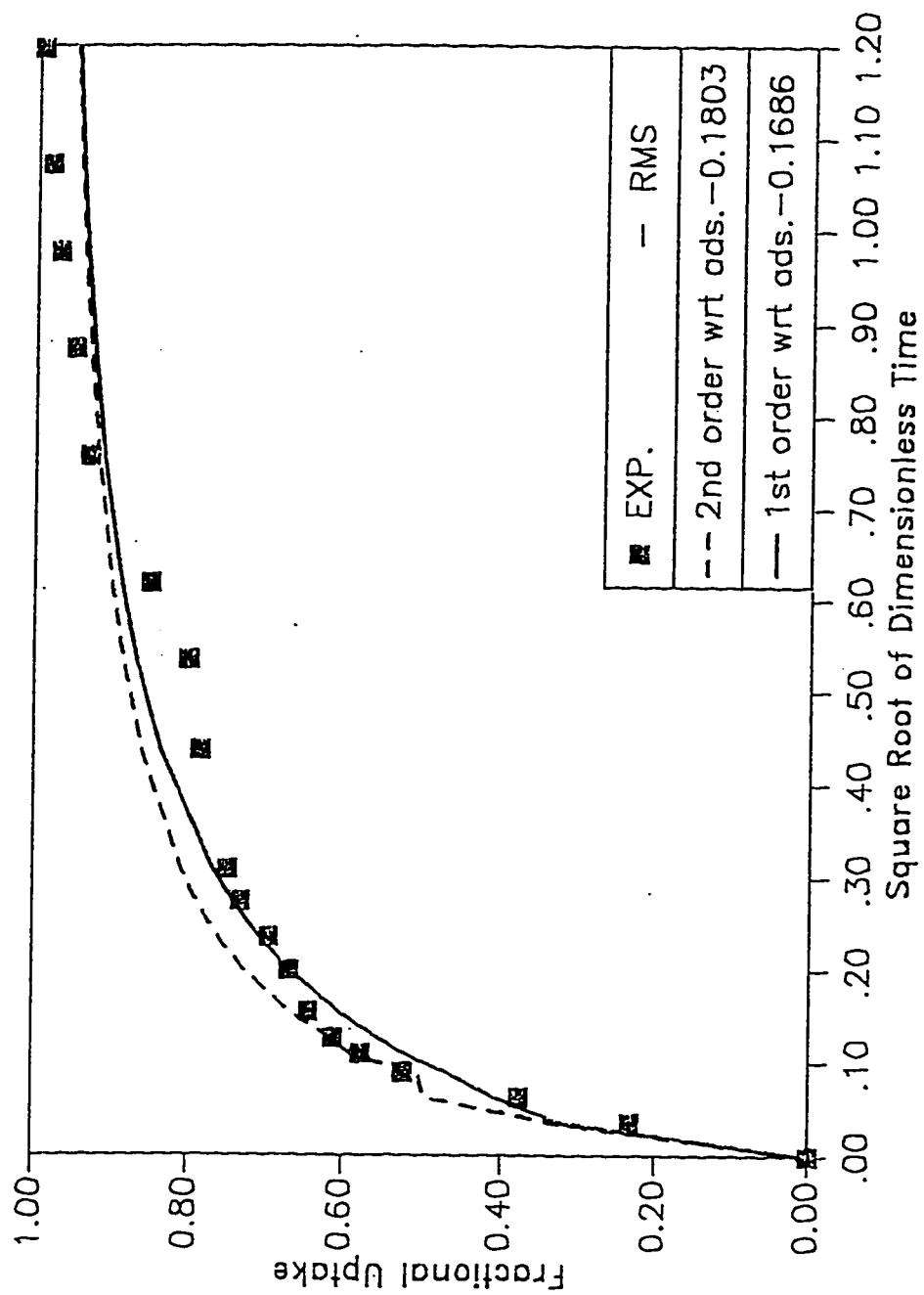


Fig 3.3: Predicted and Experimental Fractional Uptake at 308K. Adsorption with reaction of o-cresol

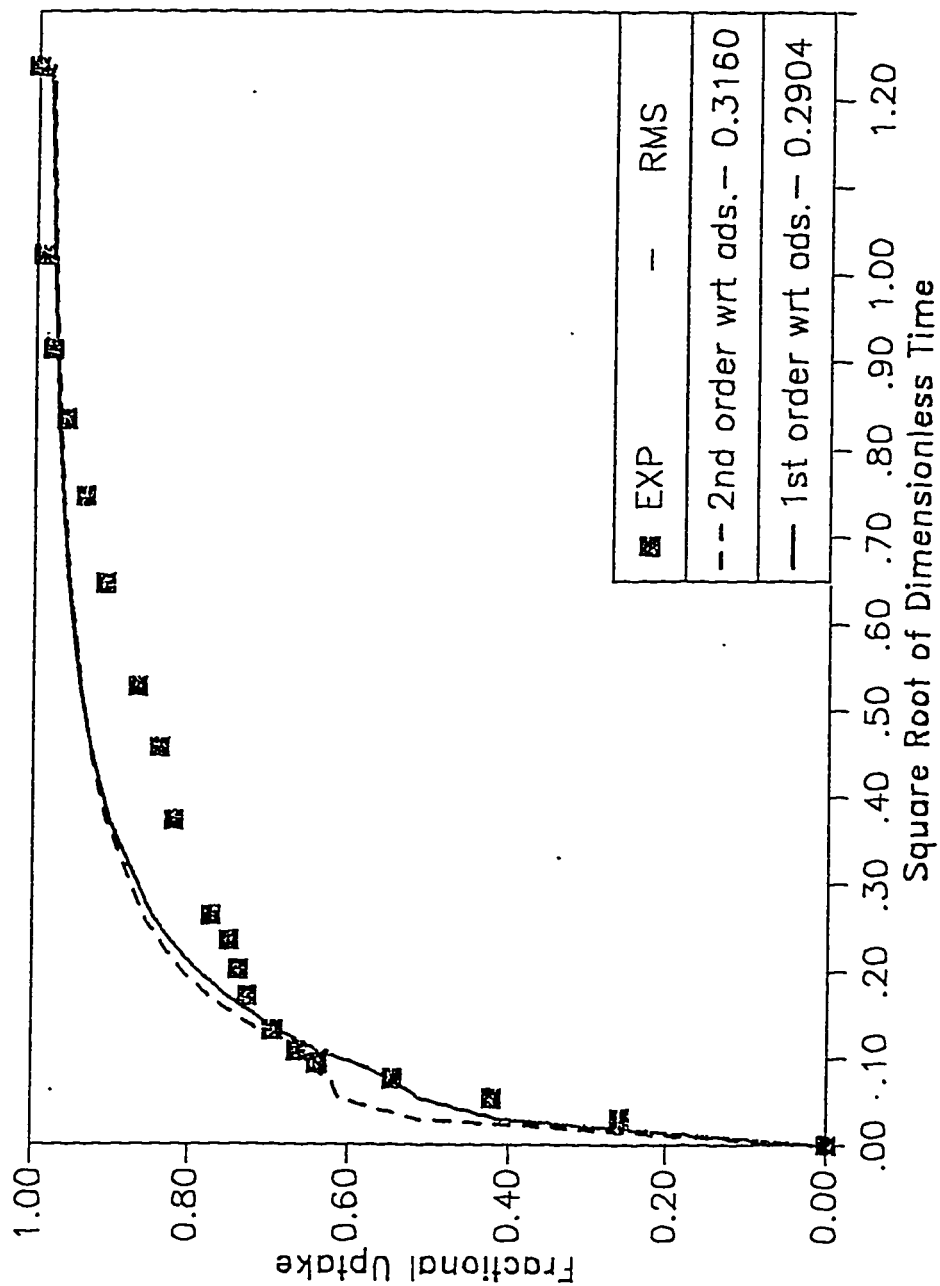


Fig 3.4: Predicted and Experimental Fractional Uptake at 281K. Adsorption with reaction of Phenol.

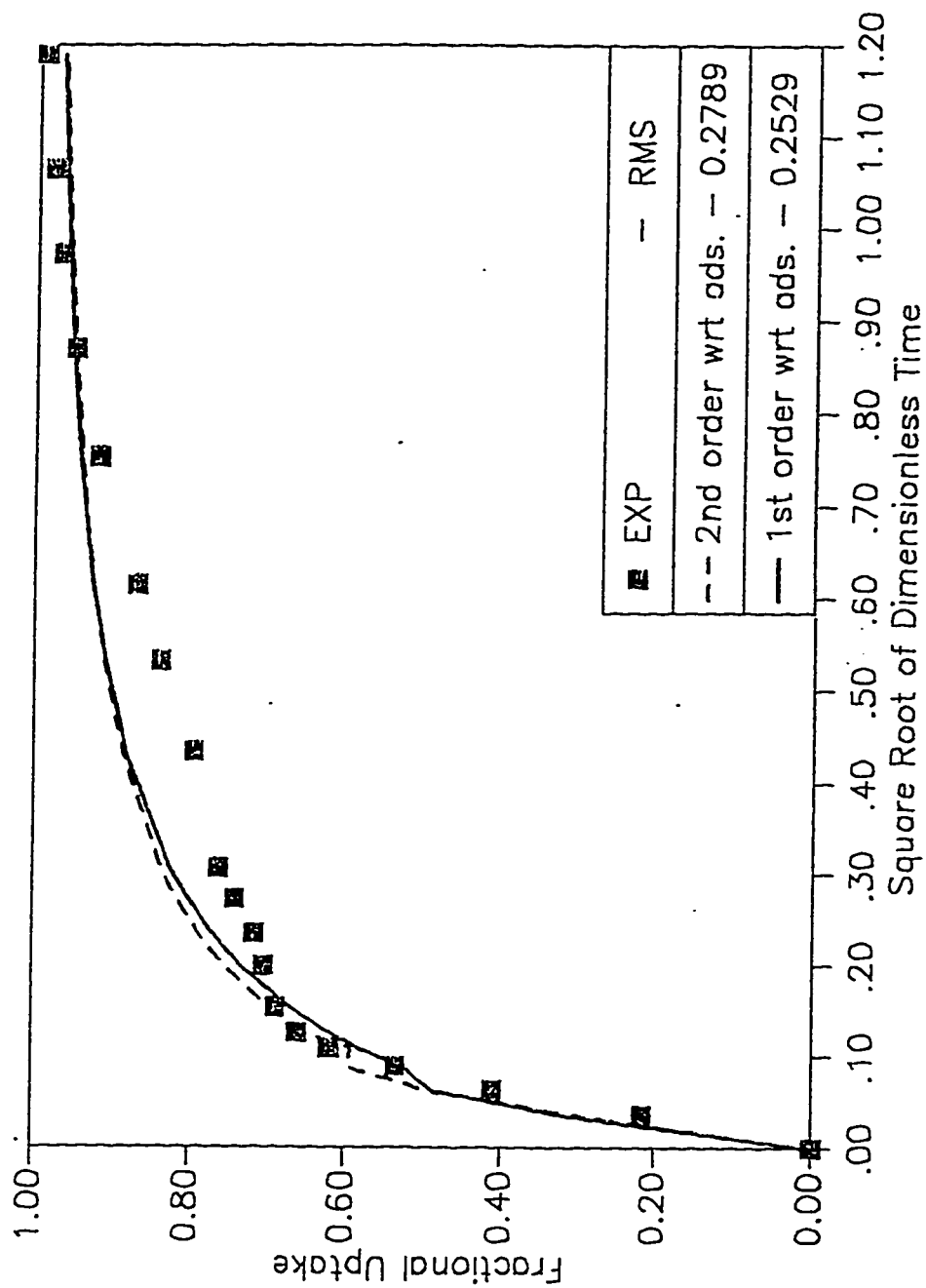


Fig 3.5: Predicted and Experimental Fractional Uptake at 294K. Adsorption with reaction of Phenol.

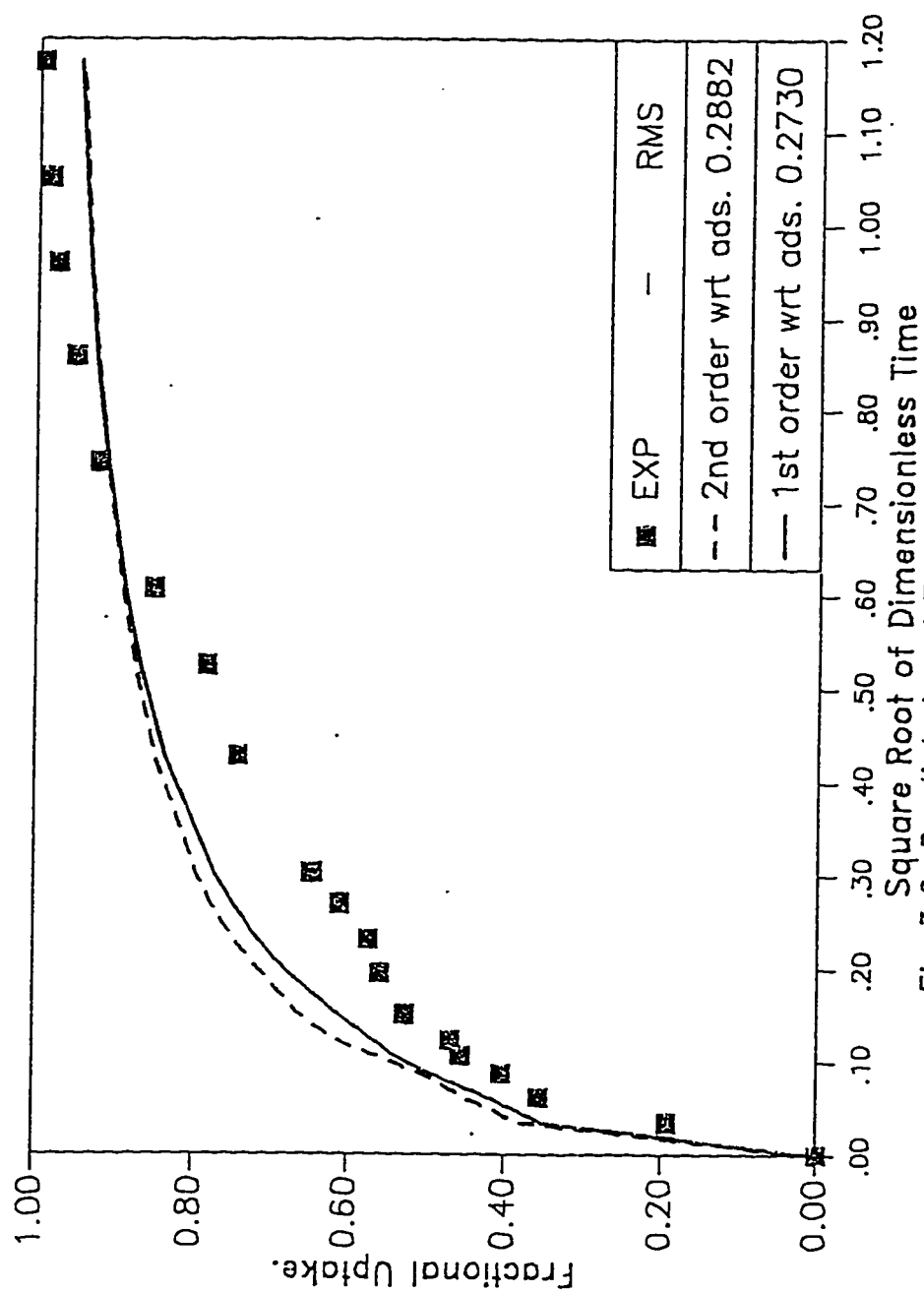


Fig 3.6: Predicted and Experimental Fractional Uptake at 308K. Adsorption of phenol with reaction

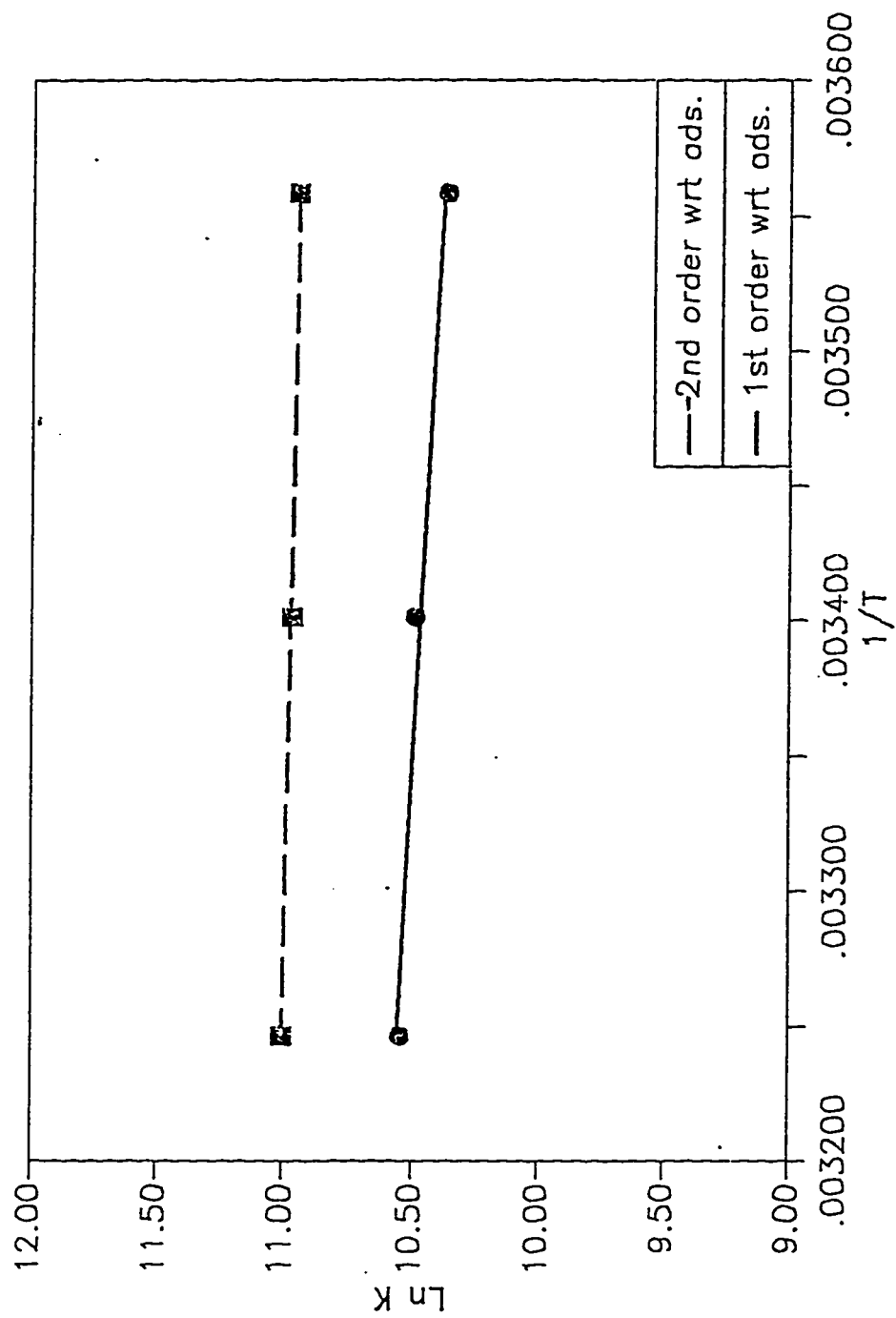


Fig 3.7: Plot of $\ln K$ vs $1/T$
Adsorption with Reaction of o-cresol

The simple empirical form of the reaction rate expression is

$$R = K \frac{Q^m}{\tau^{n^r}} \quad 3.18$$

that is, the reaction rate is proportional to sorbate concentration and inversely proportional to the time of the reaction. It is worth pointing out that the inverse proportionality to time resulted from the oxygen adsorption rate. As reaction progresses, two factors act in opposite directions. Hence, a maximum rate will occur somewhere during the reaction.

On the basis of the understanding gained from this work, the following reaction mechanism may be proposed. The sorbate molecules diffuses to the surface of the GAC and are adsorbed. Similarly, the oxygen molecules diffuses to the surface of the GAC particles and are adsorbed. Reaction of the sorbate molecules and the oxygen molecules occur on the surface of the GAC and are catalyzed by it. (Grant and King, 1990; Abuzaid, 1993).

If the reaction order with respect to the sorbate concentration is assumed to be first, then dissociation of the oxygen molecules occurs before reaction with the sorbate molecules. On the contrary, if the order is second, then the adsorbed oxygen molecules react directly with the sorbate molecules. The adsorption sites are thus occupied by sorbate and oxygen molecules that reacts creating new empty sites. The empty sites allow room for more adsorption. As time progresses, the site gets more occupied, and the reaction and adsorption decrease. From the nature of the reaction products extracted from the GAC (Abuzaid, 1993), we expect some complex interactions among the adsorbed and/or in coming molecules on the surface of the GAC.

3.5 Conclusions and Recommendations

The study presents a simple empirical rate form for predicting the reaction rate of adsorption with reaction of o-cresol and phenol in aqueous media. The reaction rate form was assumed to be m th order in adsorbate, and proportional to the oxygen imbalance to the n order.

The reaction order with respect to oxygen imbalance, n' was assumed to be first. The reaction order with respect to adsorbate concentration, m favor first order. However, the differences in RMS values of the first and second order plots are quite small. The overall rate constants increases with temperature as expected not withstanding the anomaly that was experienced at 308K in case of Phenol. The activation energies are a complex sum of

rate, adsorption and diffusion activation energies and range from 322 to 1123 cal/mole.

This work is not in anyway complete in itself to truly certify the reaction order with respect to adsorbate concentration and the actual mechanism involved in the reaction. Further experimental work is needed in conjunction with this work to ascertain the actual reaction orders and mechanism. Also, it is recommended that a mass transfer equation be written for the diffusion of oxygen and solved in conjunction with that for phenol. This will eliminate the requirement for specifying the reaction rate with a time dependence.

3.8 Literature Survey

(1) Abuzaid, N.F. "Effect of Dissolved Oxygen on Activated Carbon Uptake" PhD Dissertation Civil Engineering Department , King Fahd University of Petroleum & Minerals, Saudi Arabia, 1993.

(2) Abuzaid, N.S, and Nakhla, G.F., "Dissolved Oxygen Effects on Equilibrium and Kinetics of Phenolics Adsorption by Activated Carbon". *Environ. Sci. Technol.*, 28 , 216- 221, 1994.

(3) Boehm, H.P., Diehl, E., Heck, W., and Sappok, R., *Angew. Chem. Intern. Endl.* 3, 10, 669, 1964.

(4) Chang, C.H., Savage, D.W. and Longo, J.M., "Carbon - Sulfur Surface Compounds - Novel Regenerable Adsorbents for the Removal of Aromatics from Aqueous Solutions", *J Colloid Interface Sci.*, 79, 178 ,1981.

(5) Cooney D.O and Xi, Z.P, "Activated Carbon can Catalyze Reactions of Phenolics during Liquid Phase adsorption", First Separation Division Topical Conference on Separation Technologies : New Developments and Opportunities, AIChE Annual Conference, 415, 1992.

(6) Coughlin, R. W., "Effect of surface groups on Adsorption of Pollutants", *Water Pollution Control Research Series*, 17020 - 06170, Environ. Protection Agency, Washington, D. C, June 1970.

- (7) Garten, V.A., Weiss, D.E, and Willis, J.B., "Australian J. Chem", 10, 295, 1957.
- (8) Grant, T.M., and King, C. T., "Mechanism of Irreversible Adsorption of Phenolic compounds by activated carbons", Ind. Eng. Chem. Res., 29, 264, 1990.
- (9) Magne, P. and Walker, P. Jr. , "Phenol adsorption on activated carbon: application to the regeneration of activated carbons polluted with Phenol", Carbon, 24, 101, 1986
- (10) Mattson, J.S., Mark, H.B., Malbin, M.D., Weber, W.J., and Crittenden, J.C., "Surface Chemistry of Active Carbon: Specific Adsorption of Phenols", J. Colloid Interface Sci., 31, 116., 1969.
- (11) Modell, M., DeFilippi, R., and Krukonsis, V., "Regeneration of Activated Carbon with Supercritical Carbon Dioxide in Activated Carbon Adsorption of Organics from the aqueous Phase", Suffet, I.H., McGuire, M.J., Eds., Ann Arbor Science: Ann Arbor MI, 1980.
- (12) Prober, R., Pycha, J. J., and Kidon, W. E., "Interaction of Activated Carbon with Dissolved Oxygen ", AIChE J., 21, 1200, 1975.
- (13) Snoeyink, V. L., Lai, H. T., Johnson, J. H., and Young J. F., "Active Carbon : Dechlorination and Adsorption of Organic compounds", Chemistry of Water Supply Treatment and Distribution, A. J., Rubin ed; 232, Ann Arbor Science Publishers, Ann Arbor, Mich., 1974.

(14) Studebaker, M.L, Huffman, K.W.D., Wolfe, A.C., and Nabors, L.G., Ind. Eng. Chem. 48, 162, 1956.

(15) Suzuki, M, Adsorption Engineering, Elsevier, 9,1990.

(16) Vidic, R.D., M.T. Suidan, U.K. Traegner and G.F. Nakhla, "Adsorption Isotherms : Illusive capacity and role of oxygen", Water Resources, 24, 10, 1187 ,1990.

(17) Vidic, R.D., and Suidan, M.T, "Role of Dissolved Oxygen on the Adsorptive Capacity of Activated Carbon for Synthetic and Natural Organic Matter", Environ. Sci. Technol., 25, 1612, 1991.

(18) Vidic, R.D., and Suidan, M.T, "Selecting batch studies for adsorber design : molecular oxygen's role", J. Am. Wat. Wks. Ass., 84, 101, 1992.

(19) Vidic, R.D., Suidan, M.T, and Brenner, R.C., "Impact of oxidative Coupling on Adsorption Kinetics", Water Resources , 28, 2, 263, 1994.

3.9 Nomenclature

C_o initial phase concentration

C_∞ fluid phase equilibrium concentration

$C(t)$ fluid phase concentration as function of time.

$\bar{C}(\tau)$ dimensionless fluid phase concentration as function of dimensionless time.

C_{o_2} fluid phase concentration of oxygen as a function of time.

$C_{o_2,0}$ initial fluid phase concentration of oxygen

$C_{o_2,\infty}$ fluid phase concentration of oxygen at equilibrium

D_{so} surface diffusivity coefficient at zero adsorbate loading

D_s surface diffusivity coefficient

D_p pore volume diffusivity coefficient

H oxygen isotherm constant,

K combined constant in reaction term

k_{LF} Langmuir Freundlich isotherm constant

k' natural logarithm of the abscissa intercept in the log-log plot of oxygen imbalance versus time,

k_{o_2} reaction constant with respect to oxygen imbalance,

m reaction order with respect to adsorbate concentration,

M_t total amount of adsorbate which diffuses from the bulk phase

into the carbon particle at any time, t

M_{∞} mass adsorbed at infinite time

k_{o_2} reaction order with respect to oxygen imbalance,

n Langmuir Freundlich isotherm constant

n' reaction order with respect to oxygen imbalance,

n'' negative of the slope of the log-log plot of normalised oxygen imbalance versus time

N adsorbate flux into the particle,

q_{os} adsorbate phase concentration in equilibrium with the initial fluid phase concentration,

\bar{q}_{∞} average adsorbate concentration at infinite time

$q(r, t)$ adsorbent phase concentration as a function of radial position and time

$\bar{q}(t)$ average adsorbate concentration on the particle as a function of time, t

$\bar{Q}(\tau)$ dimensionless average adsorbate concentration as a function of dimensionless time, $\bar{q}(t)/q_{os}$

$Q(\eta, \tau)$ dimensionless adsorbent phase concentration, $q(r, t)/q_{os}$

r radial coordinate,

r_s particle radius,

R	reaction rate based on total volume of particle
t	time
u	uptake of adsorbent
V	volume of the aqueous phase
W_s	mass of the carbon particle

Greek alphabet

α	solute distribution parameter (dimensionless), Wq_{os}/VC_o ,
ε	particle porosity,
Φ	Thiele modulus
η	dimensionless radius
λ	initial surface loading, $\frac{q_o}{q_s}$
θ	loading, $\frac{q}{q_s}$
ρ_p	density of particle
τ	dimensionless time

CHAPTER FOUR

COMBINED PORE AND SURFACE DIFFUSION IN PACKED BEDS

4.1 Introduction

Practical adsorption processes are in many cases associated with adsorption in a column. Adsorption particles are packed in a column and fluid containing one or more components flows through the bed.

An ideal plug flow system has no resistance to mass transfer. In such a system, the input concentration profile is replicated by the outlet response with a time delay corresponding to the hold-up in the column. In a real system, the outlet response is dispersed. The dispersion is the result of the combined effects of axial dispersion and mass transfer resistance. Information on the adsorption equilibrium are obtained from the time delay measurement while that on the sorption kinetics and extent of axial mixing are provided by measurement of the dispersion of the outlet response. To extract this information, the experimental response must be matched with the theoretical response curve, calculated from a suitable dynamic model for the system.

The consideration of the response of an initially sorbate free column to either a step change in sorbate concentration at the column inlet (step input) or to the injection of a small pulse of sorbate at the column inlet (pulse input) is a convenient way of studying the dynamics of a fixed bed adsorption column. The response to a step input is commonly called the

breakthrough curve while the pulse response is often referred to as the chromatographic response. The chromatographic response is a derivative of the breakthrough curve since a delta function (perfect pulse) is the derivative of the Heaviside function (perfect step) for a linear system. Practical convenience rather than fundamental theoretical consideration determines the choice of input function since exactly the same information may be derived from the response to either input.

In the course of the adsorption, a saturation zone is formed near the inlet of the column and a zone with increasing concentration is observed at the frontal part. A measurement of the effluent stream concentrations reveals a seepage of the adsorbable components when the mass transfer zone approaches the exit of the bed. This of course, gives the breakthrough curve. One convenient way of classifying adsorption systems is according to number of mass transfer zones in the dynamic response to a change in feed composition.

4.2 Literature Survey

In a fixed bed of adsorbent particles, the following mass transport processes are observed: axial dispersion in the intraparticle fluid phase, fluid to particle mass transfer, intraparticle diffusion (which may include surface, micropore and/or macropore diffusion), and a reversible adsorption in the interior of the particle.

Generally, the isotherms for organic compounds on activated carbons are non-linear and analytical solutions for breakthrough curves cannot be derived. Further, the adsorbers in this field are usually not long enough to

warrant the assumption of a constant pattern concentration profile which would simplify the calculation of the breakthrough curves.

Wilmanski, and Lipinski (1989) reported that the adsorption uptake in a column increases with increase in bed height and noticed that the effective pore diffusivity decreases during column performance. They observed that the breakthrough was achieved at the same throughput values (bed volumes), without regard to the superficial velocity used in the column tests at a given particle size fraction. These results provided sufficient assurance that the external mass transfer resistance could be neglected. The breakthrough curves for smaller particles were sharper than those for larger sizes. The number of bed volume (throughput) achieved prior to breakthrough was found to decrease with increasing carbon particle size in the bed at the different breakthrough criteria. Consequently, a higher GAC solid phase concentration can be achieved for the smaller carbon particle size used in the column. This is supported by the work of Goto et al. (1986). Reschke et al. (1986) reported that the reduction of particle size to one third the standard diameter resulted in a more than a three fold increase in diffusion time constant.

In past years various numerical techniques have been employed in solving the set of descriptive column equations. However, recently, the orthogonal collocation algorithm has become more commonly used rather than other methods, as it has been proved to be more time efficient. Raghavan and Ruthven (1983), showed that the orthogonal collocation method was far more time efficient than the exact solution in evaluating a breakthrough curve. They compared their numerical solution with the exact solution presented by Rasmusson and Neretnieks, (1980).

Crittenden et al. (1986) made a review of various models used in predicting the transport of organic compounds with saturated ground water flow. A detailed discussion of the dispersed flow, film transfer, pore and surface diffusion model (DFPSDM) was presented. The mechanisms accounted for in this model include (1) constant advective flow, (2) axial dispersion and diffusion, (3) film transfer resistance to mass transport from the mobile to the stationary phase, (4) local adsorption equilibrium between the solute in the intra-aggregate stagnant fluid and (5) both surface and pore diffusion as intra-stationary phase mass transport mechanisms.

4.3 Theoretical Model

Consider a column packed with activated carbon particles through which fluid stream containing concentration $C(z, t)$ of an adsorbable species is flowing. We take an element of the bed and conduct a mass balance. If the flow pattern can be represented as axially dispersed plug flow, the differential fluid phase mass balance is:

$$-D_L \frac{\partial^2 C_b}{\partial z^2} + \frac{\partial}{\partial z}(v C_b) + \frac{\partial C_b}{\partial t} + \left(\frac{1-\varepsilon}{\varepsilon} \right) \frac{\partial \bar{q}}{\partial t} = 0 \quad (4.1)$$

The initial condition is

$$C_b(z > 0, t = 0) = 0 \quad (4.2)$$

Boundary Conditions:

The boundary conditions are the Danckwerts (1953) boundary conditions. They are obtained by equating the mass flux entering and leaving the column.

$$v[C_I(t) - C_b(z = 0^+, t)] = -D_L \frac{\partial C_b(z = 0^+, t)}{\partial z} \quad (4.3)$$

$$\frac{\partial C_b(z = L, t)}{\partial z} = 0 \quad (4.4)$$

The derivation of these boundary conditions is based on the assumption that the diffusion and dispersion occurs only within the column. Similarly, if the mass flux into the column is equated to the rate of accumulation of mass within the column, the following equivalent boundary conditions are obtained.

$$v[C_I(t) - C_b(z = L^+, t)] = \frac{\partial}{\partial t} \int_0^L \left[C_b(z, t) + \frac{3(1 - \epsilon)}{r_s^3 \epsilon} \int_0^{r_s} [\epsilon_p C_p(r, z, t) + \rho_p q(r, z, t)] r^2 dr \right] dz \quad (4.5)$$

Equation (4.4) is also the solution of the following boundary condition and its initial condition:

$$\frac{\partial^2 C_b(z = L, t)}{\partial t \partial z} = 0; \quad \frac{\partial C_b(z = L, t = 0)}{\partial z} = 0 \quad (4.6)$$

Equations (4.5) and (4.6) are used in lieu of the Danckwerts boundary conditions in the numerical solutions of the model because they simplify the numerical method.

Mass transfer rates are often correlated in terms of an effective mass transfer coefficient k_f , defined according to a linear driving force equation.

$$\begin{aligned}\frac{\partial \bar{q}}{\partial t} &= k_f a [C_b(z, t) - C_p(r = r_s, z, t)] \\ &= \frac{3k_f}{r_s} [C_b(z, t) - C_p(r = r_s, z, t)]\end{aligned}\quad (4.7)$$

where a is the external surface area per unit particle ($3/r_s$ for spherical particles) and \bar{q} is the adsorbed phase concentration averaged over a particle.

The fluid phase equations become:

$$\begin{aligned}\frac{\partial C_b(z, t)}{\partial t} &= D_L \frac{\partial^2 C_b(z, t)}{\partial z^2} - v \frac{\partial C_b(z, t)}{\partial z} \\ &\quad - \frac{3k_f(1-\epsilon)}{\epsilon r_s} [C_b(z, t) - C_p(r = r_s, z, t)]\end{aligned}\quad (4.8)$$

The terms which appear in the equation account for accumulation in the mobile liquid phase, axial dispersion and diffusion, advective flow, and rate of transport from the mobile phase to the stationary phase by liquid phase mass transfer.

The particle equations are :

$$\begin{aligned} \varepsilon_p \frac{\partial C_p(r, z, t)}{\partial t} + \rho_p \frac{\partial q(r, z, t)}{\partial t} = \\ \frac{1}{r_s^2} \left\{ r^2 \left[\varepsilon_p D_p \frac{\partial C_p(r, z, t)}{\partial r} + \rho_p D_s \frac{\partial q(r, z, t)}{\partial r} \right] \right\} \end{aligned} \quad (4.9)$$

which can also be written as :

$$\begin{aligned} \varepsilon_p \frac{\partial C_p(r, z, t)}{\partial t} + \rho_p \frac{\partial q(r, z, t)}{\partial t} = \\ \frac{1}{r_s^2} \left\{ r^2 \left[\varepsilon_p D_p \frac{\partial C_p}{\partial r} + \rho_p D_s \right] \frac{\partial q}{\partial r} \right\} \end{aligned} \quad (4.10)$$

The initial conditions are :

$$C_p(r, z, t = 0) = 0 \quad (4.11)$$

$$q(r, z, t = 0) = 0 \quad (4.12)$$

Boundary conditions:

At the center, due to symmetry, we have :

$$\frac{\partial q(r = 0, z, t)}{\partial r} = 0 \quad (4.13)$$

$$\frac{\partial C_p(r = 0, z, t)}{\partial r} = 0 \quad (4.14)$$

At the surface,

$$k_f [C_b(z, t) - C_p(r = r_s, z, t)] = D_p \epsilon_p \frac{\partial C_p(r = r_s, z, t)}{\partial r} + D_s \rho_p \frac{\partial q(r = r_s, z, t)}{\partial r} \quad (4.15)$$

Equivalently, at the surface we have :

$$k_f r_s^2 [C_b(z, t) - C_p(r = r_s, z, t)] = \frac{\partial}{\partial t} \int_0^{r_s} [\epsilon_p C_p(r = r_s, z, t) + \rho_p q(r = r_s, z, t)] r^2 dr \quad (4.16)$$

In equation (4.15), the liquid phase mass flux from the fluid phase is equated to the flux at the surface of the particle. In equation (4.16), the rate of fluid phase mass transfer is equated to the accumulation of mass within the particles. Equation (4.16) is used in the numerical method as it simplifies the solution.

The fluid in the film around the particles is assumed to be in equilibrium with the adsorbed phase concentration on the surface of the particle. Thus, the fluid phase concentration is related to the adsorbed surface concentration by an adsorption equilibrium equation.

Table 4.1 : Dimensionless Groups in Column.

Dimensionless Group	Equation	Definition
Peclet number, Pe	$\frac{vL}{D_L}$	$\frac{\text{rate of transport by advection}}{\text{rate of transport by axial dispersion}}$
Stanton number, St	$\frac{k_f L(1-\varepsilon)}{r_s \varepsilon v}$	$\frac{\text{rate of transport by film transfer}}{\text{rate of transport by advection}}$
Surface diffusion modulus, Ed _s	$\frac{LD_s Dg_s}{vr_s^2}$	$\frac{\text{rate of transport by pore diffusion}}{\text{rate of transport by advection}}$
Pore diffusion modulus, Ed _p	$\frac{LD_p Dg_p}{vr_s^2}$	$\frac{\text{rate of transport by surface diffusion}}{\text{rate of transport by advection}}$
Particle diffusion modulus, Ed	Ed _s + Ed _p	$\frac{\text{rate of transport by intra-particle diffusion}}{\text{rate of transport by advection}}$
Adsorbed solute distribution ratio, Dg _s	$\frac{(1-\varepsilon)\epsilon_p}{\varepsilon}$	$\frac{\text{mass of solute contained in immobile fluid}}{\text{mass of solute contained in the mobile phase evaluated at equilibrium with } C_o}$
Immobile fluid solute distribution ratio, Dg _p	$\frac{(1-\varepsilon)\rho_p q_e}{\varepsilon C_o}$	$\frac{\text{mass of adsorbate on the particle surface}}{\text{mass of solute contained in the mobile phase evaluated at equilibrium with } C_o}$
Solute distribution ratio, Dg	Dg _p + Dg _s	$\frac{\text{mass of adsorbate contained in the particle surface}}{\text{mass of solute contained in the mobile phase evaluated at equilibrium with } C_o}$
Throughput, T	$\frac{tv}{L(1+D_g)}$	$\frac{\text{mass of solute fed to the column}}{\text{mass of solute in a column saturated to capacity}}$

Dimensionless Form

Dimensionless variables used are:

$$\bar{z} = \frac{z}{L}; \bar{C}_1 = \frac{C_1}{C_o}; \bar{r} = \frac{r}{r_s}; \bar{C} = \frac{C}{C_o}; \bar{q} = \frac{q}{q_e};$$

$$T = \frac{tv}{L(1 - D_g)}; \bar{X}(\bar{r}, \bar{z}, T) = X(r, z, t) / X_e$$

Definitions :

$X(r, z, t)$ is the particle concentration i.e. it includes the solute in the pore water and that adsorbed on the GAC particle surface as a function of radial and axial position and time. In equation form, it is given by:

$$X(r, z, t) = \varepsilon_p C_p(r, z, t) + \rho_p q(r, z, t) \quad (4.17)$$

X_e is the particle concentration in equilibrium with C_o .

$$X_e = \varepsilon_p C_o + \rho_p q_e \quad (4.18)$$

Equation (4.17) is converted to the dimensionless form as follows :

$$\bar{X}(\bar{r}, \bar{z}, T) = X(r, z, t) / X_e \quad \text{and} \quad \bar{q} = q / q_e$$

The various dimensionless groups used in the subsequent analysis are summarized in Table 1. From Table 1:

$$D_g = \frac{(1-\varepsilon)(\rho_p q_e + \varepsilon_p C_o)}{\varepsilon C_o} = \frac{(1-\varepsilon)X_e}{\varepsilon C_o} \quad (4.19)$$

$$\bar{X}(\bar{r}, \bar{z}, T) = \frac{\varepsilon_p C_o \bar{C}_p(\bar{r}, \bar{z}, T)}{X_e} + \frac{\rho_p q_e \bar{q}(\bar{r}, \bar{z}, T)}{X_e}$$

$$\frac{Dg_s}{Dg} = \frac{(1-\varepsilon)\rho_p q_e}{\varepsilon C_o} \cdot \frac{\varepsilon C_o}{(1-\varepsilon)(\rho_p q_e + \varepsilon_p C_o)} = \frac{\rho_p q_e}{(\rho_p q_e + \varepsilon_p C_o)}$$

$$\frac{Dg_p}{Dg} = \frac{(1-\varepsilon)\varepsilon_p}{\varepsilon} \cdot \frac{\varepsilon C_o}{(1-\varepsilon)(\rho_p q_e + \varepsilon_p C_o)} = \frac{\varepsilon_p C_o}{(\rho_p q_e + \varepsilon_p C_o)}$$

Therefore,

$$\bar{X}(\bar{r}, \bar{z}, T) = \frac{Dg_p}{Dg} \bar{C}_p(\bar{r}, \bar{z}, T) + \frac{Dg_s}{Dg} \bar{q}(\bar{r}, \bar{z}, T) \quad (4.20)$$

We have :

$$\frac{\partial C_b}{\partial t} = \frac{C_o v}{L(1+D_g)} \frac{\partial \bar{C}_b}{\partial T}; \quad \frac{\partial C_b}{\partial z} = \frac{C_o}{L} \frac{\partial \bar{C}_b}{\partial \bar{z}}; \quad \text{and} \quad \frac{\partial^2 C_b}{\partial z^2} = \frac{C_o}{L^2} \frac{\partial^2 \bar{C}_b}{\partial \bar{z}^2}$$

Therefore,

$$\frac{1}{(1+D_g)} \frac{\partial \bar{C}}{\partial T} = \frac{D_L}{vL} \frac{\partial^2 \bar{C}}{\partial \bar{z}^2} - \frac{\partial \bar{C}}{\partial \bar{z}} - \frac{3(1-\varepsilon)k_f L}{\varepsilon r_s v} [\bar{C}_b(\bar{z}, T) - \bar{C}_p(1, \bar{z}, T)]$$

$$\frac{1}{(1 + D_g)} \frac{\partial \bar{C}}{\partial T} = \frac{1}{Pe} \frac{\partial^2 \bar{C}}{\partial \bar{z}^2} - \frac{\partial \bar{C}}{\partial \bar{z}} + 3St [\bar{C}_b(\bar{z}, T) - \bar{C}_p(1, \bar{z}, T)] \quad (4.21)$$

Equation (4.5) is converted to dimensionless form as follows :

$$vC_o [C_I(t) - C_b(z=1, T)] = \frac{vC_o}{L(D_g + 1)} \frac{\partial}{\partial T} \int_0^1 \left[\bar{C}_b(\bar{z}, T) + \frac{3(1-\epsilon)}{r_s^3 \epsilon} \right. \\ \left. \cdot \int_0^1 [\bar{X}(\bar{r}, \bar{z}, T) \cdot X_e] \bar{r}^2 r_s^2 \partial \bar{r} \right] L \partial \bar{z}$$

$$[C_I(t) - C_b(z=1, T)] = \frac{1}{(D_g + 1)} \frac{\partial}{\partial T} \int_0^1 \left[\bar{C}_b(\bar{z}, T) + \right. \\ \left. \frac{3(1-\epsilon)}{\epsilon C_o} (\epsilon_p C_o + \rho_p q_e) \cdot \int_0^1 \bar{X}(\bar{r}, \bar{z}, T) \cdot \bar{r}^2 \partial \bar{r} \right] \partial \bar{z}$$

This reduces to :

$$[C_I(t) - C_b(z=1, T)] = \frac{1}{(D_g + 1)} \cdot \frac{\partial}{\partial T} \cdot \int_0^1 \left[\bar{C}_b(\bar{z}, T) + 3Dg \int_0^1 \bar{X}(\bar{r}, \bar{z}, T) \cdot \bar{r}^2 \partial \bar{r} \right] \partial \bar{z} \quad (4.22)$$

Initial condition:

$$\bar{C}_b [0 < \bar{z} \leq 1, T=0] = 0 \quad (4.23)$$

Boundary conditions:

$$\bar{C}_1(T) - \bar{C}_b(\bar{z}=1, T) = -\frac{1}{Pe} \frac{\partial \bar{C}_b(\bar{z}=0^+, T)}{\partial \bar{z}} \quad (4.24)$$

$$\frac{\partial \bar{C}_b(\bar{z}=1, T)}{\partial \bar{z}} = 0 \quad (4.25)$$

Dimensionless Form of Particle Equations :

Equation (4.9) is transformed as follows :

The left hand side becomes

$$\begin{aligned} \frac{\varepsilon_p C_o v}{L(D_g + 1)} \frac{\partial \bar{C}_p}{\partial T} + \frac{\rho_p q_e v}{(D_g + 1)} \frac{\partial \bar{q}}{\partial T} &= \frac{v}{L(D_g + 1)} \left[\varepsilon_p C_o \frac{\partial \bar{C}_p}{\partial T} + \rho_p q_e \frac{\partial \bar{q}}{\partial T} \right] \\ &= \frac{\varepsilon_p C_o v}{LDg_p} \frac{D_g}{(D_g + 1)} \frac{\partial \bar{X}(\bar{r}, \bar{z}, T)}{\partial T} \end{aligned}$$

Equation (4.9) then reduces to:

$$\begin{aligned} \frac{D_g}{(D_g + 1)} \frac{\partial \bar{X}(\bar{r}, \bar{z}, T)}{\partial T} &= \frac{1}{\bar{r}^2} \frac{\partial}{\partial \bar{r}} \cdot \\ &\left\{ \bar{r}^2 \left[\frac{LDg_p}{\varepsilon_p C_o v} \cdot \frac{\varepsilon_p C_o D_p}{r_s^2} \frac{\partial \bar{C}_p}{\partial \bar{r}} + \frac{D_s \rho_p q_e}{r_s^2} \cdot \frac{\varepsilon_p C_o D_p}{r_s^2} \frac{\partial \bar{q}}{\partial \bar{r}} \right] \right\} \end{aligned}$$

We note the following :

$$Ed_s + \frac{Dg_p}{Dg_s} Ed_s = \frac{LD_s}{vr_s^2} [Dg_s + Dg_p],$$

$$Ed_s - \frac{Dg_p}{Dg_s} Ed_s = \frac{LDg_p}{vr_s^2} [D_p - D_s],$$

and, from the definition of $X(r, z, t)$,

$$\frac{\partial \bar{q}(\bar{r}, \bar{z}, T)}{\partial \bar{r}} = \frac{Dg}{Dg_s} \frac{\partial \bar{X}}{\partial \bar{r}} - \frac{Dg_p}{Dg_s} \frac{\partial \bar{C}_p}{\partial \bar{r}}$$

The term in the bracket in equation (4.9), then becomes :

$$\begin{aligned} & Ed_s \frac{\partial \bar{C}_p}{\partial \bar{r}} + \frac{LDg_p}{r_s^2 v} \left\{ \frac{D_s \rho_p q_e}{\epsilon_p C_o} \frac{D_g}{Dg_s} \frac{\partial \bar{X}}{\partial \bar{r}} - D_s \frac{\rho_p q_e}{\epsilon_p C_o} \frac{Dg_p}{Dg_s} \frac{\partial \bar{C}_p}{\partial \bar{r}} \right\} \\ &= \left(Ed_p - \frac{Dg_p}{Dg_s} Ed_s \right) \frac{\partial \bar{C}_p(\bar{r}, \bar{z}, T)}{\partial \bar{r}} + \left(Ed_s + \frac{Dg_p}{Dg_s} Ed_s \right) \frac{\partial \bar{X}(\bar{r}, \bar{z}, T)}{\partial \bar{r}} \end{aligned}$$

Equation (4.9) then becomes:

$$\begin{aligned} & \frac{D_g}{(D_g + 1)} \frac{\partial \bar{X}(\bar{r}, \bar{z}, T)}{\partial T} = \frac{1}{\bar{r}^2} \frac{\partial}{\partial \bar{r}} \left\{ \bar{r}^2 \left[\left(Ed_p - \frac{Dg_p}{Dg_s} Ed_s \right) \frac{\partial \bar{C}_p(\bar{r}, \bar{z}, T)}{\partial \bar{r}} + \left(Ed_s + \frac{Dg_p}{Dg_s} Ed_s \right) \frac{\partial \bar{X}(\bar{r}, \bar{z}, T)}{\partial \bar{r}} \right] \right\} \\ & \hspace{25em} (4.26) \end{aligned}$$

Initial conditions become:

$$\bar{C}_p(\bar{r}, \bar{z}, T=0)=0 \quad (4.27)$$

$$\bar{q}(\bar{r}, \bar{z}, T=0)=0 \quad (4.28)$$

Boundary conditions becomes:

At the center,

$$\frac{\partial \bar{q}(\bar{r}=0, \bar{z}, T)}{\partial \bar{r}}=0 \quad (4.29)$$

$$\frac{\partial \bar{C}_p(\bar{r}=0, \bar{z}, T)}{\partial \bar{r}}=0 \quad (4.30)$$

At the surface of the particle, the boundary conditions transforms as follows :

$$\begin{aligned} k_f r_s^2 C_o [\bar{C}_b(\bar{z}, T) - \bar{C}_p(\bar{r}=r_s, \bar{z}, T)] \\ = \frac{v}{L(1+D_g)} r_s^3 X_e \frac{\partial}{\partial T} \int_0^1 \bar{X}(\bar{r}, \bar{z}, T) \bar{r}^2 d\bar{r} \end{aligned}$$

We note that

$$X_e = \varepsilon_p C_o + \rho_p q_e = \frac{\varepsilon C_o}{(1-\varepsilon)} Dg$$

Hence,

$$\left(\frac{k_f L(1-\varepsilon)}{r_s \varepsilon v} \right) \cdot \left(\frac{1+D_g}{D_g} \right) \left[\bar{C}_b(\bar{z}, T) - \bar{C}_p(\bar{r} = r_s, \bar{z}, T) \right]$$

$$= \frac{\partial}{\partial T} \int_0^1 \bar{X}(\bar{r}, \bar{z}, T) \bar{r}^2 d\bar{r}$$

Or,

$$\text{St.} \left(\frac{1+D_g}{D_g} \right) \left[\bar{C}_b(\bar{z}, T) - \bar{C}_p(\bar{r} = r_s, \bar{z}, T) \right]$$

$$= \frac{\partial}{\partial T} \int_0^1 \bar{X}(\bar{r}, \bar{z}, T) \bar{r}^2 d\bar{r} \quad (4.31)$$

The dispersion coefficient was calculated using the correlation given in Ruthven (1978)

$$D_L = \delta_1 D_M + \delta_2 d_p v \quad (4.32)$$

where $\delta_1 = 0.7$; $\delta_2 = 0.5$

v = interstitial velocity,

d_p = particle density

The following equation (Wakao and Funzkri) was used to calculate the film transfer coefficient. The correlation is valid for Reynolds number between 3 and 1000.

$$\frac{2k_f r}{D_M} = 2 + 1.1 R^{0.6} \text{Sc}^{0.333} \quad (4.33)$$

Where k_f is the liquid - phase mass transfer coefficient, R is Reynolds number, and Sc is Schmidt number. The dimensionless groups are defined as follows:

$$Sc = \frac{\mu}{\rho_1 D_M} \quad (4.34)$$

$$R = \frac{2 \rho_1 r v}{\mu} \quad (4.35)$$

where , μ is viscosity of water ($9.8E-4$ kg.s/m), ρ_1 is density of water (997.8 kg/m³), r is mean radius of adsorbent particle, v is the superficial velocity ($3.286E-3$ m/s) , and D_M is the diffusivity of the adsorbate in water calculated using the Wilke - Chang equation . The values of D_M and r were presented in chapter two.

Solution Scheme

Equations (21) and (26) were coupled by assuming local equilibrium at the surface of the carbon particle. The isotherm equation was used to relate the surface and pore concentrations within the immobile phase by equation (20).

Equations (4.20) to (4.30) represents a set of simultaneous, nonlinear, partial differential equations (PDEs) that can be solved numerically by orthogonal collocation (OC) (Finlayson, 1980). The orthogonal collocation method converts the set of PDEs to a set of linear polynomials. The dependence of concentration on position within the particles and column is now represented by linear combination of orthogonal polynomials. These polynomials are used in integration and differentiation algorithms that only require values for the dependent variables, concentration, at specific collocation points. The collocation points are located at the roots of the polynomials where the polynomials approximations agree exactly with the true values of the dependent variables. The PDEs are converted to a series of ordinary differential equations (ODEs) which describe the temporal variation of the dependent variable at the collocation points.

Applying OC to the equations yields the following MC ODEs for the mobile phase in the axial direction:

$$\begin{aligned} \frac{d\bar{C}_b(k, T)}{dT} = & (Dg + 1) \sum_{i=1}^{MC} \left[\frac{B_{i,k}^z}{Pe} - A_{i,k}^z \right] \bar{C}_b(k, T) \\ & - 3(Dg + 1) St [\bar{C}_b(k, T) - \bar{C}_p(NC, k, T)] \end{aligned} \quad (4.36)$$

for $k = 2$ to $MC - 1$

$$\begin{aligned}
\frac{d\bar{C}_b(k=1, T)}{dT} = & \left\{ [(Dg + 1)[\bar{C}_l(T) - \bar{C}_b(MC, T)] \right. \\
& - \sum_{k=2}^{MC-1} \left(W_k^z - W_{MC}^z \frac{A_{MC,k}^z}{A_{MC,MC}^z} \right) \frac{d\bar{C}_b(k, T)}{dT} \Bigg] \\
& \cdot \left(W_1^z - W_{MC}^z \frac{A_{MC,1}^z}{A_{MC,MC}^z} \right)^{-1} \Bigg\} \\
& - \left\{ 3Dg \left(\sum_{k=1}^{MC} W_k^z \left(\sum_{j=1}^{NC} W_j^r \frac{d\bar{X}(j, k, T)}{dT} \right) \right) \right\} \\
& \cdot \left(W_1^z - W_{MC}^z \frac{A_{MC,1}^z}{A_{MC,MC}^z} \right)^{-1} \Bigg\}
\end{aligned} \tag{4.37}$$

$$\frac{d\bar{C}_b(MC, T)}{dT} = - \sum_{k=1}^{MC-1} \frac{A_{MC,k}^z}{A_{MC,MC}^z} \frac{d\bar{C}_b(k, T)}{dT} \tag{4.38}$$

The entrance condition (equation (4.37)) was derived by the simultaneous solution of the ODEs that result from the application of OC to (4.23) to (4.25). The initial conditions for the bulk solution concentration at axial locations $k = 1$ to MC are

$$\bar{C}_b(k, T=0) = 0 \tag{4.39}$$

Time- variable influent concentrations are utilized in (4.37) by using $\bar{C}_I(T)$ for the influent concentration as a function of time.

Applying OC to (4.26) and (4.31) gives the following set of ODEs at NC collocation points in the immobile phase:

$$\frac{d\bar{X}(NC,k,T)}{dT} = \frac{(Dg+1)}{Dg} \sum_{i=1}^{NC} \left[\left(\left(Ed_p - \frac{Dg_p}{Dg_s} Ed_s \right) St [\bar{C}_b(k,T) - \right] \right. \\ \left. \cdot B_{i,j}^r \bar{C}_p(i,k,T) + \left(Ed_s + \frac{Dg_p}{Dg_s} Ed_s \right) B_{i,j}^r \bar{X}(i,k,T) \right] \quad (4.40)$$

for $j = 1$ to $NC-1$ and $k = 1$ to MC .

$$\frac{d\bar{X}(NC,k,T)}{dT} = \frac{(Dg+1)}{Dg W_{NC}^r} St [\bar{C}_b(k,T) - \bar{C}_p(NC,k,T)] \\ - \sum_{j=1}^{NC-1} \frac{W_j^r}{W_{NC}^r} \frac{d\bar{X}(j,k,T)}{dT} \quad (4.41)$$

for $k = 1$ to MC

Equations (4.300 is satisfied by using symmetrical orthogonal polynomials to represent the spatial derivatives.

The initial conditions for the surface and pore concentrations at axial locations $k = 1$ to MC are:

$$\bar{X}(j,k,T=0)=0; \quad \bar{C}_p(j,k,T=0) \quad (4.42)$$

The OC method was applied to (4.20) as follows :

$$\bar{X}(j,k,T) = \frac{Dg_p}{Dg} \bar{C}_p(j,k,T) + \frac{Dg_s}{Dg} \left(\frac{K_{LF} \bar{C}_o \bar{C}_p(j,k,T)^{1/N_{LF}}}{1 + K_{LF} \bar{C}_o \bar{C}_p(j,k,T)^{1/N_{LF}}} \right) \quad (4.43)$$

$A_{i,k}^z$, $B_{i,k}^z$ and W_i^z are the OC matrices and vector that are used to approximate the first derivatives, the second derivative, and the integral of relative concentration with respect to axial position, respectively. These were derived using unsymmetric jacobi polynomials with weighting factors of $(1 - x^2)$. $B_{i,k}^z$ and W_i^z are the OC matrix and vector that approximate the second derivatives and the integral in the radial direction using symmetric Legendre polynomials (Villadsen and Michelsen, 1978).

The ODEs were solved using an algorithm called IVPAG, from the IMSL package. The system of ODEs were solved by first solving (4.43) for $\bar{C}_p(j,k,T)$. Next, the various derivatives were evaluated in this order : equations (4.40), (4.41), (4.36), (4.38), and (4.37). This was done starting with initial conditions given in equations (4.39) and (4.42) and the time-variable influent concentration given in equation (4.37).

The above algorithm has been used, tested and proved highly efficient by Crittenden et al (1986). The accuracy of the program used was attested by reproducing the results of Crittenden et al. (1986).

4.4 Results And Discussion

The column parameters and their values are presented in the Tables 4.2 and 4.3 below:

Table 4.2 : Column Parameters

Column Parameters	Value
Influent Concentration, C_o	70 mg/L
Temperature	21 °C
Column length, L	60 cm
Particle density, ρ_p	0.67E6 mg/L
Interstitial velocity, v	0.8418 cm/s
Bed porosity, ε	0.39
Particle porosity, ε_p	0.63
Film transfer coefficient, k_f	phenol - 3.88E-3 cm ² /s o-cresol - 3.60E-3 cm ² /s
Dispersion coefficient, D_L	phenol - 6.657 cm ² /s o-cresol - 6.657 cm ² /s

Table 4.3 : Program Input for column system.

Program Input		
Dim. groups / Parameters	Phenol	o-cresol
Pe	769.2	769.2
St	5.545	5.1449
$fs = \frac{Dg_s}{Dg}$	0.99925	0.99965
Ed	2.486	2.0583
K_{LF}	0.1345	0.1353
n_{LF}	3.125	3.448

The program was used to fit the data by Abuzaid (1993). The program was found to be sensitive to the value of Station number used which in turn depends on the value of the film transfer coefficient. The correlation used in predicting the film transfer coefficient affects the value to some extent. This was shown in the work by Abuzaid (1993).

The fits are presented in Figures 4.1 and 4.2. The experimental effluent concentration data did not rise up to the inlet concentration as expected. Consequently, the experimental values were more reliably predicted at the earlier portion of the plots than at the later.

4.5 Conclusions and Recommendations.

The pore and surface diffusion model for a column was done. The model parameters used are those determined in chapter two of this work. The fits obtained predicted the experimental data favorably well at low reduced effluent concentration than at higher values. The discrepancies were noted to be due to the difficulty encountered in purging the column completely of oxygen before the experiment.

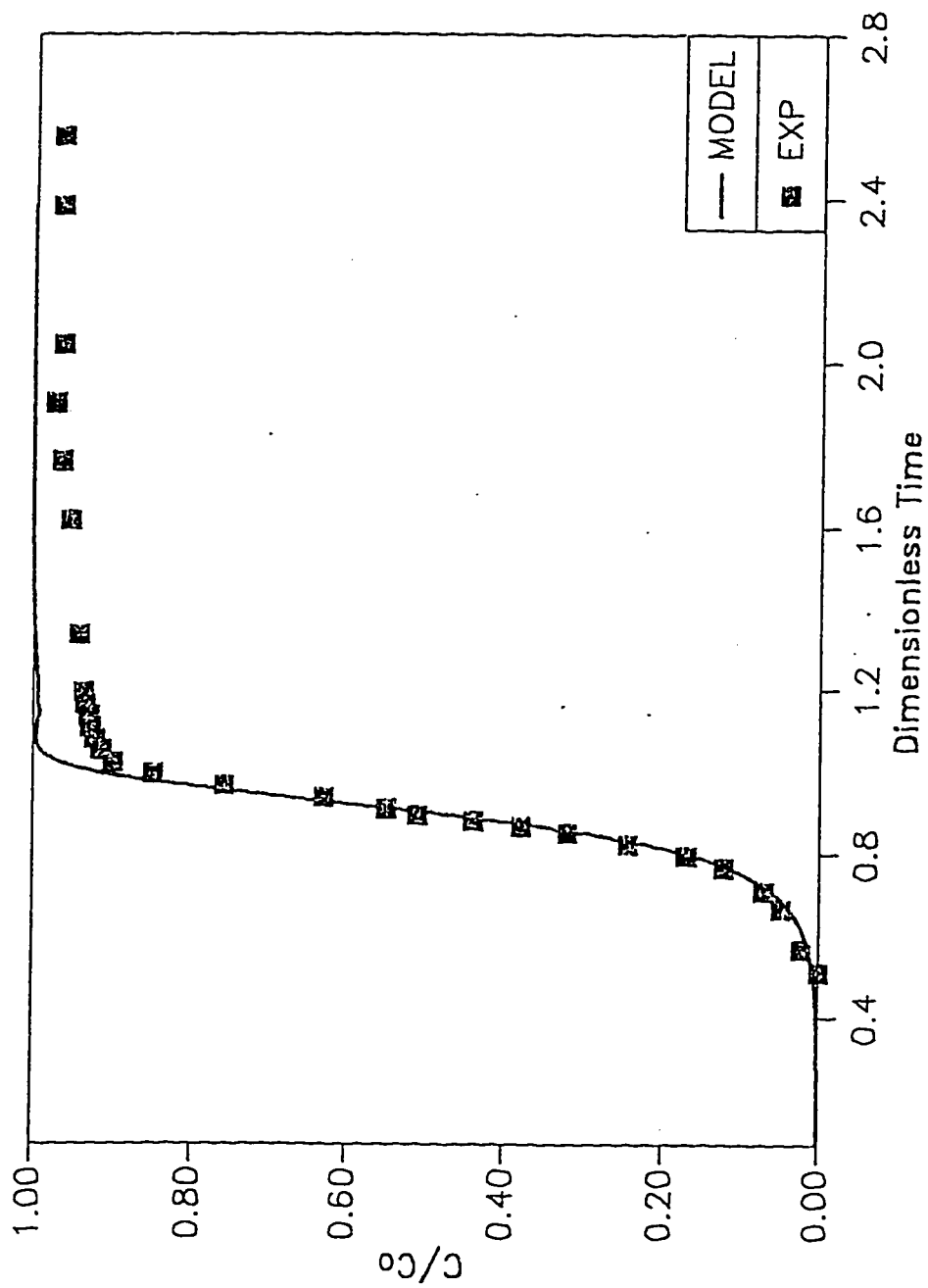


Fig 4.1: Predicted and Experimental Breakthrough Curves
Adsorption of o-cresol in column at 294K

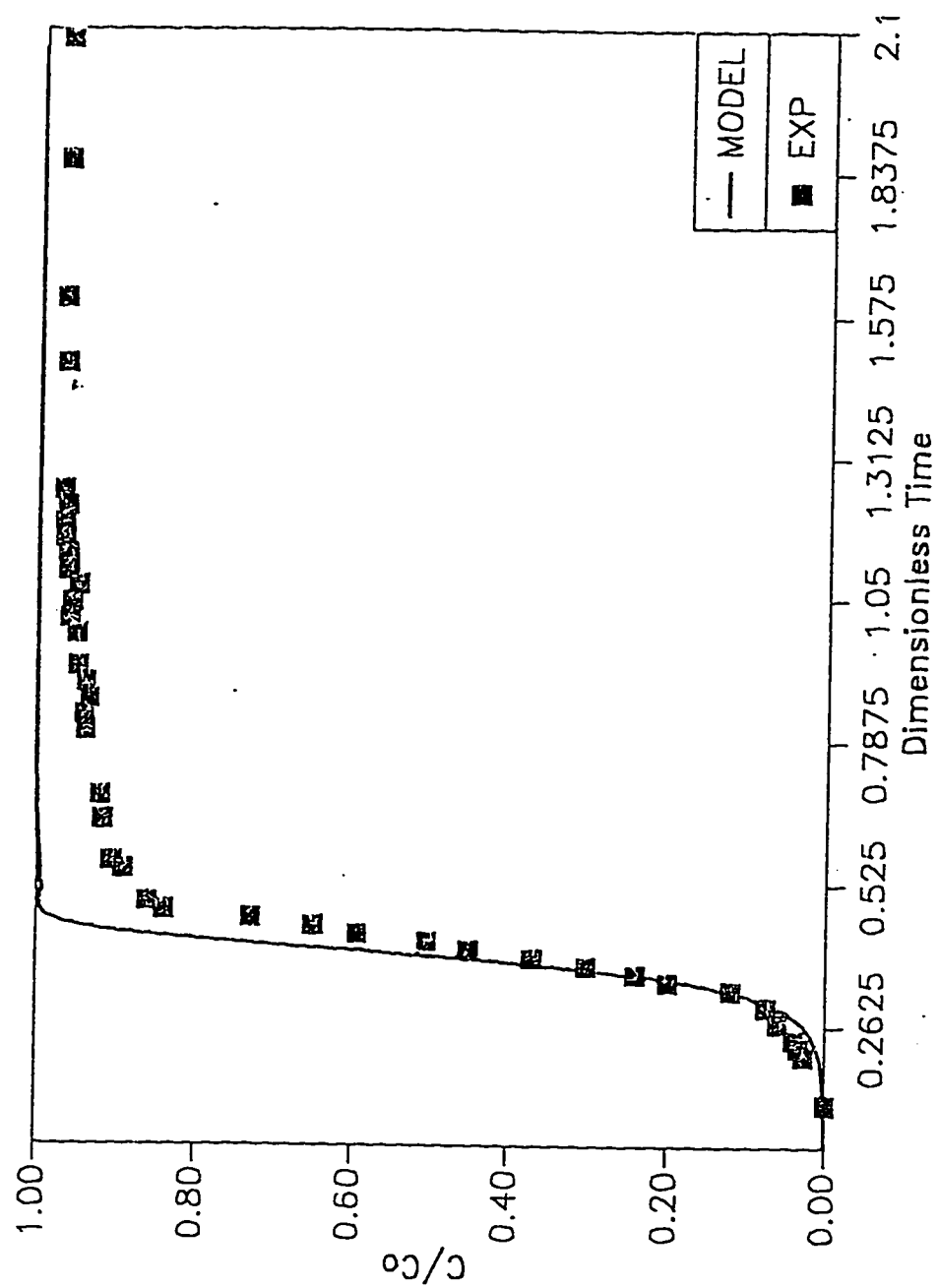


Fig.4.2: Predicted and Experimental Breakthrough Curves
Adsorption of phenol in columns at 294K

4.6 Literature Cited

(1) Crittenden, J., Hutzler, N. J., Geyer, D. G., Oravitz, J.L., and Friedman, G., "Transport of Organic Compounds With Saturated Groundwater Flow : Model Development and Parameter Sensitivity ", Wat. Resour. Research, 22(3),271-283, 1986.

(2) Danckwerts, P.V., "Continuous flow systems", Chem. Eng. Sci., 2, 1,1953.

(3) Finlayson, B.A., "Nonlinear Analysis in Chemical Engineering", McGraw-Hill, New York, 1980

(4) Goto, M., Hayashi, N., Goto, S., "Adsorption and Desorption of Phenol on Anion - Exchange resin and Activated Carbon", Environ. Sci. Technol., 20,463-467, 1986.

(5) Raghavan N.S., and D.M. Ruthven, "Numerical simulation of a Fixed-Bed Adsorption Column by method of orthogonal collocation", AIChE J., 29(6),922-925, 1983.

(6) Rasmusson, A., and I. Nerenieks, "Exact Solution of a Model for Diffusion in Particle and Longitudinal Dispersion in packed Beds", AIChE J, 26, 1980.

(7) Reschke, G., K.H., Radeke and D., Gelbin. "Breakthrough curves for single solutes in beds of Activated Carbon with a broad pore - size distribution - II. Measuring and calculating breakthrough curves of Phenol and Indole from aqueous solutions on activated carbons", Chem. Eng. Sci., 41(3),549-554, 1986.

(8) Villadsen, J., and M. L. Michelsen, "Solution of Differential Equation Models by Approximation", Prentice-Hall, Englewood Cliffs, New Jersey, 1978.

(9) Wakao, N., and Funckri T., "Effect of Fluid Dispersion Coefficients in Dilute Solutions", Chem. Eng. Sci., 33, 1375, 1978.

(10) Wilmanski, K., and Lipinski, K., "Adsorption Kinetics in GAC. systems for water treatment", J. Environ. Eng. 115(1),91-107, 1989.

4.7 Nomenclature

A	column cross sectional area (L^2)
$A_{i,k}^z$	orthogonal collocation matrix that approximates the first derivative in the axial direction.
Bi_p	pore diffusion Biot number, ratio of the external liquid phase mass transfer rate to the pore diffusion rate within the particle, equal to $(1 - \epsilon)k_f r_s / (\epsilon D_p D g_p)$ (dimensionless)
Bi_s	surface diffusion Biot number, ratio of the external liquid phase mass transfer rate to the surface diffusion rate within the particle equal to $(1 - \epsilon)k_f r_s / (\epsilon D_s D g_s)$ (dimensionless)
$B_{i,j}^r$	orthogonal collocation matrix that approximates the Laplacian quadrature in radial direction
$B_{i,k}^z$	orthogonal collocation matrix that approximates the Laplacian quadrature in axial direction
$C_b(z, t)$	bulk fluid phase concentration in mobile phase as a function of axial position and time (M / L^3)
$\bar{C}_b(\bar{z}, T)$	$\bar{C}_b(z, t) / C_o$ (dimensionless)
$\bar{C}_I(T)$	$C_I(T) / C_o$ (dimensionless)
C_o	arbitrary concentration used to normalize dimensionless equations, usually the maximum influent concentration (M / L^3)

$C_p(r, z, T)$ $C_p(r, z, T) / C_o$ (dimensionless)

Dg solute distribution ratio, the ratio of the mass of adsorbate contained in the particle phase to the mass of solute contained in the mobile phase evaluated at equilibrium with C_o equal to $Dg_p + Dg_s$ (dimensionless).

Dg_p immobile fluid solute distribution ratio, the ratio of the mass of solute contained in immobile fluid to the mass of solute contained in the mobile phase evaluated at equilibrium with C_o equal to $(1 - \epsilon)\epsilon_p / \epsilon$ (dimensionless)

Dg_s adsorbed solute distribution ratio, the ratio of the mass of adsorbate on the soil surface to the mass of solute contained in the mobile phase evaluated at equilibrium with C_o , equal to $(1 - \epsilon)\rho_p q_e / (\epsilon C_o)$ (dimensionless)

D_M molecular diffusion coefficient of Phenol in water, (L^2 / t)

D_L axial dispersion and diffusion coefficient, (L^2 / t)

D_p pore diffusion coefficient, equal to D_M / τ_p , (L^2 / t)

D_s surface diffusion coefficient (L^2 / t)

Ed particle diffusion modulus, the ratio of the rate of mass transfer due to diffusion within the particle to the rate of mass transfer due to advection, equal $Ed_p + Ed_s$ (dimensionless)

Ed_p pore diffusion modulus, the ratio of the of mass transfer due to pore diffusion within the particle to the rate of mass due to

	advection, equal to $LD_p Dg_p / vr_s^2$ (dimensionless)
Ed_s	surface diffusion modulus, the ratio of the of mass transfer due to surface diffusion within the particle to the rate of mass due to advection, equal to $LD_s Dg_s / vr_s^2$ (dimensionless)
k_f	film transfer coefficient (L / t)
K_{LF}	Langmuir Freundlich isotherm constant, $(L^3/M)^{1/n}$
L	length of column (L)
MC	number of collocation points in the axial direction.
MTZ	mass transfer zone
n	Langmuir Freundlich isotherm constant (dimensionless)
NC	number of collocation points in radial direction
Pe	Peclet number, equal to vL / D_L (dimensionless)
Q	flow rate (L^3 / t)
$q(r, z, t)$	particle phase concentration as a function of radial and axial position and time (M/M)
q_e	particle phase concentration in equilibrium with C_o , (M/M)
r_s	radius of particle, (L)
Re	Reynolds number, (dimensionless)
St	Stanton number, the ratio of the mass transfer due to external liquid phase mass transfer to the mass transfer due to advection, equal to $(1 - \epsilon)k_f L / (\epsilon vr_s)$ (dimensionless)
T	throughput, the ratio of mass of solute fed to the column to the mass of solute in a column saturated to capacity, equal to

	$tv / L(1 + D_g)$ (dimensionless)
t	elapsed time (t)
v	v_s/ε , average interstitial velocity in pores (L/t)
v_s	specific discharge, equal to Q/A (L/t)
W_j^r	orthogonal collocation vector that approximates the Gauss quadrature in the radial direction.
W_i^z	orthogonal collocation vector that approximates the Gauss quadrature in the axial direction.
$X(r, z, t)$	particle concentration including solute pore water and adsorbed on particle surface as a function of radial and axial position and time, equal to $\varepsilon_p C_p(r, z, t) + \rho_p q(r, z, t)$ (M / L ³)
X_e	particle concentration in equilibrium with C_o , $\varepsilon_p C_o + \rho_p q_e$, (M / L ³)
$\bar{X}(\bar{r}, \bar{z}, T)$	$\bar{X}(r, z, t) / X_e$ (dimensionless)
z	axial direction (L)
\bar{z}	z/L (dimensionless)
ε	void fraction of column filled b mobile fluid (dimensionless)
ε_p	void fraction of particle (dimensionless)
μ	fluid viscosity (M/Lt)
ρ_p	particle density, (M / L ³)
τ_p	tortuosity (dimensionless)

CHAPTER FIVE

COMBINED PORE AND SURFACE DIFFUSION WITH REACTION IN PACKED BEDS

5.1 Introduction

Adsorption with reaction studies are usually conducted in batch systems. Practical cases, however, are conducted in packed columns. The adsorption of phenol with reaction conducted in columns exhibits similar characteristics as the batch reactor studies. The principal characteristics have been already discussed in chapter three of this work.

5.2 Literature Survey

Vidic and Suidan (1992) studied the influence of dissolved oxygen on the breakthrough curve for o-cresol. They observed that the size of GAC particles and the initial o-cresol concentration had no detectable influence on either the aerobic and anaerobic adsorption isotherms. There was no biological activity in the isotherm bottles and Freundlich isotherm gave a good fit. The increase in adsorption uptake due to the presence of dissolved oxygen ranges from 22% to 200%. The oxidative coupling reaction accounted for the increase in adsorption uptake. This phenomenon was used to explain the characteristics tail observed in the breakthrough curves for o-cresol reported by Liu and Weber, (1981); Peel and Benedek (1981) and, Seidel and Gelbin (1986).

Abuzaid (1993) conducted parametric studies of the adsorption of phenol, and o-cresol on GAC under the influence of dissolved oxygen in both batch and column systems. The influence of dissolved oxygen level, temperature and

pressure were emphasised. When the adsorption temperature, pH and dissolved oxygen level are fixed, the uptake increases directly with the mass of the GAC used. The uptake increases directly with increase in dissolved oxygen concentration. This fact was noted in the batch studies. The increase in uptake was shown to be the result of the oxidative coupling reactions occurring primarily on the surface of the GAC particles. The uptake for phenol, o-cresol and nitrophenol at 1mg/L under aerobic conditions were respectively 163%, 114%, and 18% higher than the anaerobic uptakes. The reaction, plausibly catalysed by the GAC, takes place between the physisorbed sorbate and chemisorbed oxygen molecules. The products of the reaction were identified as 2,2-dihydroxyl-1, 1-biphenyl, 4-phenoxyphenol and a phenolic trimer. The oxidative coupling reaction is favoured by high temperature and pH (Abuzaid, 1993; Grant and King, 1990; Cooney and Xi, 1992).

Abuzaid (1993) conducted desorption studies to access the reversibility of the adsorption. The recovery efficiencies observed for the anaerobic and aerobic cases were respectively 70% and 23%. The reduction in recovery in the aerobic test is attributed partly to the oxidative coupling reaction occurring on the GAC during the adsorption process. This is supported by the earlier work of Grant and King (1990).

5.3 Theoretical Model

The general descriptive equation are similar to that of the case of adsorption without reaction as presented in section 4.3 of chapter four. The only difference however, is in the particle equation which now includes a reaction term. The initial and boundary conditions are exactly the same.

The general particle equation now becomes

$$\epsilon_p \frac{\partial C_p}{\partial t} + \rho_p \frac{\partial q}{\partial t} = \frac{1}{r^2} \frac{\partial}{\partial r} \left\{ r^2 \left[\epsilon_p D_p \frac{\partial C_p}{\partial r} + \rho_p D_{so} \frac{n}{1 - \bar{q}\lambda} \frac{\partial q}{\partial r} \right] \right\} - R \quad (5.1)$$

where R is the reaction term.

In dimensionless form , we have

$$\begin{aligned} \frac{Dg}{(Dg+1)} \frac{\partial \bar{X}}{\partial T} = \frac{1}{\bar{r}^2} \frac{\partial}{\partial \bar{r}} \left\{ \bar{r}^2 \left[\left(Ed_p - \frac{Dg_p}{Dg_s} \frac{Ed_{so} \cdot n}{1 - \lambda \bar{q}} \right) \frac{\partial \bar{C}_p}{\partial \bar{r}} + \right. \right. \\ \left. \left. \left(1 + \frac{Dg_p}{Dg_s} \right) \left(\frac{Ed_{so} \cdot n}{1 - \lambda \bar{X}} \right) \frac{\partial \bar{X}}{\partial \bar{r}} \right] \right\} - \frac{Dg_p L}{\epsilon_p \nu C_o} R \end{aligned} \quad (5.2)$$

The reaction term R, as defined in chapter three is

$$R = k_{o_2} k_{phe} q_e^m \bar{q}^m (q_{o_2} - q_{o_2, \infty})^n \quad (5.3)$$

A plot of the normalised oxygen concentration decay against time on a log - log basis gave a straight line. The log - log relationship was of the form:

$$\log_e \left(\frac{C_{o_2} - C_{o_2, \infty}}{C_{o_2, 0} - C_{o_2, \infty}} \right) = \log_e k - n'' \log_e t \quad (5.4)$$

where the negative of b is the slope of the plot and natural log of k is the intercept. This reduces to the following :

$$\frac{q_{o_2} - q_{o_2, \infty}}{q_{o_2, 0} - q_{o_2, \infty}} = \frac{C_{o_2} - C_{o_2, \infty}}{C_{o_2, 0} - C_{o_2, \infty}} = kt^{-n''} \quad (5.5)$$

The throughput which is the dimensionless time in this case is defined as

$$T = \frac{tv}{L(Dg + 1)} \quad (5.6)$$

Therefore,

$$t = \frac{TL(Dg + 1)}{v} = \sigma T \quad (5.7)$$

where

$$\sigma = \frac{L(Dg + 1)}{v}$$

We assume a linear isotherm for the oxygen, i.e.

$$q_{o_2} = HC_{o_2} \quad (5.8)$$

Therefore, we have the following ;

$$q_{o_2} - q_{o_2,\infty} = H(C_{o_2,0} - C_{o_2,\infty})kt^{-n''}$$

or

$$q_{o_2} - q_{o_2,\infty} = H(C_{o_2,0} - C_{o_2,\infty})k\sigma^{-n''}t^{-n''} \quad (5.9)$$

The reaction term becomes:

$$R = k_{phc} k_{o_2} q_c^m \left[H(C_{o_2,0} - C_{o_2,\infty})k\sigma^{-n''}T^{-n''} \right]^{n'} \bar{q}^m$$

$$R = \left\{ k_{\text{phe}} k_{\text{o}_2} q_e^m \left[H(C_{\text{o}_2,0} - C_{\text{o}_2,\infty}) k \sigma^{-n''} \right]^{n'} \right\} \bar{q}^m T^{-n''n'} \quad (5.10)$$

Let,

$$K = k_{\text{phe}} k_{\text{o}_2} q_e^m \left[H(C_{\text{o}_2,0} - C_{\text{o}_2,\infty}) k \sigma^{-n''} \right]^{n'} \quad (5.11)$$

The value of n' is assumed to be one. Thus, the reaction rate expression becomes :

$$R = K \bar{q}^m T^{-n''} \quad (5.12)$$

The overall particle equation then becomes ;

$$\begin{aligned} \frac{Dg}{(Dg+1)} \frac{\partial \bar{X}}{\partial T} = \frac{1}{\bar{r}^2} \frac{\partial}{\partial \bar{r}} \left\{ \bar{r}^2 \left[\left(Ed_p - \frac{Dg_p}{Dg_s} \frac{Ed_{so}n}{1-\bar{X}\lambda} \right) \frac{\partial \bar{C}_p}{\partial \bar{r}} + \right. \right. \\ \left. \left. \left(1 + \frac{Dg_p}{Dg_s} \right) \left(\frac{Ed_{so}n}{1-\bar{X}\lambda} \right) \frac{\partial \bar{X}}{\partial \bar{r}} \right] \right\} - \frac{Dg_p I K}{\epsilon_p \nu C_o} T^{-n''} \bar{q}^m \end{aligned} \quad (5.13)$$

The reaction rate is rearranged as follows to facilitate the calculation of the value of the rate constant, K in the particle equation above

$$R = \left[k_{\text{phe}} k_{\text{o}_2} (C_{\text{o}_2,0} - C_{\text{o}_2,\infty}) q_e^m H k \right] \sigma^{-n''} T^{-n''} \bar{q}^m \quad (5.14)$$

The overall rate constants determined in chapter three were given as :

$$K_b = \left[k_{phe} k_{o_2} (C_{o_2,0} - C_{o_2,\infty}) q_e^m H k \right] \left[\frac{r_s^2}{q_{os} D_{os}} \right] \left[\frac{r_s^2}{D_{os}} \right]^{-n''} \quad (5.15)$$

$$K_c = K_b q_{os} \left[\frac{r_s^2}{D_{os}} \right]^{1-n''} \quad (5.16)$$

$$K = K_c \sigma^{-n''} \quad (5.17)$$

The set of descriptive PDEs were converted to a system of ODEs and solved by orthogonal collocation method as described in chapter four. The boundary conditions and initial conditions are unchanged. The particle equation, however is replaced by equation (5.13) to account for the reaction occurring in the particle.

5.4 Results And Discussion.

All other parameters and program input are as presented in chapter four. The only additional parameters are reaction constants. The overall reaction rate calculated as described above are given in Table 5.1. The fits for phenol and o-cresol are shown in Figures 5.1 to 5.4. The RMS values for the fits were in the range of 0.33 - 0.4. The fits for the first order and second order cases were almost identical. The same observation was made in the batch systems.

The fits are general good at the earlier portion of the curve, but deviate more from the experimental readings as the dimensionless concentration tends to unity. This observation may be due to either of two reasons. First, there may be experimental error associated with the difficulty of ensuring accurate measurement

Table 5.1 : Reaction orders and overall constants for column systems

	$n = 0.6$	$n = 0.6$
	order = 1	order = 2
K (phenol)	4.06E-2	9.22E-2
K (o-cresol)	7.68E-2	1.24E-1

of oxygen concentration in the system. Secondly, there may be the problem of oxygen diffusion which is not accounted for by the present reaction model in column systems. Generally, the quality of fits obtained in the batch systems are better than those of the column systems. This is probably due to the fact that in the experimental set-up in the in the column systems there continued to be an input of dissolved oxygen into the system. whereas in the batch system the oxygen was consumed.

5.5 Conclusions and Recommendations.

The adsorption of phenol and its reaction with dissolved oxygen was modelled. The reaction constants used were obtained from the results got in the batch studies. The fits obtained, though representative of the general trend of the experimental data, are not good enough. There is a need to investigate the reaction process separately in a column and devise a more appropriate reaction model.

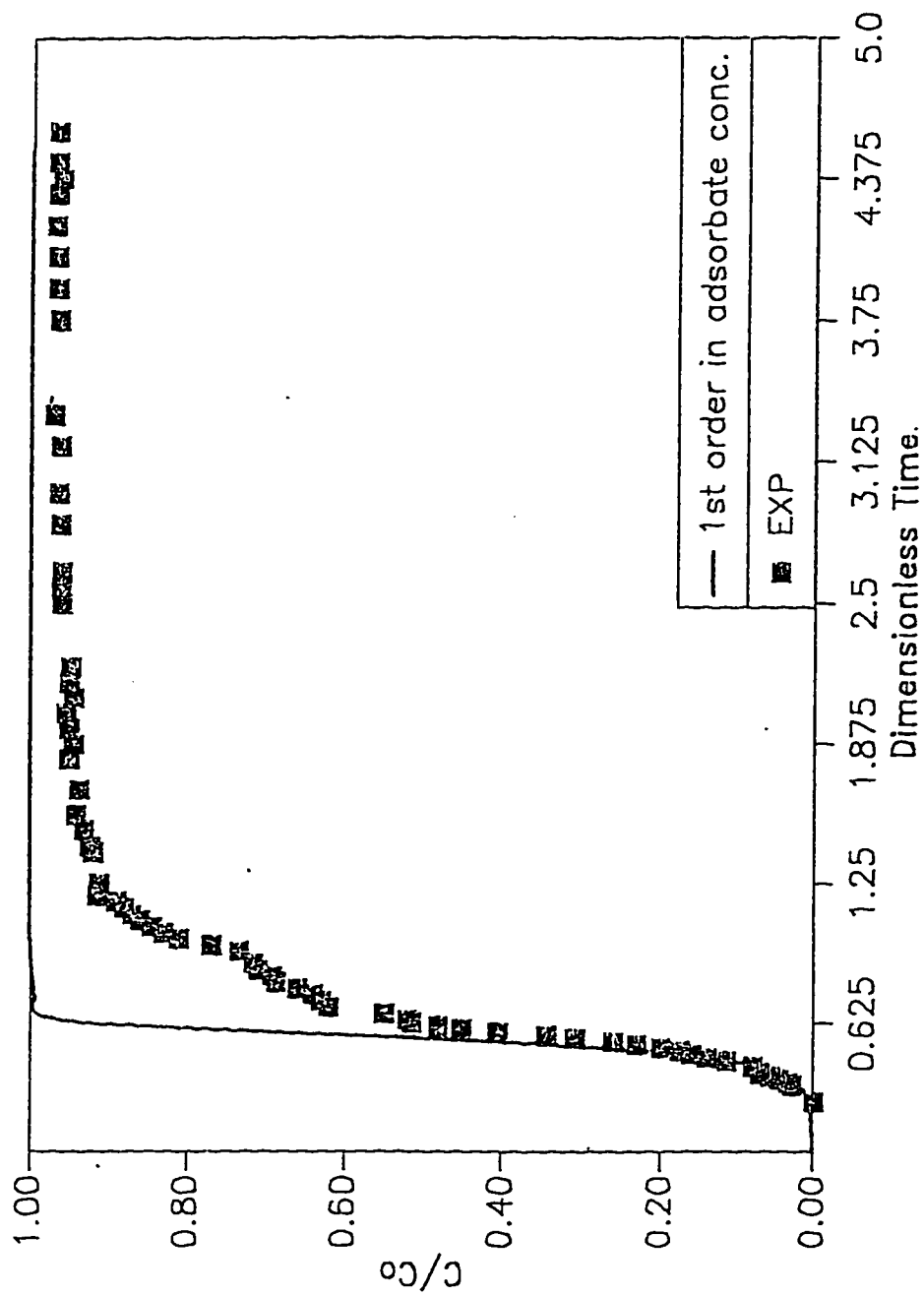


Fig 5.1: Predicted and Experimental Breakthrough Curves
Adsorption with Reaction of phenol in column at 294K.(1st order)

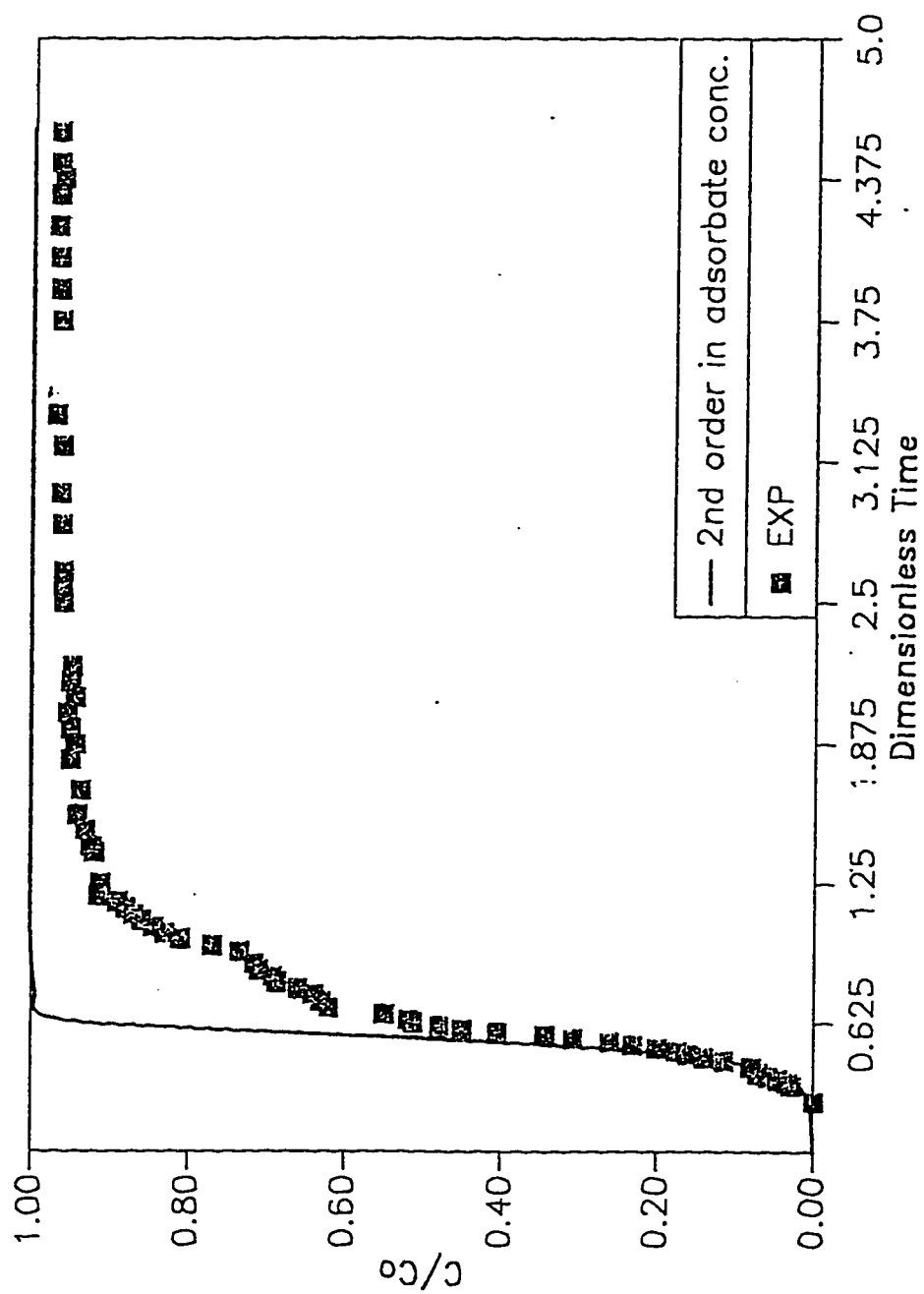


Fig 5.2: Predicted and Experimental Breakthrough Curves
Adsorption with Reaction of Phenol in column at 294K. (2nd order)

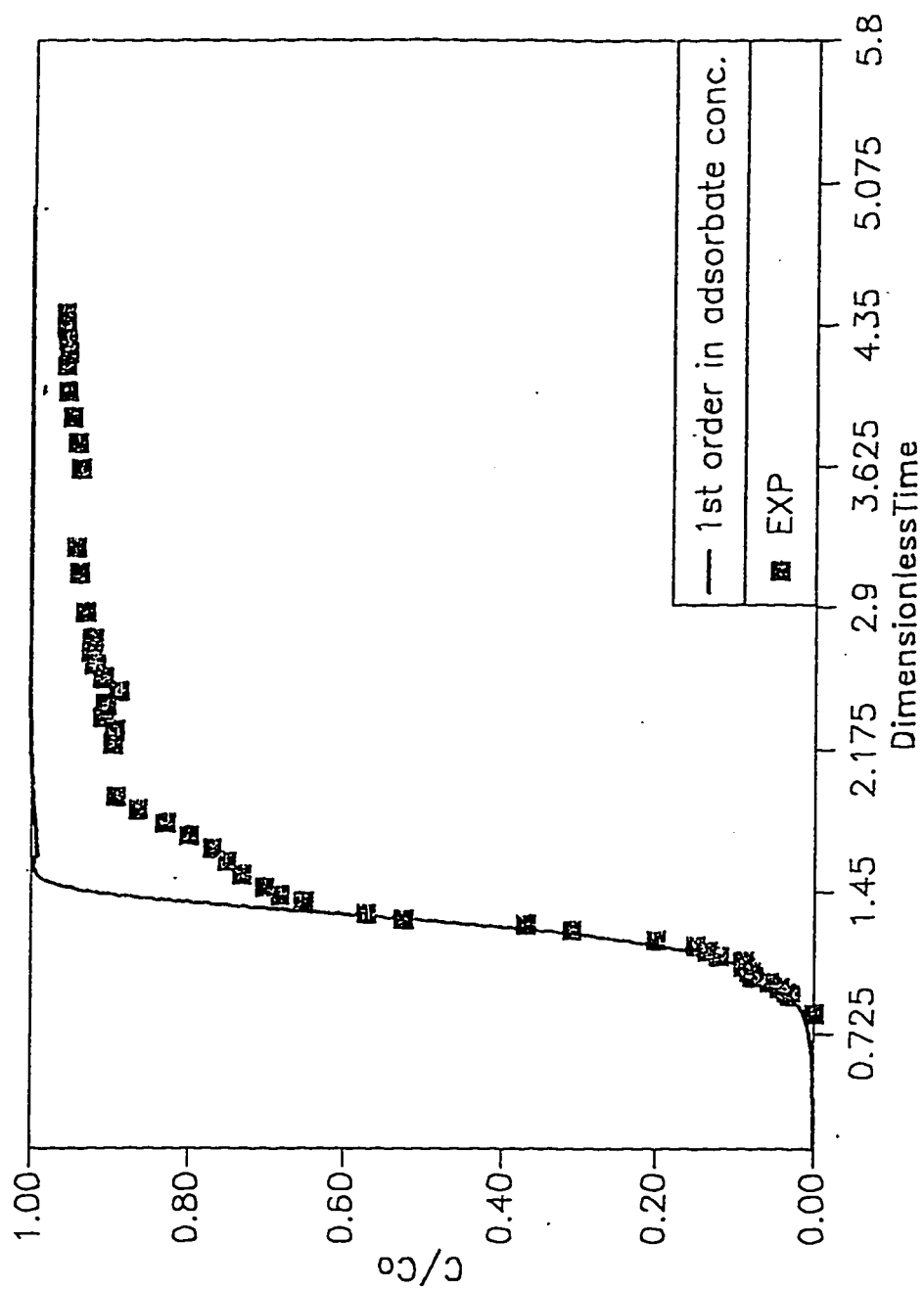


Fig 5.3: Predicted and Experimental Breakthrough Curves
Adsorption with Reaction of o-cresol at 294K. (1st order)

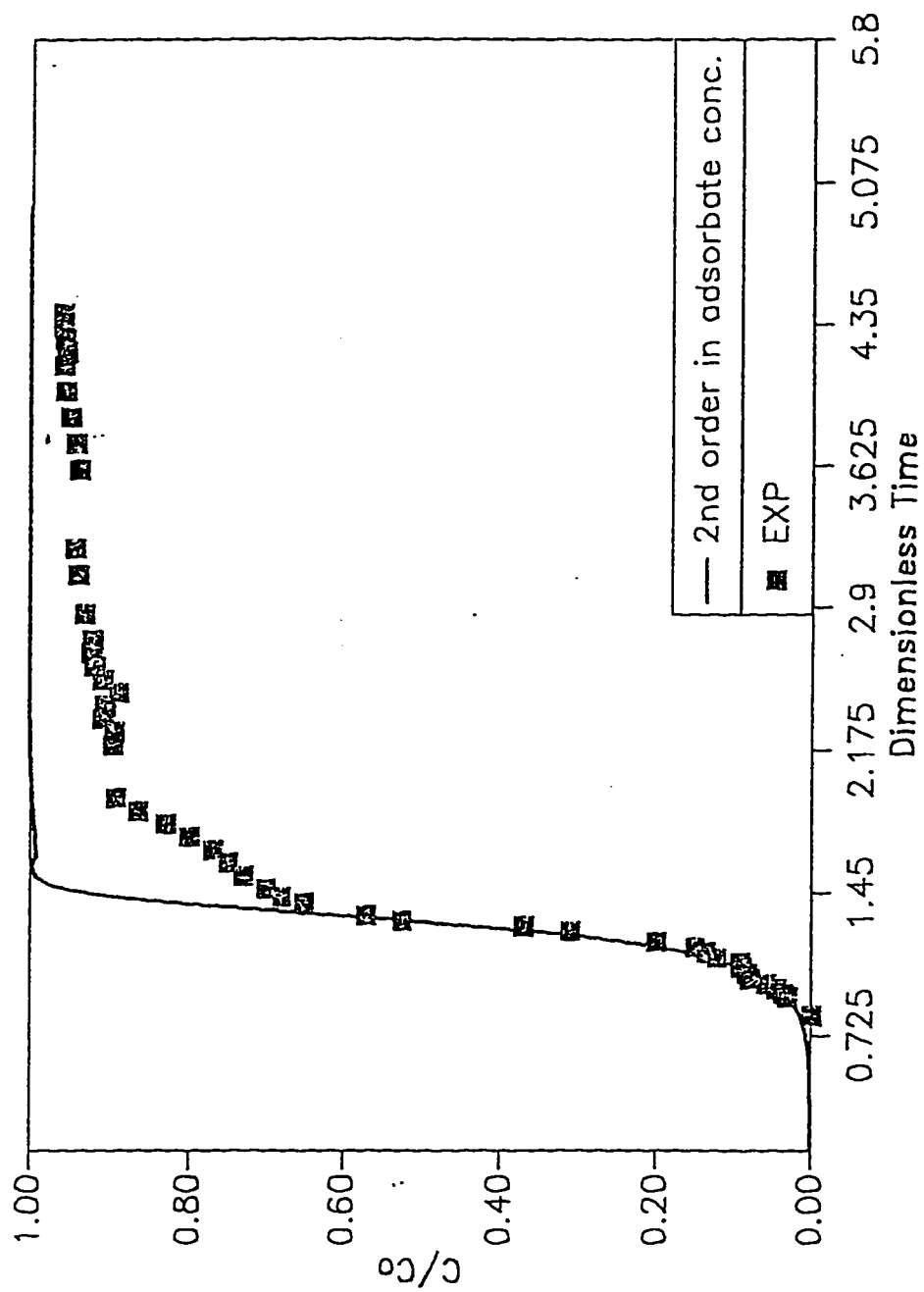


Fig 5.4: Predicted and Experimental Breakthrough Curves. Adsorption with Reaction of o-cresol at 294K. (2nd order)

5.6 Literature Cited

(1) Abuzaid, N. F., "Effect of Dissolved oxygen on Activated Carbon Uptake", PhD Dissertation, Civil Engineering Department, King Fahd University of Petroleum & Minerals, Saudi Arabia, 1993.

(2) Cooney, D.O. and Xi, Z. P., "Activated Carbon can Catalyze Reactions of Phenolics during Liquid Phase adsorption", Separation Division Tropical Conference on Separation Technologies : New Developments and Opportunities, AIChE annual Conference, 415-418, 1992.

(3) Grant, T. M., and King, C. T., "Mechanism of Irreversible Adsorption of Phenolic Compounds by Activated Carbons", Ind. Eng. Chem. Res., 29, 264, 1990.

(4) Liu, K. T., and Weber, W.J., Jr., "Characterisation of mass transfer parameters for adsorber modelling and design", J. Wat. Pollut. Control Fed. 53, 1541, 1981.

(5) Peel, R.G. and Benedek, A., "Dual rate kinetic model of fix bed adsorber." J. Environ. Engng. Div., Am. Soc. Civ Engrs EE4, 797, 1986.

(6) Seidel, A., and Gelbin, D., "Breakthrough curves for single solutes in beds of activated carbon with a broad pore - size distribution - I. Mathematical models of breakthrough curves in beds of activated carbons", Chem. Eng. Sci. 41, 3, 541, 1986.

(7) Vidic, R. D., and Suidan, M. T., "Selecting batch studies for adsorber design : molecular oxygen's role", J. Am. Wat. Wks. Ass." 84, 101, 1992.

CHAPTER SIX

CONCLUSIONS AND RECOMMENDATIONS

Conclusions

- (1) The adsorption of phenol on granular activated carbon (GAC) was effectively modeled using five different models. The models used are the pore diffusion model (PDM), the homogeneous surface diffusion model (HSDM) with constant D_s , the HSDM but accounting for the variation of D_s with adsorbed phase concentration, the pore and surface diffusion model (PSDM) with constant D_s , and the PSDM but accounting for the variation of D_s for the adsorbed phase concentration.
- (2) The PDM proved to be grossly inadequate in predicting the adsorption process when the concentration level of the data is high (1000mg/L)
- (3) The HSDM and PSDM fits were almost identical indicating that the pore diffusion contribution is only significant at the early part of the process and it exerts a notable influence on the shape of D_s versus time plot.
- (4) The variation of D_s with time is significant. However, the influence of this variation on the overall fit is not conspicuous. Hence, compensation for D_s by Darken's relation, though significant on its own, was only slightly reflected in the curves.
- (5) The reaction of phenol with dissolved oxygen at the surface of the GAC was successfully modeled. On final analysis, the best rate form was first order in adsorbed phase concentration and -0.6 order in reaction time.

(6) The actual order with respect to oxygen imbalance was assumed to be 1. There were insufficient data to determine this. The reaction mechanism presented, though plausible, is purely speculative. Actual mechanism and order in oxygen imbalances can only be obtained from further studies with objectives focused on these needs.

(7) The column fits were generally poor. The data were adequately modeled at low reduced concentrations, but at high reduced concentrations (0.86-1.0), there exist some irreconcilable discrepancies. These were attributed to the difficulties experienced in handling the dissolved oxygen during the experimental work as this is continually added to the system during the column studies whereas it diminishes during the batch operation.

Recommendations

(1) Further experimental investigation is needed to truly certify the reaction mechanism and order of the oxygen imbalance.

(2) The influence of the diffusion of oxygen should be investigated in the column by the inclusion of an equation that will account for the diffusion of oxygen .

APPENDICES

Appendix A1

Program for Pore and Surface Diffusion in Batch Systems

FILE: CRANK6N FORTRAN A1 KING FAHD UNIVERSITY OF PETROLEUM AND MINERALS. DIAHRAN

```

***** CRA00010
* APPENDIX A1 * CRA00020
* PROGRAM FOR PORE AND SURFACE DIFFUSION IN BATCH SYSTEMS * CRA00030
* * CRA00040
***** CRA00050
* PROGRAM CRANK6 * CRA00060
* * CRA00070
* * CRA00080
* LAGMUIR FREUNDLICH ISOTHERM : GENERAL PROGRAM FOR PORE AND SURFACE * CRA00090
* DIFFUSION MODEL AND SURFACE DIFFUSION MODEL WITH PROVISION MADE FOR * CRA00100
* ACCOUNTING FOR CONCENTRATION DEPENDENCE VIA DARKEN'S RELATION. * CRA00110
* * CRA00120
* * CRA00130
  IMPLICIT DOUBLE PRECISION ( A-H, O-Z) * CRA00140
  DOUBLE PRECISION KF,NF,LAMBDA * CRA00150
  PARAMETER(N=51,M=1000,NEXP=15) * CRA00160
  DIMENSION Q(N,0:M),QNEW(N),QOLD(N),QAVG(0:M),QMID(N), * CRA00170
  / CBAR(0:M),TAU(0:M),A(N),B(N),C(N),D(N), * CRA00180
  / CCAL(NEXP), TEXP(NEXP),CEXP(NEXP),ETAU(NEXP),DSCAL(NEXP), * CRA00190
  / CTAU(NEXP), SQTAU(NEXP), UPCAL(NEXP),UPEXP(NEXP) * CRA00200
  COMMON /INEXP/TEXP,CEXP * CRA00210
  COMMON /INDATA1/EP,QS,DP,DS,KF,CEOCO,RS,NF * CRA00220
  COMMON /INDATA2/RHOP,CO,TEMP * CRA00230
  COMMON /EPSI/ EPSI1, EPSI2, ERROR * CRA00240
  EXTERNAL AVERAGE,THOMAS,LOAD,INTER,POLATE,INITIA,OUTPUT * CRA00250
  * CRA00260
  CALL INITIA (N,M,PSI,CEQUIL,DTAU,DR,LAMBDA,QINFQO,ALPHA, * CRA00270
  / * CRA00280
  Q,QMID, QAVG,CBAR ) * CRA00290
  * CRA00300
  X = DS/DP * CRA00310
  * CRA00320
*** GENERAL LOOP * CRA00330
  * CRA00340
  DO 400 J = 0, M-1 * CRA00350
  ITER1 = 0 * CRA00360
  ITER2 = 0 * CRA00370
  TAU(J) = REAL(J)*DTAU * CRA00380
399 CONTINUE * CRA00390
  DO 20 I = 1, N * CRA00400
  20 QOLD(I) = Q(I,J) * CRA00410
  IF ( ITER1 .EQ. 0) THEN * CRA00420
  * CRA00430
  QAVG(J+1) = QAVG(J) + EPSI1 * CRA00440
  CHECK = EPSI1 * CRA00450
  ELSE * CRA00460
  * CRA00470
  CALL AVERAGE ( N,QNEW,DR,QAV ) * CRA00480
  CHECK = ABS ( QAVG(J+1) - QAV ) * CRA00490
  QAVG(J+1) = QAV * CRA00500
  * CRA00510
  ENDIF * CRA00520
  * CRA00530
  CBAR(J+1) = CBAR(0)- ALPHA*QAVG(J+1) * CRA00540
  Q(N,J+1) = KF*( CO*CBAR(J+1) )*(1.0D0/NF)/LAMBDA/ * CRA00550
  & ( 1.0D0+KF*(CO*CBAR(J+1))*(1.0D0/NF) )

```

FILE: CRANK6N FORTRAN A1 KING FAHD UNIVERSITY OF PETROLEUM AND MINERALS, DHAHRAN

```

QNEW      = Q(N,J+1)
IF ( ITER2 .EQ. 0 ) THEN
DO 30 I = 1 , N
30 QMID(I) = QMID(I) + EPSI2*(I)
ELSE
DO 40 I = 1 , N
40 QMID(I) = ( Q(I,J) + Q(I,J+1) )/ 2.0D0
ENDIF

ITER1 = ITER1 + 1
ITER2 = ITER2 + 1

CALL LOAD ( X,N,DTAU,DR,LAMBDA,QOLD,QMID,QNEW,A,B,C,D )
CALL THOMAS ( N,A,B,C,D,QNEW )

DO 50 I = 1, N
Q(I,J+1) = QNEW(I)
50 CONTINUE

IF ( (CHECK .GT. ERROR ) .AND. ( ITER1 .LT. 50) ) GOTO 399

C PRINT17, TAU(J), CBAR(J)
C 17 FORMAT(2X,E15.8,2X,E15.8 )

400 CONTINUE
CALL POLATE (M,NEXP,RS,CEOCO,X,CBAR,TAU,TEXP,DP,CEXP,
/          CCAL,DSFIT,SQTAU,UPCAL,UPEXP,RMS,RMS2)

CALL INTER(M,NEXP,RS,X,CEOCO,CBAR,TAU,TEXP,CEXP,CTAU,DSCAL)
CALL OUTPUT(NEXP,CTAU,DSCAL,DSFIT,SQTAU,UPCAL,UPEXP,RMS,RMS2)

END

*****
SUBROUTINE THOMAS ( N,A,B,C,D,X)
IMPLICIT DOUBLE PRECISION ( A-H, O-Z)
*****
* THOMAS ALGORYTHM FOR SOLVING A TRIDIAGONAL MATRIX *
*****

PARAMETER( M =100)
DIMENSION A(N),B(N),C(N),D(N),X(N),GAM(M),BET(M)

BET(1) = B(1)
GAM(1) = D(1)/B(1)
DO 320 I = 2, N
BET(I) = B(I) - A(I)*C(I-1)/BET(I-1)
GAM(I) = ( D(I) - A(I)*GAM(I-1) )/BET(I)
320 CONTINUE
X(N) = GAM(N)
DO 330 I = N -1,1,-1

```

CRA00560
CRA00570
CRA00580
CRA00590
CRA00600
CRA00610
CRA00620
CRA00630
CRA00640
CRA00650
CRA00660
CRA00670
CRA00680
CRA00690
CRA00700
CRA00710
CRA00720
CRA00730
CRA00740
CRA00750
CRA00760
CRA00770
CRA00780
CRA00790
CRA00800
CRA00810
CRA00820
CRA00830
CRA00840
CRA00850
CRA00860
CRA00870
CRA00880
CRA00890
CRA00900
CRA00910
CRA00920
CRA00930
CRA00940
CRA00950
CRA00960
CRA00970
CRA00980
CRA00990
CRA01000
CRA01010
CRA01020
CRA01030
CRA01040
CRA01050
CRA01060
CRA01070
CRA01080
CRA01090
CRA01100

C	CB = C(I)/BET(I)	CRA01110
C	X(I) = GAM(I) - CB*X(I+1)	CRA01120
	X(I) = GAM(I) - C(I)*X(I+1)/BET(I)	CRA01130
330	CONTINUE	CRA01140
		CRA01150
	RETURN	CRA01160
	END	CRA01170
		CRA01180
	*****	CRA01190
	SUBROUTINE AVERAGE(N,Q,DR,QAVG)	CRA01200
*	INTEGRATION VIA SIMPSON'S COMPOSITE RULE	CRA01210
*	RETURNS THE AVERAGE VALUE OF THE SOLID PHASE CONCENTRATION	CRA01220
		CRA01230
	IMPLICIT DOUBLE PRECISION (A-H,O-Z)	CRA01240
	DIMENSION Q(N)	CRA01250
		CRA01260
		CRA01270
	XI0 = Q(1)*0.0*0.0 + Q(N)*1.0*1.0	CRA01280
	XI1 = 0.0D0	CRA01290
	XI2 = 0.0D0	CRA01300
	DO 350 I = 2, N-1	CRA01310
	IF (MOD(I,2) .EQ. 0) THEN	CRA01320
	XI2 = XI2 + Q(I)* ((DR*REAL(I-1))**2)	CRA01330
	ELSE	CRA01340
	XI1 = XI1 + Q(I)* ((DR*REAL(I-1))**2)	CRA01350
	ENDIF	CRA01360
350	CONTINUE	CRA01370
	XI = (DR/3.0D0)*(XI0 + 4.0D0*XI2 + 2.0D0*XI1)	CRA01380
	QAVG = 3.0D0*XI	CRA01390
		CRA01400
	RETURN	CRA01410
	END	CRA01420
		CRA01430
	*****	CRA01440
	SUBROUTINE LOAD (X,N,DTAU,DR,LAMBDA,QOLD,QMID,QNNEW,A,B,C,D)	CRA01450
*		CRA01460
*	THIS PROGRAM CALCULATES THE VALUES OF A,B,C AND D REQUIRED IN THOMAS	CRA01470
*	ALGORYTHM.	CRA01480
*		CRA01490
	IMPLICIT DOUBLE PRECISION (A-H,O-Z)	CRA01500
	DOUBLE PRECISION KF,NF,LAMBDA	CRA01510
	COMMON /INDATA1/EP,QS,DP,DS,KF,CEOCO,RS,NF	CRA01520
	COMMON /INDATA2/RHOP,CO,TEMP	CRA01530
	PARAMETER (M =100)	CRA01540
	DIMENSION QOLD(N),QMID(N),A(M),B(M),C(M),D(M),P(M),F(M),OMEGA(M),	CRA01550
	PO(M)	CRA01560
		CRA01570
	PHI = DTAU/DR**2	CRA01580
	NM1 = N-1	CRA01590
	PSI = EP/RHOP	CRA01600
		CRA01610
	DO 10 I = 1, N	CRA01620
	IF (QMID(I) .GT. 1.0) THEN	CRA01630
	QMID(I) = 0.999990D0	CRA01640
	ELSE	CRA01650

FILE: CRANK6N FORTRAN A1 KING FAHD UNIVERSITY OF PETROLEUM AND MINERALS, DHAHRAN

```

ENDIF
QL = LAMBDA*QMID(I)
IF ( ( QMID(I) .EQ. 0.0).OR.(QL .LT. 1.0E-75) ) THEN
DCDQ = (NF/(KF**NF)/QS)
ELSE
DCDQ = (NF/(KF**NF)/QS)*(QL**((NF-1.0))/((1.0-QL)**(NF+1.0)))
ENDIF

** FOR HSDM CONSTANT DS MODEL :
C PO(I) = X
** FOR HSDM CONCENTRATION DEPEDENT DS MODEL :
C PO(I) = PSI*DCDQ + X
** FOR PSD CONSTANT DS MODEL :
PO(I) = X*NF/(1.0 - QL)
** FOR PSD CONCENTRATION DEPEDENT DS MODEL :
C PO(I) = PSI*DCDQ + X*NF/(1.0 - QL)

10 CONTINUE

DO 20 I = 2, NM1
F(I) = (PHI/4.0D0)*(2.0D0*PO(I)/DBLE(I-1)+(PO(I+1)-PO(I-1))/2.0D0 )
20 CONTINUE

*
* BOUNDARY NODE 1
*
A(1) = 0.0
B(1) = 1.0D0 + 3.0D0*PHI*PO(1)
C(1) = - 3.0D0*PHI*PO(1)
D(1) = ( 2.0D0 - B(1))*QOLD(1) - C(1)*QOLD(2)

*
* INTERIOR NODES 2 TO NM1
*
DO 30 I = 2, NM1
A(I) = -PHI*PO(I)/2.0D0 + F(I)
B(I) = 1.0D0 + PHI*PO(I)
C(I) = -PHI*PO(I)/2.0D0 - F(I)
D(I) = -A(I)*QOLD(I-1)+(2.0-B(I))*QOLD(I)- C(I)*QOLD(I+1)
30 CONTINUE

*
* BOUNDARY NODE N
*
A(N) = 0.0
B(N) = 1.0D0
C(N) = 0.0
D(N) = QNNEW

RETURN
END

*****

SUBROUTINE INTER ( M,NEXP,RS,X,CEOCO,CBAR,TAU,TEXP,
/
CEXP,CTAU,CSCAL)
*****
* THIS SUBROUTINE INTERPOLATES A SET OF DATA LINEARLY.

```

CRA01660
CRA01670
CRA01680
CRA01690
CRA01700
CRA01710
CRA01720
CRA01730
CRA01740
CRA01750
CRA01760
CRA01770
CRA01780
CRA01790
CRA01800
CRA01810
CRA01820
CRA01830
CRA01840
CRA01850
CRA01860
CRA01870
CRA01880
CRA01890
CRA01900
CRA01910
CRA01920
CRA01930
CRA01940
CRA01950
CRA01960
CRA01970
CRA01980
CRA01990
CRA02000
CRA02010
CRA02020
CRA02030
CRA02040
CRA02050
CRA02060
CRA02070
CRA02080
CRA02090
CRA02100
CRA02110
CRA02120
CRA02130
CRA02140
CRA02150
CRA02160
CRA02170
CRA02180
CRA02190
CRA02200

FILE: CRANK6N FORTRAN A1 KING FAHD UNIVERSITY OF PETROLEUM AND MINERALS, DHAHRAN

```

* THE DIFFUSIVITY COEFFICIENT IS CALCULATED FROM THE          * CRA02210
* RELATION : DSCAL = TAU*RS*RS/TIME                            * CRA02220
*                                                              * CRA02230
*****                                                         * CRA02240
*                                                              * CRA02250
      IMPLICIT DOUBLE PRECISION ( A-H, O-Z)                   * CRA02260
      DIMENSION CBAR(M),TAU(M),TEXP(NEXP),CEXP(NEXP),CTAU(NEXP), * CRA02270
      /              DSCAL(NEXP)                               * CRA02280
                                                              * CRA02290
      DO 100 IEXP = 2, NEXP                                    * CRA02300
*                                                              * CRA02310
* SCAN THROUGH THE DATA                                       * CRA02320
*                                                              * CRA02330
      ISCAN = 0                                                 * CRA02340
10 CONTINUE                                                     * CRA02350
      ISCAN = ISCAN + 1                                          * CRA02360
      IF ( CEXP(IEXP) .LT. CBAR(ISCAN) ) GOTO 10                * CRA02370
*                                                              * CRA02380
* INTERPOLATE USING LINEAR INTERPOLATION SCHEME               * CRA02390
*                                                              * CRA02400
      CTAU(IEXP) = ( TAU(ISCAN) - TAU(ISCAN+1) ) .             * CRA02410
      /                *( ( CEXP(IEXP) - CBAR(ISCAN+1)) /      * CRA02420
      /                (CBAR(ISCAN)-CBAR(ISCAN+1))) + TAU(ISCAN+1) * CRA02430
      DPCAL = CTAU(IEXP)*RS*RS/( TEXP(IEXP)*60.0**2)           * CRA02440
      DSCAL(IEXP) = DPCAL*X                                       * CRA02450
                                                              * CRA02460
100 CONTINUE                                                    * CRA02470
                                                              * CRA02480
      RETURN                                                     * CRA02490
      END                                                         * CRA02500
                                                              * CRA02510
*****                                                         * CRA02520
      SUBROUTINE POLATE (M,NEXP,RS,CEOCO,X,CBAR,TAU,TEXP,DP,CEXP, * CRA02530
      /              CCAL,DSFIT,SQTAU,UPCAL,UPEXP,RMS,RMS2)      * CRA02540
                                                              * CRA02550
*****                                                         * CRA02560
* THIS SUBROUTINE INTERPOLATES A SET OF DATA LINEARLY AND    * CRA02570
* CALCULATES THE ROOT MEAN SQUARE OF THE DEVIATIONS OF        * CRA02580
* PREDICTED CONCENTRATION VALUES FROM EXPERIMENTAL VALUES   * CRA02590
*****                                                         * CRA02600
*                                                              * CRA02610
*                                                              * CRA02620
      IMPLICIT DOUBLE PRECISION ( A-H, O-Z)                   * CRA02630
      PARAMETER ( N = 20 )                                     * CRA02640
      DIMENSION CBAR(M),TAU(M),TEXP(NEXP),CEXP(NEXP),SQTAU(N), * CRA02650
      /              ETAU(N),CCAL(N),UPCAL(N),UPEXP(N)          * CRA02660
                                                              * CRA02670
      DO 10 I = 1, NEXP                                         * CRA02680
      ETAU(I) = DP*TEXP(I)*60.0**2/RS**2                       * CRA02690
10 CONTINUE                                                     * CRA02700
                                                              * CRA02710
      RMS = 0.0                                                 * CRA02720
      RMS2 = 0.0                                                * CRA02730
                                                              * CRA02740
      DO 100 I = 2, NEXP                                        * CRA02750

```


FILE: CRANK6N FORTRAN A1 KING FAHD UNIVERSITY OF PETROLEUM AND MINERALS, DHAHRAN

```

      ISCAN = 0
20  CONTINUE
      ISCAN = ISCAN + 1
      IF ( ETAU(I) .GT. TAU(ISCAN) ) GOTO 20
*
* INTERPOLATE USING LINEAR INTERPOLATION SCHEME
*
      CCAL(I) = (CBAR(ISCAN) - CBAR(ISCAN+1)) * ((ETAU(IEXP) - TAU(ISCAN)) /
/      (TAU(ISCAN) - TAU(ISCAN+1))) + CBAR(ISCAN+1)

      IF ( I .NE. 1 ) THEN
      RMS2 = ( (CEXP(I) - CCAL(I)) / CEXP(I) ) ** 2 + RMS2
      ELSE
      ENDIF
      RMS = ( (CEXP(I) - CCAL(I)) / CEXP(I) ) ** 2 + RMS

      SQTAU(I) = SQRT( ETAU(I) )
      UPCAL(I) = ABS(1.0 - CCAL(I)) / (1.0 - CEOCO )
      UPEXP(I) = ABS(1.0 - CEXP(I)) / (1.0 - CEOCO )

100 CONTINUE

      RMS = 100.0 * SQRT(RMS / REAL(NEXP))
      RMS2 = 100.0 * SQRT(RMS2 / REAL(NEXP-1))
      DSFIT = DP * X

      RETURN
      END

*****
      BLOCK DATA
      IMPLICIT DOUBLE PRECISION (A-H, O-Z)
      DOUBLE PRECISION KF, NF
      PARAMETER ( N = 15 )
      DIMENSION TEXP(N), CEXP(N)
      COMMON /INDATA1/ EP, QS, DP, DS, KF, CEOCO, RS, NF
      COMMON /INDATA2/ RHOP, CO, TEMP
      COMMON /INEXP/ TEXP, CEXP
      COMMON /EPSI/ EPSI1, EPSI2, ERROR

      DATA EPSI1, EPSI2, ERROR / 1.0D-8, 1.0D-9, 1.0D-13 /
      DATA EP, RHOP, QS, DP, DS, KF, CEOCO, TEMP, RS, NF, CO / 0.63, 0.67E6, 0.25,
/ 1.3957E-6, 1.12E-8, 0.1873, 0.213, 8.0, 0.078, 3.125, 1000.0 /

* PH 7, TEMP 8 C; OXYGEN PURGED = 0.00, C MASS = 28.6
* EXPERIMENTAL TIME AND REDUCED CONCENTRATION

      DATA TEXP / 0.0, 0.16, 0.50, 1.083, 1.583, 2.083, 3.083, 5.083, 7.083,
/ 9.583, 12.083, 24.083, 36.083, 48.083, 72.083 /
      DATA CEXP / 1.0, 0.751, 0.595, 0.465, 0.373, 0.355, 0.328, 0.296,
/ 0.289, 0.281, 0.271, 0.249, 0.237, 0.226, 0.213 /

      END
*****

```

FILE: CRANK6N FORTRAN A1 KING FAHD UNIVERSITY OF PETROLEUM AND MINERALS. DIAHRAN

```

      SUBROUTINE INITIA (N,M,PSI,CEQUIL,DTAU,DR,LAMBDA,QINFQO,ALPHA,
      /
      Q,QMID, QAVG,CBAR )
      *
      * THIS SUBROUTINE CALCULATES THE INITIAL VALUES OF THE REQUIRED
      * PARAMETERS
      *
      IMPLICIT DOUBLE PRECISION (A-H, O-Z)
      DOUBLE PRECISION KF,NF,LAMBDA
      PARAMETER ( NN = 100 )
      DIMENSION Q(NN,0:1),QMID(NN), QAVG(0:1),CBAR(0:1)
      C DIMENSION Q(NN,0),QMID(NN), QAVG(MM),CBAR(MM)
      COMMON /INDATA1/EP,QS,DP,KF,CEOCO,RS,NF
      COMMON /INDATA2/RHOP,CO,TEMP
      COMMON /EPSI/ EPSI1, EPSI2, ERROR

      PSI = EP/RHOP
      CEQUIL = CO*CEOCO
      UPTAKE = 1.0D0 - CEOCO
      DTAU = 100.0D0/DBLE( M )
      DR = 1.0D0/DBLE( N-1 )

      LAMBDA = KF*CO**((1.0/NF))/( 1.0D0 + KF*CO**((1.0/NF) )
      QINFQO = KF*(CEQUIL)**((1.0D0/NF)/LAMBDA/
      & ( 1.0D0+KF*(CEQUIL)**((1.0D0/NF) )
      ALPHA = (1.0D0 - CEOCO)/QINFQO

      *** INITIALIZATION : AT TAU = 0
      DO 10 I = 1,N
      Q(I,0) = 0.0D0
      QMID(I) = EPSI2*DBLE(I)
      10 CONTINUE
      QAVG(0) = 0.0D0
      CBAR(0) = 1.0D0

      WRITE(7,*) NF,KF,CO,CEOCO
      PRINT20, NF,KF,CO,CEOCO
      20 FORMAT(7X,' ADSORPTION OF PHENOL ON GAC ',
      / ,7X, 30('-'), /,
      / ,3X,'LANGMUIR FREUNDLICH ISOTHERM CONSTANT = ',F9.3.
      / ,3X,'LANGMUIR FREUNDLICH EQUILIBRIUM PARAMETER = ',F9.3.
      / ,3X,'INITIAL CONCENTRATION = ',F9.3.
      / ,3X,'CBAR AT INFINITY = ',F9.3)

      PRINT30, LAMBDA, UPTAKE, QINFQO,ALPHA
      30 FORMAT( 1X, ' LAMBDA = ',F6.3.
      / ,1X, ' UPTAKE = ',F6.3.
      / ,1X, ' QBAR AT INFINITY(QINFQO) = ',F6.3.
      / ,1X, ' ALPHA = ',F6.3 )

      RETURN
      END

      *****
      SUBROUTINE OUTPUT(N,CTAU,DSCAL,DSFIT,SQTAU,UPCAL,UPEXP,RMS,RMS2)

```

FILE: CRANK6N FORTRAN A1 KING FAHD UNIVERSITY OF PETROLEUM AND MINERALS, DHAHRAN

IMPLICIT DOUBLE PRECISION (A-H, O-Z)	CRA03860
DIMENSION SQTAU(N),CTAU(N),DSCAL(N),UPCAL(N),UPEXP(N)	CRA03870
	CRA03880
PRINT5	CRA03890
5 FORMAT(/,4X,'I',11X,'SQTAU(I)',9X,'UPEXP(I)',9X,'UPEXP(I)',/,	CRA03900
/ 65('=')))	CRA03910
DO 10 I = 1, N	CRA03920
10 PRINT20,I, SQTAU(I), UPEXP(I), UPCAL(I)	CRA03930
20 FORMAT(3X,I2, 5X,F12.6, 5X, F12.6,5X,F12.6./)	CRA03940
	CRA03950
PRINT30	CRA03960
30 FORMAT(/,4X,'I',11X,'CTAU(I)',9X,'DSCAL(I)',/,	CRA03970
/ 45('=')))	CRA03980
DO 40 I = 1, N	CRA03990
40 PRINT50,I, CTAU(I), DSCAL(I)	CRA04000
50 FORMAT(3X,I2, 5X,F12.6, 5X, E12.6./)	CRA04010
PRINT*, 'BEST FIT DS VALUE IS =', DSFIT	CRA04020
PRINT*, 'RMS VALUE IS =', RMS2	CRA04030
	CRA04040
	CRA04050
RETURN	CRA04060
END	CRA04070
	CRA04080

Appendix A2

Optimization Program to Calculate Parameters for Batch Diffusion Systems.

FILE: A2 FORTRAN A1 KING FAHD UNIVERSITY OF PETROLEUM AND MINERALS, DHAHRAN

```

***** A2 00010
* APPENDIX A2 * A2 00020
* OPTIMIZATION PROGRAM TO CALCULATE PARAMETERS FOR DIFFUSION * A2 00030
* * A2 00040
* THIS PROGRAM CALCULATES  $X = DS/DP$  FROM WHICH  $DS$  IS OBTAINED * A2 00050
* * A2 00060
***** A2 00070
C----- A2 00080
C IMSL Name: ECPOL/DBCPOL (Single/Double precision version) A2 00090
C A2 00100
C Purpose: Minimize a function of N variables subject to bounds on A2 00110
C the variables using a direct search complex algorithm. A2 00120
C A2 00130
C Usage: CALL BCPOL (FCN, N, XGUESS, IBTYPE, XLB, XUB, FTOL, A2 00140
C MAXFCN, X, FVALUE) A2 00150
C A2 00160
C----- A2 00170
C A2 00180
C INTEGER N A2 00190
C PARAMETER (N=1) A2 00200
C A2 00210
C INTEGER IBTYPE, K, MAXFCN, NOUT A2 00220
C REAL FTOL, FVALUE, X(N), XGUESS(N), XLB(N), XUB(N) A2 00230
C EXTERNAL BCPOL, FCN, UMACH A2 00240
C A2 00250
C DATA XGUESS/1.2/, XLB/2.0E-5/, XUB/1.0/ A2 00260
C A2 00270
C FTOL = 1.0E-5 A2 00280
C IBTYPE = 0 A2 00290
C MAXFCN = 300 A2 00300
C A2 00310
C CALL BCPOL (FCN, N, XGUESS, IBTYPE, XLB, XUB, FTOL, MAXFCN, X, A2 00320
C & FVALUE) A2 00330
C A2 00340
C CALL UMACH (2, NOUT) A2 00350
C WRITE (NOUT,99) X(1), FVALUE A2 00360
99 FORMAT (' THE BEST ESTIMATE FOR THE MINIMUM VALUE OF THE', /, A2 00370
C & ' FUNCTION IS X = (', (2X,F4.2), ')', /, ' WITH ' A2 00380
C & 'function value FVALUE = ', E12.6) A2 00390
C A2 00400
C END A2 00410
C A2 00420
C External function to be minimized A2 00430
C A2 00440
C SUBROUTINE FCN (N, X, F) A2 00450
C INTEGER N A2 00460
C REAL X(N), F A2 00470
C A2 00480
C CALL CRANK6N ( X, RMS ) A2 00490
C F = RMS A2 00500
C RETURN A2 00510
C END A2 00520
C A2 00530
***** A2 00540
* A2 00550

```

FILE: A2 FORTRAN A1 KING FAHD UNIVERSITY OF PETROLEUM AND MINERALS, DHAIRAN

```

SUBROUTINE CRANK6N (X, RMS)
*
* LAGMUIR FREUNDLICH ISOTHERM : GENERAL PROGRAM FOR PORE AND SURFACE
* DIFFUSION MODEL AND SURFACE DIFFUSION MODEL WITH PROVISION MADE FOR
* ACCOUNTING FOR CONCENTRATION DEPENDENCE VIA DARKEN'S RELATION.
*
*
      IMPLICIT DOUBLE PRECISION ( A-H, O-Z)
      DOUBLE PRECISION KF,NF,LAMBDA
      PARAMETER(N=51,M=1000,NEXP=15)
      DIMENSION Q(N,0:M),QNEW(N),QOLD(N),QAVG(0:M),QMID(N),
/ CBAR(0:M),TAU(0:M),A(N),B(N),C(N),D(N),
/ CCAL(NEXP), TEXP(NEXP),CEXP(NEXP),ETAU(NEXP),DSCAL(NEXP),
/ CTAU(NEXP), SQTAU(NEXP), UPCAL(NEXP),UPEXP(NEXP)
      COMMON /INEXP/TEXP,CEXP
      COMMON /INDATA1/EP,QS,DP,KF,CEOCO,RS,NF
      COMMON /INDATA2/RHOP,CO,TEMP
      COMMON /EPSI/ EPSI1, EPSI2, ERROR
      EXTERNAL AVERAGE,THOMAS,LOAD,INTER,POLATE,INITIA,OUTPUT

      CALL INITIA (N,M,PSI,CEQUIL,DTAU,DR,LAMBDA,QINFQO,ALPHA,
/ Q,QMID, QAVG,CBAR )

*** GENERAL LOOP

      DO 400 J = 0, M-1
      ITER1 = 0
      ITER2 = 0
      TAU(J) = REAL(J)*DTAU
399 CONTINUE
      DO 20 I = 1, N
      20 QOLD(I) = Q(I,J)
      IF ( ITER1 .EQ. 0 ) THEN

      QAVG(J+1) = QAVG(J) + EPSI1
      CHECK = EPSI1
      ELSE

      CALL AVERAGE ( N,QNEW,DR,QAV )
      CHECK = ABS ( QAVG(J+1) - QAV )
      QAVG(J+1) = QAV

      ENDIF

      CBAR(J+1) = CBAR(0)- ALPHA*QAVG(J+1)
      Q(N,J+1) = KF*( CO*CBAR(J+1) )*(1.0D0/NF)/LAMBDA/
& ( 1.0D0+KF*(CO*CBAR(J+1))*(1.0D0/NF) )

      QNEW = Q(N,J+1)

      IF ( ITER2 .EQ. 0 ) THEN

      DO 30 I = 1, N
      30 QMID(I) = QMID(I) + EPSI2*(I)
      ELSE

```

FILE: A2 FORTRAN A1 KING FAHD UNIVERSITY OF PETROLEUM AND MINERALS, DHAHRAN

```

DO 40 I = 1, N
40 QMID(I) = ( Q(I,J) + Q(I,J+1) ) / 2.000
ENDIF

ITER1 = ITER1 + 1
ITER2 = ITER2 + 1

CALL LOAD ( X,N,DTAU,DR,LAMBDA,QOLD,QMID,QNEW,A,B,C,D )
CALL THOMAS ( N,A,B,C,D,QNEW )

DO 50 I = 1, N
Q(I,J+1) = QNEW(I)
50 CONTINUE

IF ( (CHECK.GT.ERROR) .AND. ( ITER1.LT.50) ) GOTO 399

400 CONTINUE
CALL POLATE (M,NEXP,RS,CEOCO,X,CBAR,TAU,TEXP,DP,CEXP,
/          CCAL,DSFIT,SQTAU,UPCAL,UPEXP,RMS,RMS2)

C CALL INTER(M,NEXP,RS,X,CEOCO,CBAR,TAU,TEXP,CEXP,CTAU,DSCAL)
CALL OUTPUT(NEXP,CTAU,DSCAL,DSFIT,SQTAU,UPCAL,UPEXP,RMS,RMS2)

END

*****
SUBROUTINE THOMAS ( N,A,B,C,D,X)
IMPLICIT DOUBLE PRECISION ( A-H, O-Z)
*****
* THOMAS ALGORYTHM FOR SOLVING A TRIDIAGONAL MATRIX *
*****

PARAMETER( M =100)
DIMENSION A(N),B(N),C(N),D(N),X(N),GAM(M),BET(M)

BET(1) = B(1)
GAM(1) = D(1)/B(1)
DO 320 I = 2, N
BET(I) = B(I) - A(I)*C(I-1)/BET(I-1)
GAM(I) = ( D(I) - A(I)*GAM(I-1) )/BET(I)
320 CONTINUE
X(N) = GAM(N)
DO 330 I = N -1,1,-1
X(I) = GAM(I) - C(I)*X(I+1)/BET(I)
330 CONTINUE

RETURN
END

*****
SUBROUTINE AVERAGE( N,Q,DF,QAVG)
* INTEGRATION VIA SIMPSON'S COMPOSITE RULE

```

FILE: A2 FORTRAN A1 KING FAHD UNIVERSITY OF PETROLEUM AND MINERALS, DHAHRAN

```

* RETURNS THE AVERAGE VALUE OF THE SOLID PHASE CONCENTRATION
      IMPLICIT DOUBLE PRECISION (A-H,O-Z)
      DIMENSION Q(N)

      X10 = Q(1)*0.0*0.0 + Q(N)*1.0*1.0
      X11 = 0.0D0
      X12 = 0.0D0
      DO 350 I = 2, N-1
        IF ( MOD(I,2) .EQ. 0 ) THEN
          X12 = X12 + Q(I)*( (DR*REAL(I-1))**2 )
        ELSE
          X11 = X11 + Q(I)*( (DR*REAL(I-1))**2 )
        ENDIF
      350 CONTINUE
      XI = (DR/3.0D0)*( X10 + 4.0D0*X12 + 2.0D0*X11 )
      QAVG = 3.0D0*XI

      RETURN
      END

*****
      SUBROUTINE LOAD ( X,N,DTAU,DR,LAMBDA,QOLD,QMID,QNNEW,A,B,C,D )
*
*THIS PROGRAM CALCULATES THE VALUES OF A,B,C AND D REQUIRED IN THOMAS
* ALGORYTHM.
*
      IMPLICIT DOUBLE PRECISION ( A-H,O-Z)
      DOUBLE PRECISION KF,NF,LAMBDA
      COMMON /INDATA1/EP,QS,DP,KF,CEOCO,RS,NF
      COMMON /INDATA2/RHOP,CO,TEMP
      PARAMETER ( M =100 )
      DIMENSION QOLD(N),QMID(N),A(M),B(M),C(M),D(M),P(M),F(M),OMEGA(M),
      /      PO(M)

      PHI = DTAU/DR**2
      NM1 = N-1
      PSI = EP/RHOP

      DO 10 I = 1, N
        IF ( QMID(I) .GT. 1.0 ) THEN
          QMID(I) = 0.999990D0
        ELSE
          ENDIF
          QL = LAMBDA*QMID(I)
          IF ( ( QMID(I) .EQ. 0.0 ).OR. (QL .LT. 1.0E-75) ) THEN
            DCDQ = (NF/(KF**NF))/QS
          ELSE
            DCDQ = (NF/(KF**NF))/QS*(QL**(NF-1.0))/((1.0-QL)**(NF+1.0))
          ENDIF

** FOR HSDM CONSTANT DS MODEL :
C      PO(I) = X
** FOR HSDM CONCENTRATION DEPEDENT DS MODEL :
C      PO(I) = PSI*DCDQ + X

```


FILE: A2 FORTRAN A1 KING FAHD UNIVERSITY OF PETROLEUM AND MINERALS. DHAHRAN

```

** FOR PSD CONSTANT DS MODEL :
    PO(I) = X*NF/(1.0 - QL)
** FOR PSD CONCENTRATION DEPEDENT DS MODEL :
C    PO(I) = PSI*DCDQ + X*NF/(1.0 - QL)

10 CONTINUE

    DO 20 I = 2, NM1
        F(I) = (PHI/4.0D0)*(2.0D0*PO(I)/DBLE(I-1) + (PO(I+1)-PO(I-1))/2.0D0 )
    20 CONTINUE
*
* BOUNDARY NODE 1
*
    A(1) = 0.0
    B(1) = 1.0D0 + 3.0D0*PHI*PO(1)
    C(1) = - 3.0D0*PHI*PO(1)
    D(1) = ( 2.0D0 - B(1))*QOLD(1) - C(1)*QOLD(2)
*
* INTERIOR NODES 2 TO NM1
*
    DO 30 I = 2, NM1
        A(I) = -PHI*PO(I)/2.0D0 + F(I)
        B(I) = 1.0D0 + PHI*PO(I)
        C(I) = -PHI*PO(I)/2.0D0 - F(I)
        D(I) = -A(I)*QOLD(I-1) + (2.0-B(I))*QOLD(I) - C(I)*QOLD(I+1)
    30 CONTINUE
*
* BOUNDARY NODE N
*
    A(N) = 0.0
    B(N) = 1.0D0
    C(N) = 0.0
    D(N) = QNNEW

    RETURN
    END

*****
      SUBROUTINE INTER ( M,NEXP,RS,X,CEOCO,CBAR,TAU,TEXP,
/                   CEXP,CTAU,DSCAL)
*****
* THIS SUBROUTINE INTERPOLATES A SET OF DATA LINEARLY.
* THE DIFFUSIVITY COEFFICIENT IS CALCULATED FROM THE
* RELATION : DSCAL = TAU*RS*RS/TIME
*
*****
*
      IMPLICIT DOUBLE PRECISION ( A-H, O-Z)
      DIMENSION CBAR(M),TAU(M),TEXP(NEXP),CEXP(NEXP),CTAU(NEXP),
/              DSCAL(NEXP)

      DO 100 IEXP = 2, NEXP
*
* SCAN THROUGH THE DATA

```

FILE: A2 FORTRAN A1 KING FAHD UNIVERSITY OF PETROLEUM AND MINERALS, DHAHRAN

```

*
      ISCAN = 0
10  CONTINUE
      ISCAN = ISCAN + 1
      IF ( CEXP(IEXP) .LT. CBAR(ISCAN) ) GOTO 10
*
* INTERPOLATE USING LINEAR INTERPOLATION SCHEME
*
      CTAU(IEXP) = ( TAU(ISCAN) - TAU(ISCAN+1) )
/
      * ( ( CEXP(IEXP) - CBAR(ISCAN+1)) /
/
      (CBAR(ISCAN) - CBAR(ISCAN+1)) ) + TAU(ISCAN+1)
      DPCAL = CTAU(IEXP) * RS * RS / ( TEXP(IEXP) * 60.0 ** 2 )
      DSCAL(IEXP) = DPCAL * X
100 CONTINUE

      RETURN
      END
*****
      SUBROUTINE POLATE (M,NEXP,RS,CEOCO,X,CBAR,TAU,TEXP,DP,CEXP,
/
      CCAL,DSFIT,SQTAU,UPCAL,UPEXP,RMS,RMS2)
*****
* THIS SUBROUTINE INTERPOLATES A SET OF DATA LINEARLY AND
* CALCULATES THE ROOT MEAN SQUARE OF THE DEVIATIONS OF
* PREDICTED CONCENTRATION VALUES FROM EXPERIMENTAL VALUES
*****
*
      IMPLICIT DOUBLE PRECISION ( A-H, O-Z)
      PARAMETER ( N = 20 )
      DIMENSION CBAR(M),TAU(M),TEXP(NEXP),CEXP(NEXP),SQTAU(N),
/
      ETAU(N),CCAL(N),UPCAL(N),UPEXP(N)

      DO 10 I = 1, NEXP
      ETAU(I) = DP * TEXP(I) * 60.0 ** 2 / RS ** 2
10  CONTINUE

      RMS = 0.0
      RMS2 = 0.0

      DO 100 I = 2, NEXP
      ISCAN = 0
20  CONTINUE
      ISCAN = ISCAN + 1
      IF ( ETAU(I) .GT. TAU(ISCAN) ) GOTO 20
*
* INTERPOLATE USING LINEAR INTERPOLATION SCHEME
*
      CCAL(I) = (CBAR(ISCAN) - CBAR(ISCAN+1)) * ((ETAU(IEXP) - TAU(ISCAN)) /
/
      (TAU(ISCAN) - TAU(ISCAN+1))) + CBAR(ISCAN+1)

      IF ( I .NE. 1 ) THEN
      RMS2 = ( (CEXP(I) - CCAL(I)) / CEXP(I) ) ** 2 + RMS2

```

FILE: A2 FORTRAN A1 KING FAHD UNIVERSITY OF PETROLEUM AND MINERALS, DHAHRAN

```

ELSE
ENDIF
RMS = ( (CEXP(I)-CCAL(I))/CEXP(I) )**2 + RMS

SQTau(I) = SQRT( ETAU(I) )
UPCAL(I) = ABS(1.0 - CCAL(I) )/( 1.0 - CEOCO )
UPEXP(I) = ABS(1.0 - CEXP(I) )/( 1.0 - CEOCO )

100 CONTINUE

RMS = 100.0*SQRT(RMS/REAL(NEXP))
RMS2 = 100.0*SQRT(RMS2/REAL(NEXP-1))
DSFIT = DP*X

RETURN
END

*****
BLOCK DATA
IMPLICIT DOUBLE PRECISION (A-H, O-Z)
DOUBLE PRECISION KF,NF
PARAMETER ( N =15 )
DIMENSION TEXP(N), CEXP(N)
COMMON /INDATA1/EP, QS, DP, KF, CEOCO, RS, NF
COMMON /INDATA2/RHOP, CO, TEMP
COMMON /INEXP/TEXP, CEXP
COMMON /EPSI/ EPSI1, EPSI2, ERROR

DATA EPSI1, EPSI2, ERROR / 1.0D-8,1.0D-9,1.0D-13/
DATA EP, RHOP, QS, DP, KF, CEOCO, TEMP, RS, NF, CO / 0.63, 0.67E6, 0.25,
/ 1.3957E-6, 0.1873, 0.213, 8.0, 0.078, 3.125, 1000.0 /

* PH 7, TEMP 8 C; OXYGEN PURGED = 0.00, C MASS = 28.6
* EXPERIMENTAL TIME AND REDUCED CONCENTRATION

DATA TEXP / 0.0, 0.16, 0.50, 1.083, 1.583, 2.083, 3.083, 5.083, 7.083,
/ 9.583, 12.083, 24.083, 36.083, 48.083, 72.083 /
DATA CEXP / 1.0, 0.751, 0.595, 0.465, 0.373, 0.355, 0.328, 0.296,
/ 0.289, 0.281, 0.271, 0.249, 0.237, 0.226, 0.213 /

END

*****
SUBROUTINE INITIA (N,M,PSI,CEQUIL,DTAU,DR,LAMBDA,QINFQO,ALPHA,
/ Q,QMID, QAVG,CBAR )
*
* THIS SUBROUTINE CALCULATES THE INITIAL VALUES OF THE REQUIRED
* PARAMETERS
*
IMPLICIT DOUBLE PRECISION (A-H, O-Z)
DOUBLE PRECISION KF,NF,LAMBDA
PARAMETER ( NN = 100 )
DIMENSION Q(NN,0:1),QMID(NN), QAVG(0:1),CBAR(0:1)
C DIMENSION Q(NN,0),QMID(NN), QAVG(MM),CBAR(MM)
COMMON /INDATA1/EP, QS, DP, KF, CEOCO, RS, NF

```

FILE: A2 FORTRAN A1 KING FAHD UNIVERSITY OF PETROLEUM AND MINERALS. DHAHRAN

```

COMMON /INDATA2/RHOP,CO,TEMP -
COMMON /EPSI/ EPSI1, EPSI2, ERROR

PSI = EP/RHOP
CEQUIL = CO*CEOCO
UPTAKE = 1.0D0 - CEOCO
DTAU = 100.0D0/DBLE( M )
DR = 1.0D0/DBLE( N-1 )

LAMBDA = KF*CO**((1.0/NF)/( 1.0D0 + KF*CO**((1.0/NF) )
QINFQO = KF*(CEQUIL)**((1.0D0/NF)/LAMBDA/
& ( 1.0D0+KF*(CEQUIL)**((1.0D0/NF) )
ALPHA = (1.0D0 - CEOCO)/QINFQO

*** INITIALIZATION : AT TAU = 0
DO 10 I = 1,N
  Q(I,0) = 0.0D0
  QMID(I) = EPSI2*DBLE(I)
10 CONTINUE
  QAVG(0) = 0.0D0
  CBAR(0) = 1.0D0

  WRITE(7,*) NF,KF,CO,CEOCO
  PRINT20, NF,KF,CO,CEOCO
20 FORMAT(7X,' ADSORPTION OF PHENOL ON GAC ',
/      /,7X, 30(' '), /,
/      /,3X,'LANGMUIR FREUNDLICH ISOTHERM CONSTANT = ',F9.3,
/      /,3X,'LANGMUIR FREUNDLICH EQUILIBRIUM PARAMETER = ',F9.3,
/      /,3X,'INITIAL CONCENTRATION = ',F9.3,
/      /,3X,'CBAR AT INFINITY = ',F9.3)

  PRINT30, LAMBDA, UPTAKE, QINFQO,ALPHA
30 FORMAT( 1X, ' LAMBDA = ',F6.3,
/      /,1X, ' UPTAKE = ',F6.3,
/      /,1X, ' QBAR AT INFINITY(QINFQO) = ',F6.3,
/      /,1X, ' ALPHA = ',F6.3 )

  RETURN
END

***** (*****
SUBROUTINE OUTPUT(N,CTAU,DSCAL,DSFIT,SQTAU,UPCAL,UPEXP,RMS,RMS2)
IMPLICIT DOUBLE PRECISION ( A-H, O-Z)
DIMENSION SQTAU(N),CTAU(N),DSCAL(N),UPCAL(N),UPEXP(N)

PRINT5
5 FORMAT(/,4X,'I',11X,'SQTAU(I)',9X,'UPEXP(I)',9X,'UPEXP(I)',/,
/      65(' ') )
DO 10 I = 1, N
10 PRINT20,I, SQTAU(I), UPEXP(I), UPCAL(I)
20 FORMAT( 3X,I2, 5X,F12.6, 5X, F12.6,5X,F12.6,/ )

PRINT30

```

FILE: A2 FORTRAN A1 KING FAHD UNIVERSITY OF PETROLEUM AND MINERALS, DHAHRAN

30	FORMAT(/,4X,'I',11X,'CTAU(I)',9X,'DSCAL(I)'.//,	A2 04410
	/ 45('='))	A2 04420
	DO 40 I = 1, N	A2 04430
40	PRINT50,I, CTAU(I), DSCAL(I)	A2 04440
50	FORMAT(3X,I2, 5X,F12.6, 5X, E12.6,/)	A2 04450
	PRINT*, 'BEST FIT DS VALUE IS =', DSFIT	A2 04460
	PRINT*, 'RMS VALUE IS =', RMS2	A2 04470
	RETURN	A2 04480
	END	A2 04490
		A2 04500

Appendix A3

Program for Pore and Surface Diffusion with Reaction in Batch Systems.

FILE: CRANK8N FORTRAN A1 KING FAHD UNIVERSITY OF PETROLEUM AND MINERALS. DHAHRAN

```

*****
*                               *
*      APPENDIX A3              *
*  PROGRAM FOR PORE & SURFACE DIFFUSION WITH REACTION IN BATCH  *
*  SYSTEMS                      *
*                               *
*****
      PROGRAM CRANK8N
*
*  LAGMUIR FREUNDLICH ISOTHERM : PORE AND SURFACE DIFFUSION MODEL
*  WITH REACTION
*
      IMPLICIT DOUBLE PRECISION ( A-H, O-Z)
      DOUBLE PRECISION KF,NF,LAMBDA
      PARAMETER(N=61,M=2000,NEXP=20 )
      DIMENSION Q(N,0:M),QNEW(N),QOLD(N),QAVG(0:M),QMID(N),
/ CBAR(0:M),TAU(0:M),A(N),B(N),C(N),D(N),
/ CCAL(NEXP), TEXP(NEXP), CEXP(NEXP), ETAU(NEXP), DSCAL(NEXP),
/ CTAU(NEXP),SQTAU(NEXP),UFCAL(NEXP),UPEXP(NEXP), RTERM(NEXP)
      COMMON /INDATA1/EP,QS,DP,KF,CEOCO,RS,NF
      COMMON /INDATA2/RHOP,CO,TEMP
      COMMON /INEXP/TEXP,CEXP
      COMMON /EPSI/ EPSI1, EPSI2, ERROR
      COMMON /RRX/ CONST, ORDER1, ORDER2, RCONC

      EXTERNAL AVERAGE, THOMAS, LOAD, INTER, POLATE,RXN

      CALL INITIA (N,M,PSI,CEQUIL,DTAU,DR,LAMBDA,QINFQO,ALPHA,
/          Q,QMID, QAVG,CBAR )

      DS = 0.98E-8
      DP = 1.3957E-6
C
      X = DP/DS

*** GENERAL LOOP

      DO 400 J = 0, M-1

          ISUME1 = 0
          ISUME2 = 0
          TAU(J) = REAL(J)*DTAU
399 CONTINUE

          DO 20 I = 1, N
20 QOLD(I) = Q(I,J)

          IF ( ISUME1 .EQ. 0) THEN

              QAVG(J+1) = QAVG(J) + EPSI1
              CHECK = EPSI1
              ELSE

              CALL AVERAGE ( N,QNEW,DR,QAV )
              CHECK = ABS ( QAVG(J+1) - QAV )
              QAVG(J+1) = QAV

```

CRA00010
CRA00020
CRA00030
CRA00040
CRA00050
CRA00060
CRA00070
CRA00080
CRA00090
CRA00100
CRA00110
CRA00120
CRA00130
CRA00140
CRA00150
CRA00160
CRA00170
CRA00180
CRA00190
CRA00200
CRA00210
CRA00220
CRA00230
CRA00240
CRA00250
CRA00260
CRA00270
CRA00280
CRA00290
CRA00300
CRA00310
CRA00320
CRA00330
CRA00340
CRA00350
CRA00360
CRA00370
CRA00380
CRA00390
CRA00400
CRA00410
CRA00420
CRA00430
CRA00440
CRA00450
CRA00460
CRA00470
CRA00480
CRA00490
CRA00500
CRA00510
CRA00520
CRA00530
CRA00540
CRA00550

FILE: CRANK8N FORTRAN A1 KING FAHD UNIVERSITY OF PETROLEUM AND MINERALS, DHAHRAN

```

ENDIF
CRA00560

CBAR(J+1) = CBAR(0) - ALPHA*QAVG(J+1)
CRA00570
Q(N,J+1) = KF*( CO*CBAR(J+1) )**((1.0D0/NF)/LAMBDA/
CRA00580
&      ( 1.0D0+KF*(CO*CBAR(J+1))**((1.0D0/NF) )
CRA00590
CRA00600
QNEW      = Q(N,J+1)
CRA00610
CRA00620
IF ( ISUME2 .EQ. 0 ) THEN
CRA00630
CRA00640
CRA00650
CRA00660
DO 30 I = 1 , N
CRA00670
30 QMID(I) = QMID(I) + EPSI2*(I)
CRA00680
ELSE
CRA00690
DO 40 I = 1 , N
CRA00700
40 QMID(I) = ( Q(I,J) + Q(I,J+1) )/ 2.0D0
CRA00710
ENDIF
CRA00720
CRA00730
ISUME1 = ISUME1 + 1
CRA00740
ISUME2 = ISUME2 + 1
CRA00750
CRA00760
DO 45 I = 1 , N
CRA00770
45 RTERM(I) = 0.0
CRA00780
CRA00790
** CALL SUBROUTINE LOAD TO SET UP THE TRIDIAGONAL MATRIX
CRA00800
CALL LOAD (X,RTERM,N,DTAU,DR,QOLD,QMID,QNEW,A,B,C,D,DS,LAMBDA)
CRA00810
CALL THOMAS ( N,A,B,C,D,QNEW )
CRA00820
CRA00830
DO 50 I = 1, N
CRA00840
Q(I,J+1) = QNEW(I)
CRA00850
50 CONTINUE
CRA00860
TAUJ = TAU(J)
CRA00870
CRA00880
IF ( (CHECK .GT. ERROR) .AND. ( ISUME1 .LT. 50) ) GOTO 399
CRA00890
CRA00900
CALL RXN(N,TAUJ,DTAU,RS,DS,RCONC,ORDER1,ORDER2,CONST,QOLD,RTERM)
CRA00910
CRA00920
CALL LOAD (X,RTERM,N,DTAU,DR,QOLD,QMID,QNEW,A,B,C,D,DS,LAMBDA)
CRA00930
CRA00940
CALL THOMAS ( N,A,B,C,D,QNEW )
CRA00950
CRA00960
CBAR(J+1) = CBAR(0) - ALPHA*QAVG(J+1)
CRA00970
Q(N,J+1) = KF*( CO*CBAR(J+1) )**((1.0D0/NF)/LAMBDA/
CRA00980
&      ( 1.0D0+KF*(CO*CBAR(J+1))**((1.0D0/NF) )
CRA00990
CRA01000
QNEW      = Q(N,J+1)
CRA01010
CRA01020
DO 60 I = 1, N
CRA01030
Q(I,J+1) = QNEW(I)
CRA01040
60 CONTINUE
CRA01050
CRA01060
C
PRINT*, TAU(J) , CBAR(J)
CRA01070
WRITE(7,*) TAU(J) , CBAR(J)
CRA01080
CRA01090
CRA01100

```


FILE: CRANK8N FORTRAN A1 KING FAHD UNIVERSITY OF PETROLEUM AND MINERALS, DHAHRAN

```

400 CONTINUE
CALL POLATE (M,NEXP,RS,CEOCO,X,CBAR,TAU,TEXP,DP,CEXP,
/          CCAL,DSFIT,SQTAU,UPCAL,UPEXP,RMS,RMS2)
CALL INTER ( M,NEXP,RS,X,CEOCO,CBAR,TAU,TEXP,
/          CEXP,CTAU,DSCAL)
CALL OUTPUT(NEXP,CTAU,DSCAL,DSFIT,SQTAU,UPCAL,UPEXP,RMS,RMS2)
END

*****
SUBROUTINE THOMAS ( N,A,B,C,D,X)
IMPLICIT DOUBLE PRECISION ( A-H, O-Z)
*****
* THOMAS ALGORYTHM FOR SOLVING A TRIDIAGONAL MATRIX *
*****

PARAMETER( M =100)
DIMENSION A(N),B(N),C(N),D(N),X(N),GAM(M),BET(M)

BET(1) = B(1)
GAM(1) = D(1)/B(1)
DO 320 I = 2, N
  BET(I) = B(I) - A(I)*C(I-1)/BET(I-1)
  GAM(I) = ( D(I) - A(I)*GAM(I-1) )/BET(I)
320 CONTINUE
  X(N) = GAM(N)
  DO 330 I = N -1,1,-1
    IF (X(I+1) .LT. 1.0E-77 ) THEN
      X(I+1) = GAM(I)
    ELSE
      X(I) = GAM(I) - C(I)*X(I+1)/BET(I)
    ENDIF
330 CONTINUE

  DO 333 I = 1,N
333 CONTINUE
  RETURN
END

*****
SUBROUTINE AVERAGE( N,Q,DR,QAVG)
* INTEGRATION VIA SIMPSON'S COMPOSITE RULE
IMPLICIT DOUBLE PRECISION (A-H,O-Z)
DIMENSION Q(N)

XI0 = Q(1)*0.0*0.0 + Q(N)*1.0*1.0
XI1 = 0.000
XI2 = 0.000

```

CRA01110
CRA01120
CRA01130
CRA01140
CRA01150
CRA01160
CRA01170
CRA01180
CRA01190
CRA01200
CRA01210
CRA01220
CRA01230
CRA01240
CRA01250
CRA01260
CRA01270
CRA01280
CRA01290
CRA01300
CRA01310
CRA01320
CRA01330
CRA01340
CRA01350
CRA01360
CRA01370
CRA01380
CRA01390
CRA01400
CRA01410
CRA01420
CRA01430
CRA01440
CRA01450
CRA01460
CRA01470
CRA01480
CRA01490
CRA01500
CRA01510
CRA01520
CRA01530
CRA01540
CRA01550
CRA01560
CRA01570
CRA01580
CRA01590
CRA01600
CRA01610
CRA01620
CRA01630
CRA01640
CRA01650

FILE: CRANK8N FORTRAN A1 KING FAHD UNIVERSITY OF PETROLEUM AND MINERALS, DHAHRAN

```

DO 350 I = 2, N-1
IF ( MOD(I,2) .EQ. 0 ) THEN
XI2 = XI2 + Q(I)*( (DR*REAL(I-1))*2 )
ELSE
XI1 = XI1 + Q(I)*( (DR*REAL(I-1))*2 )
ENDIF
350 CONTINUE
XI = (DR/3.0D0)*( XI0 + 4.0D0*XI2 + 2.0D0*XI1 )
QAVG = 3.0D0*XI

RETURN
END

*****
SUBROUTINE LOAD (X,RTerm,N,DTAU,DR,QOLD,QMID,QNNEW, A,B,C,D,DS,
/
LAMBDA )

IMPLICIT DOUBLE PRECISION ( A-H,O-Z)
DOUBLE PRECISION KF,NF,LAMBDA
COMMON /INDATA1/EP,QS,DP,KF,CEOCO,RS,NF
COMMON /INDATA2/RHOP,CO,TEMP
PARAMETER ( M =100 )
DIMENSION QOLD(N),QMID(N),A(M),B(M),C(M),D(M),P(M),F(M),
/
PO(M),RTerm(N)

PHI = DTAU/DR**2
NM1 = N-1
PSI = EP/RHOP

DO 10 I = 1, N

IF ( QMID(I) .GT. 1.0 ) THEN
QMID(I) = 0.999999990D0
ELSE
ENDIF
CK = 1.0 - QL
IF ( ( QL .LT. 0.0 ) .OR. (CK .LT. 0.0 ) ) THEN
DCDQ = 0.0
ELSE
QL = LAMBDA*QMID(I)
DCDQ =(NF/(KF**NF)/QS)*(QL**(NF-1.0))/((1.0-QL)**(NF+1.0))
ENDIF

* FOR PSD CONSTANT DS MODEL
* PO(I) = PSI*DCDQ*X + 1.0
* FOR PSD WITH VARIABLE DS MODEL
PO(I) = PSI*DCDQ*X + NF/(1.0D0 - LAMBDA*QMID(I) )
* FOR HSSD WITH VARIABLE DS MODEL
* PO(I) = NF/(1.0D0 - LAMBDA*QMID(I) )

10 CONTINUE

DO 20 I = 2, NM1
F(I) =(PHI/4.0D0)*(2.0D0*PO(I)/DBLE(I-1)+(PO(I+1)-PO(I-1))/2.0D0 )
20 CONTINUE

```

CRA01660
CRA01670
CRA01680
CRA01690
CRA01700
CRA01710
CRA01720
CRA01730
CRA01740
CRA01750
CRA01760
CRA01770
CRA01780
CRA01790
CRA01800
CRA01810
CRA01820
CRA01830
CRA01840
CRA01850
CRA01860
CRA01870
CRA01880
CRA01890
CRA01900
CRA01910
CRA01920
CRA01930
CRA01940
CRA01950
CRA01960
CRA01970
CRA01980
CRA01990
CRA02000
CRA02010
CRA02020
CRA02030
CRA02040
CRA02050
CRA02060
CRA02070
CRA02080
CRA02090
CRA02100
CRA02110
CRA02120
CRA02130
CRA02140
CRA02150
CRA02160
CRA02170
CRA02180
CRA02190
CRA02200

FILE: CRANK8N FORTRAN A1 KING FAHD UNIVERSITY OF PETROLEUM AND MINERALS, DHAHRAN

```

*
* BOUNDARY NODE 1
*
      A(1) = 0.0
      B(1) = 1.0D0 + 3.0D0*PHI*PO(1)
      C(1) = - 3.0D0*PHI*PO(1)
      D(1) = ( 2.0D0 - B(1))*QOLD(1) - C(1)*QOLD(2)-RTERM(1)
*
* INTERIOR NODES 2 TO NM1
*
      DO 30 I = 2, NM1
      A(I) = -PHI*PO(I)/2.0D0 + F(I)
      B(I) = 1.0D0 + PHI*PO(I)
      C(I) = -PHI*PO(I)/2.0D0 - F(I)
      D(I) = -A(I)*QOLD(I-1)+(2.0-B(I))*QOLD(I)-C(I)*QOLD(I+1)-RTERM(I)
30  CONTINUE
*
* BOUNDARY NODE N
*
      A(N) = 0.0
      B(N) = 1.0D0
      C(N) = 0.0
      D(N) = QNNEW - RTERM(N)

      RETURN
      END
*****
      SUBROUTINE RXN (N,TAUJ, DTAU, RS,DS,RCONC,ORDER1,ORDER2,
/              CONST,QOLD,RTERM)
      IMPLICIT DOUBLE PRECISION ( A-H, O-Z)
      DIMENSION QOLD(N),RTERM(N)
      TAUJO = 0.0

      SIGMA = RCONC*((RS**2/DS)**ORDER1)
      T2 = TAUJ + DTAU/2.0
      TM = (T2**ORDER1)*SIGMA

      DO 20 I = 1, N
      IF ( QOLD(I) .LT. 0.0 ) THEN
      RTERM(I) = DTAU*CONST*TM
      ELSE
      RTERM(I) = DTAU*CONST*TM*(QOLD(I)**ORDER2)
      ENDIF
20  CONTINUE

      RETURN
      END
*****
      SUBROUTINE INTER ( M,NEXP,RS,X,CEOCO,CBAR,TAU,TEXP,
/              CEXP,CTAU,DSCAL)
*****
* THIS SUBROUTINE INTERPOLATES A SET OF DATA LINEARLY.
* THE DIFFUSIVITY COEFFICIENT IS CALCULATED FROM THE

```

CRA02210
CRA02220
CRA02230
CRA02240
CRA02250
CRA02260
CRA02270
CRA02280
CRA02290
CRA02300
CRA02310
CRA02320
CRA02330
CRA02340
CRA02350
CRA02360
CRA02370
CRA02380
CRA02390
CRA02400
CRA02410
CRA02420
CRA02430
CRA02440
CRA02450
CRA02460
CRA02470
CRA02480
CRA02490
CRA02500
CRA02510
CRA02520
CRA02530
CRA02540
CRA02550
CRA02560
CRA02570
CRA02580
CRA02590
CRA02600
CRA02610
CRA02620
CRA02630
CRA02640
CRA02650
CRA02660
CRA02670
CRA02680
CRA02690
CRA02700
CRA02710
CRA02720
CRA02730
CRA02740
CRA02750

FILE: CRANK8N FORTRAN A1 KING FAHD UNIVERSITY OF PETROLEUM AND MINERALS, DHAHRAN

```

* RELATION : DSCAL = TAU*RS*RS/TIME * CRA02760
* * CRA02770
***** CRA02780
* CRA02790
      IMPLICIT DOUBLE PRECISION ( A-H, O-Z)
      DIMENSION CBAR(M),TAU(M),TEXP(NEXP),CEXP(NEXP),CTAU(NEXP),
/        DSCAL(NEXP)
      DO 100 IEXP = 2, NEXP
*
* SCAN THROUGH THE DATA
*
      ISCAN = 0
10  CONTINUE
      ISCAN = ISCAN + 1
      IF ( CEXP(IEXP) .LT. CBAR(ISCAN) ) GOTO 10
*
* INTERPOLATE USING LINEAR INTERPOLATION SCHEME
*
      CTAU(IEXP) = ( TAU(ISCAN) - TAU(ISCAN+1) )
/        *( ( CEXP(IEXP) - CBAR(ISCAN+1)) /
/        (CBAR(ISCAN)-CBAR(ISCAN+1))) + TAU(ISCAN+1)
      DPCAL = CTAU(IEXP)*RS*RS/( TEXP(IEXP)*60.0**2)
      DSCAL(IEXP) = DPCAL*X
      100 CONTINUE
      RETURN
      END
*****CRA03060
      SUBROUTINE POLATE (M,NEXP,RS,CEOCO,X,CBAR,TAU,TEXP,DP,CEXP,
/        CCAL,DSFIT,SQTAU,UPCAL,UPEXP,RMS,RMS2)
*****CRA03070
* THIS SUBROUTINE INTERPOLATES A SET OF DATA LINEARLY AND
* CALCULATES THE ROOT MEAN SQUARE OF THE DEVIATIONS OF
* PREDICTED CONCENTRATION VALUES FROM EXPERIMENTAL VALUES
*****CRA03110
*
      IMPLICIT DOUBLE PRECISION ( A-H, O-Z)
      PARAMETER ( N = 20 )
      DIMENSION CBAR(M),TAU(M),TEXP(NEXP),CEXP(NEXP),SQTAU(N),
/        ETAU(N),CCAL(N),UPCAL(N),UPEXP(N)
      DO 10 I = 1, NEXP
      ETAU(I) = (DP/X)*TEXP(I)*60.0**2/RS**2
10  CONTINUE
      RMS = 0.0
      RMS2 = 0.0
      DO 100 I = 2, NEXP
      ISCAN = 0

```

FILE: CRANK8N FORTRAN A1 KING FAHD UNIVERSITY OF PETROLEUM AND MINERALS. DHAHRAN

```

20 CONTINUE                                CRA03310
  ISCAN = ISCAN + 1                        CRA03320
  IF ( ETAU(I) .GT. TAU(ISCAN) ) GOTO 20  CRA03330
*                                           CRA03340
* INTERPOLATE USING LINEAR INTERPOLATION SCHEME CRA03350
*                                           CRA03360
  CCAL(I)=(CBAR(ISCAN)-CBAR(ISCAN+1))*((ETAU(IEXP)-TAU(ISCAN))/
/      (TAU(ISCAN) - TAU(ISCAN+1))) + CBAR(ISCAN+1) CRA03370
                                           CRA03380
                                           CRA03390
  IF ( I .NE. 1 ) THEN                    CRA03400
    RMS2 = ( (CEXP(I)-CCAL(I))/CEXP(I) )**2 + RMS2 CRA03410
  ELSE                                     CRA03420
    ENDIF                                  CRA03430
  RMS = ( (CEXP(I)-CCAL(I))/CEXP(I) )**2 + RMS CRA03440
                                           CRA03450
  SQTAU(I) = SQRT( ETAU(I) )              CRA03460
  UPCAL(I) = ABS(1.0 - CCAL(I) )/( 1.0 - CEOCO ) CRA03470
  UPEXP(I) = ABS(1.0 - CEXP(I) )/( 1.0 - CEOCO ) CRA03480
                                           CRA03490
  PRINT*, CCAL(I), UPCAL(I)               CRA03500
                                           CRA03510
                                           CRA03520
100 CONTINUE                              CRA03530
                                           CRA03540
  RMS = 100.0*SQRT(RMS/REAL(NEXP))        CRA03550
  RMS2 = 100.0*SQRT(RMS2/REAL(NEXP-1))    CRA03560
  DSFIT = DP/X                             CRA03570
                                           CRA03580
  RETURN                                   CRA03590
  END                                       CRA03600
                                           CRA03610
*****CRA03620
  BLOCK DATA                             CRA03630
  IMPLICIT DOUBLE PRECISION (A-H, O-Z)    CRA03640
  DOUBLE PRECISION KF,NF                  CRA03650
  PARAMETER ( N =20 )                     CRA03660
  DIMENSION TEXP(N), CEXP(N)              CRA03670
  COMMON /INDATA1/EP, QS, DP, KF, CEOCO, RS, NF CRA03680
  COMMON /INDATA2/RHOP, CO, TEMP          CRA03690
  COMMON /INEXP/TEXP, CEXP                 CRA03700
  COMMON /EPSI/ EPSI1, EPSI2, ERROR       CRA03710
  COMMON /RRX/ CONST, ORDER1, ORDER2, RCONC CRA03720
                                           CRA03730
  DATA CONST, ORDER1, ORDER2, RCONC /200.0,-0.6,1.0,240.0/ CRA03740
                                           CRA03750
  DATA EPSI1, EPSI2, ERROR / 1.0D-8,1.0D-9,1.0D-13/ CRA03760
                                           CRA03770
  DATA EP, RHOP, QS, DP, KF, CEOCO, TEMP, RS, NF, CO/0.63,0.67E6,0.25,
/ 1.3957E-6,0.1873,0.021,8.0,0.078,3.125,1000.0/ CRA03780
                                           CRA03790
CCCCCCCCCCCC PH 7,TEMP 8 C; OXYGEN PURGED = 31.1 MG/L,C MASS = 28.6 CRA03800
  DATA TEXP /0.0,0.16,0.50,1.0,1.5,2.0,3.0,5.0,7.0,9.5,12.0,24.0,
/ 36.0,48.0,72.0,96.0,120.0,144.0,180.0,264.0/ CRA03820
  DATA CEXP / 1.0,0.747,0.587,0.467,0.376,0.351,0.322,0.291,
/ 0.279,0.267,0.244,0.197,0.179,0.151,0.110,0.084, CRA03840
                                           CRA03850

```

/	0.059,0.042,0.029,0.021/	CRA03860
END		CRA03870
*****		CRA03880
SUBROUTINE INITIA (N,M,PSI,CEQUIL,DTAU,DR,LAMBDA,QINFQO,ALPHA,		CRA03890
/ Q,MID, QAVG,CBAR)		CRA03900
IMPLICIT DOUBLE PRECISION (A-H, O-Z)		CRA03910
DOUBLE PRECISION KF,NF,LAMBDA		CRA03920
PARAMETER (NN = 100)		CRA03930
DIMENSION Q(NN,0:1),QMID(NN), QAVG(0:1),CBAR(0:1)		CRA03940
COMMON /INDATA1/EP,QS,DP,KF,CEOCO,RS,NF		CRA03950
COMMON /INDATA2/RHOP,CO,TEMP		CRA03960
COMMON /EPSI/ EPSI1, EPSI2, ERROR		CRA03970
		CRA03980
PSI = EP/RHOP		CRA03990
CEQUIL = CO*CEOCO		CRA04000
UPTAKE = 1.0D0 - CEOCO		CRA04010
DTAU = 2.1D0/DBLE(M)		CRA04020
DR = 1.0D0/DBLE(N-1)		CRA04030
		CRA04040
LAMBDA = KF*CO**((1.0/NF)/(1.0D0 + KF*CO**((1.0/NF))		CRA04050
QINFQO = KF*(CEQUIL)**((1.0D0/NF)/LAMBDA/		CRA04060
& (1.0D0+KF*(CEQUIL)**((1.0D0/NF))		CRA04070
ALPHA = (1.0D0 - CEOCO)/QINFQO		CRA04080
		CRA04090
*** INITIALIZATION : AT TAU = 0		CRA04100
DO 10 I = 1,N		CRA04110
Q(I,0) = 0.0D0		CRA04120
QMID(I) = EPSI2*DBLE(I)		CRA04130
10 CONTINUE		CRA04140
QAVG(0) = 0.0D0		CRA04150
CBAR(0) = 1.0D0		CRA04160
		CRA04170
WRITE(7,*) NF,KF,CO,CEOCO		CRA04180
PRINT20, NF,KF,CO,CEOCO		CRA04190
20 FORMAT(7X,' ADSORPTION OF PHENOL ON GAC ',		CRA04200
/ ,7X, 30('-',), /,		CRA04210
/ ,3X,'LANGMUIR FREUNDLICH ISOTHERM CONSTANT = ',F9.3.		CRA04220
/ ,3X,'LANGMUIR FREUNDLICH EQUILIBRIUM PARAMETER = ',F9.3.		CRA04230
/ ,3X,'INITIAL CONCENTRATION = ',F9.3.		CRA04240
/ ,3X,'CBAR AT INFINITY = ',F9.3)		CRA04250
		CRA04260
PRINT30, LAMBDA, UPTAKE, QINFQO,ALPHA		CRA04270
30 FORMAT(1X, ' LAMBDA = ',F6.3,		CRA04280
/ ,1X, ' UPTAKE = ',F6.3,		CRA04290
/ ,1X, ' QBAR AT INFINITY(QINFQO) = ',F6.3,		CRA04300
/ ,1X, ' ALPHA = ',F6.3)		CRA04310
		CRA04320
C PRINT40, TEMP,OXY,CMASS		CRA04330
		CRA04340
RETURN		CRA04350
END		CRA04360
		CRA04370
		CRA04380
*****		CRA04390
		CRA04400

FILE: CRANK8N FORTRAN A1 KING FAHD UNIVERSITY OF PETROLEUM AND MINERALS. DHAHRAN

```

SUBROUTINE OUTPUT(N,CTAU,DSCAL,DSFIT,SQTAU,UPCAL,UPEXP,RMS,RMS2) CRA04410
IMPLICIT DOUBLE PRECISION ( A-H, O-Z) CRA04420
DIMENSION SQTAU(N),CTAU(N),DSCAL(N),UPCAL(N),UPEXP(N) CRA04430
PRINT5 CRA04440
5 FORMAT(/,4X,'I',11X,'SQTAU(I)',9X,'UPEXP(I)',9X,'UPEXP(I)',/, CRA04450
/ 65('=')) CRA04460
DO 10 I = 1, N CRA04470
10 PRINT20,I, SQTAU(I), UPEXP(I), UPCAL(I) CRA04480
20 FORMAT( 3X,I2, 5X,F12.6, 5X, F12.6,5X,F12.6,/ ) CRA04490
PRINT30 CRA04500
30 FORMAT(/,4X,'I',11X,'CTAU(I)',9X,'DSCAL(I)',/, CRA04510
/ 45('=')) CRA04520
DO 40 I = 1, N CRA04530
40 PRINT50,I, CTAU(I), DSCAL(I) CRA04540
50 FORMAT( 3X,I2, 5X,F12.6, 5X, E12.6,/ ) CRA04550
PRINT*, 'BEST FIT DS VALUE IS =', DSFIT CRA04560
PRINT*, 'RMS VALUE IS =', RMS2 CRA04570
RETURN CRA04580
END CRA04590
CRA04600
CRA04610
CRA04620
CRA04630
CRA04640

```

Appendix A4

**Optimization Program to Calculate Parameters for Pore & Surface Diffusion
with Reaction in Batch Systems.**

FILE: A4 FORTRAN A1 KING FAHD UNIVERSITY OF PETROLEUM AND MINERALS, DHAHRAN

```

***** A4 00010
* APPENDIX A4 * A4 00020
* OPTIMIZATION PROGRAM TO CALCULATE PARAMETERS FOR PORE & SURFACE * A4 00030
* DIFFUSION WITH REACTION IN BATCH SYSTEMS * A4 00040
* * A4 00050
***** A4 00060
C A4 00070
C IMSL Name: BCPOL/DBCPOL (Single/Double precision version) A4 00080
C A4 00090
C Purpose: Minimize a function of N variables subject to bounds on A4 00100
C the variables using a direct search complex algorithm. A4 00110
C A4 00120
C Usage: CALL BCPOL (FCN, N, XGUESS, IBTYPE, XLB, XUB, FTOL, A4 00130
C MAXFCN, X, FVALUE) A4 00140
C A4 00150
C Variable declarations A4 00160
C A4 00170
C INTEGER N A4 00180
C PARAMETER (N=3) A4 00190
C A4 00200
C INTEGER IBTYPE, K, MAXFCN, NOUT A4 00210
C REAL FTOL, FVALUE, X(N), XGUESS(N), XLB(N), XUB(N) A4 00220
C EXTERNAL BCPOL, FCN, UMACH A4 00230
C A4 00240
C DATA XGUESS/-0.7E0, 2.0E0, 24.E1/, XLB/-0.8E0, 1.0E0, 17.5E1/, A4 00250
C & XUB/-0.6E0, 3.0E0, 28.5E1 / A4 00260
C A4 00270
C FTOL = 1.0E-5 A4 00280
C IBTYPE = 0 A4 00290
C MAXFCN = 300 A4 00300
C A4 00310
C CALL BCPOL (FCN, N, XGUESS, IBTYPE, XLB, XUB, FTOL, MAXFCN, X, A4 00320
C & FVALUE) A4 00330
C A4 00340
C CALL UMACH (2, NOUT) A4 00350
C WRITE (NOUT,99) (X(K),K=1,N), FVALUE A4 00360
C 99 FORMAT (' THE BEST ESTIMATE FOR THE MINIMUM VALUE OF THE', /, A4 00370
C & ' FUNCTION IS X = (', 3(2X,E12.6), '), /, ' WITH ', A4 00380
C & 'function value FVALUE = ', E12.6) A4 00390
C A4 00400
C END A4 00410
***** A4 00420
* EXTERNAL FUNCTION TO BE MINIMIZED A4 00430
C A4 00440
C SUBROUTINE FCN (N, X, F) A4 00450
C INTEGER N A4 00460
C REAL X(N), F, ORDER1, ORDER2, RCONC A4 00470
C A4 00480
C A4 00490
C ORDER1 = X(1) A4 00500
C ORDER2 = X(2) A4 00510
C RCONC = X(3) A4 00520
C A4 00530
C CALL CRANK8N ( ORDER1, ORDER2, RCONC ) A4 00540
C A4 00550

```

FILE: A4 FORTRAN A1 KING FAHD UNIVERSITY OF PETROLEUM AND MINERALS, DHAHRAN

```

      F = RMS
      RETURN
      END
      A4 00560

      A4 00570
      A4 00580
      A4 00590
      A4 00600
      A4 00610
      A4 00620
      A4 00630
      A4 00640
      A4 00650
      A4 00660
      A4 00670
      A4 00680
      A4 00690
      A4 00700
      A4 00710
      A4 00720
      A4 00730
      A4 00740
      A4 00750
      A4 00760
      A4 00770
      A4 00780
      A4 00790
      A4 00800
      A4 00810
      A4 00820
      A4 00830
      A4 00840
      A4 00850
      A4 00860
      A4 00870
      A4 00880
      A4 00890
      A4 00900
      A4 00910
      A4 00920
      A4 00930
      A4 00940
      A4 00950
      A4 00960
      A4 00970
      A4 00980
      A4 00990
      A4 01000
      A4 01010
      A4 01020
      A4 01030
      A4 01040
      A4 01050
      A4 01060
      A4 01070
      A4 01080
      A4 01090
      A4 01100

      *****
      *
      SUBROUTINE CRANK8N (ORDER1, ORDER2, RCONC )
      *
      ***** APPENDIX A3 *****
      *
      * LAGMUIR FREUNDLICH ISOTHERM : PORE AND SURFACE DIFFUSION MODEL
      * WITH REACTION
      *
      IMPLICIT DOUBLE PRECISION ( A-H, O-Z)
      DOUBLE PRECISION KF,NF,LAMBDA
      PARAMETER(N=61,M=2000,NEXP=20 )
      DIMENSION Q(N,0:M),QNEW(N),QOLD(N),QAVG(0:M),QMID(N),
      / CBAR(0:M),TAU(0:M),A(N),B(N),C(N),D(N),
      / CCAL(NEXP), TEXP(NEXP), CEXP(NEXP), ETAU(NEXP), DSCAL(NEXP),
      / CTAU(NEXP),SQTAU(NEXP),UPCAL(NEXP),UPEXP(NEXP), RTERM(NEXP)
      COMMON /INDATA1/EP,QS,DP,KF,CEOCO,RS,NF
      COMMON /INDATA2/RHOP,CO,TEMP
      COMMON /INEXP/TEXP,CEXP
      COMMON /EPSI/ EPSI1, EPSI2, ERROR
      COMMON /RRX/ CONST
      C COMMON /RRX/ CONST, ORDER1, ORDER2, RCONC

      EXTERNAL AVERAGE, THOMAS, LOAD, INTER, POLATE,RXN

      CALL INITIA (N,M,PSI,CEQUIL,DTAU,DR,LAMBDA,QINFQO,ALPHA,
      / Q,QMID, QAVG,CBAR )

      DS = 0.98E-8
      X = DP/DS

      *** GENERAL LOOP

      DO 400 J = 0, M-1

      ISUME1 = 0
      ISUME2 = 0
      TAU(J) = REAL(J)*DTAU
      399 CONTINUE

      DO 20 I = 1, N
      20 QOLD(I) = Q(I,J)

      IF ( ISUME1 .EQ. 0) THEN

      QAVG(J+1) = QAVG(J) + EPSI1
      CHECK = EPSI1
      ELSE

      CALL AVERAGE ( N,QNEW,DR,QAV )

```

FILE: A4 FORTRAN A1 KING FAHD UNIVERSITY OF PETROLEUM AND MINERALS, DHAHRAN

```

CHECK = ABS ( QAVG(J+1) - QAV )
QAVG(J+1) = QAV
ENDIF

CBAR(J+1) = CBAR(0) - ALPHA*QAVG(J+1)
Q(N,J+1) = KF*( CO*CBAR(J+1) )**((1.0D0/NF)/LAMBDA/
&          ( 1.0D0+KF*(CO*CBAR(J+1))**((1.0D0/NF) )

QNNEW      = Q(N,J+1)

IF ( ISUME2 .EQ. 0 ) THEN

DO 30 I = 1 , N
30 QMID(I) = QMID(I) + EPSI2*(I)
ELSE
DO 40 I = 1 , N
40 QMID(I) = ( Q(I,J) + Q(I,J+1) ) / 2.0D0
ENDIF

ISUME1 = ISUME1 + 1
ISUME2 = ISUME2 + 1

DO 45 I = 1 , N
45 RTERM(I) = 0.0

** CALL SUBROUTINE LOAD TO SET UP THE TRIDIAGONAL MATRIX

CALL LOAD (X,RTERM,N,DTAU,DR,QOLD,QMID,QNNEW,A,B,C,D,DS,LAMBDA)

CALL THOMAS ( N,A,B,C,D,QNEW )

DO 50 I = 1, N
Q(I,J+1) = QNEW(I)
50 CONTINUE
TAUJ = TAU(J)

IF ( (CHECK .GT. ERROR) .AND. ( ISUME1 .LT. 50) ) GOTO 399

CALL RXN(N,TAUJ,DTAU,RS,DS,RCONC,ORDER1,ORDER2,CONST,QOLD,RTERM)

CALL LOAD (X,RTERM,N,DTAU,DR,QOLD,QMID,QNNEW,A,B,C,D,DS,LAMBDA)

CALL THOMAS ( N,A,B,C,D,QNEW )

CBAR(J+1) = CBAR(0) - ALPHA*QAVG(J+1)
Q(N,J+1) = KF*( CO*CBAR(J+1) )**((1.0D0/NF)/LAMBDA/
&          ( 1.0D0+KF*(CO*CBAR(J+1))**((1.0D0/NF) )

QNNEW      = Q(N,J+1)

DO 60 I = 1, N
Q(I,J+1) = QNEW(I)
60 CONTINUE

```

FILE: A4 FORTRAN A1 KING FAHD UNIVERSITY OF PETROLEUM AND MINERALS. DHAHRAN 174

```

C   PRINT*, TAU(J) , CBAR(J)
    WRITE(7,*) TAU(J) , CBAR(J)

400 CONTINUE

    CALL POLATE (M,NEXP,RS,CEOCO,X,CBAR,TAU,TEXP,DP,CEXP,
/              CCAL,DSFIT,SQTAU,UPCAL,UPEXP,RMS,RMS2)

    CALL INTER ( M,NEXP,RS,X,CEOCO,CBAR,TAU,TEXP,
/              CEXP,CTAU,DSCAL)

    CALL OUTPUT(NEXP,CTAU,DSCAL,DSFIT,SQTAU,UPCAL,UPEXP,RMS,RMS2)

END

*****
SUBROUTINE THOMAS ( N,A,B,C,D,X)
  IMPLICIT DOUBLE PRECISION ( A-H, O-Z)
  *****
  * THOMAS ALGORITHM FOR SOLVING A TRIDIAGONAL MATRIX *
  *****

  PARAMETER( M =100)
  DIMENSION A(N),B(N),C(N),D(N),X(N),GAM(M),BET(M)

  BET(1) = B(1)
  GAM(1) = D(1)/B(1)
  DO 320 I = 2, N
    BET(I) = B(I) - A(I)*C(I-1)/BET(I-1)
    GAM(I) = ( D(I) - A(I)*GAM(I-1) )/BET(I)
320 CONTINUE
    X(N) = GAM(N)
    DO 330 I = N -1,1,-1
      IF (X(I+1) .LT. 1.0E-77 ) THEN
        X(I+1) = GAM(I)
      ELSE
        X(I) = GAM(I) - C(I)*X(I+1)/BET(I)
      ENDIF
330 CONTINUE

    DO 333 I = 1,N
333 CONTINUE
    RETURN
  END

*****
SUBROUTINE AVERAGE( N,Q,DR,QAVG)
  * INTEGRATION VIA SIMPSON'S COMPOSITE RULE
  IMPLICIT DOUBLE PRECISION (A-H,O-Z)
  DIMENSION Q(N)

  X10 = Q(1)*0.0*0.0 + Q(N)*1.0*1.0

```

FILE: A4 FORTRAN A1 KING FAHD UNIVERSITY OF PETROLEUM AND MINERALS. DHAHRAN

```

      XI1 = 0.0D0
      XI2 = 0.0D0
      DO 350 I = 2, N-1
      IF ( MOD(I,2) .EQ. 0 ) THEN
      XI2 = XI2 + Q(I)*( (DR*REAL(I-1))*2 )
      ELSE
      XI1 = XI1 + Q(I)*( (DR*REAL(I-1))*2 )
      ENDIF
350 CONTINUE
      XI = (DR/3.0D0)*( XI0 + 4.0D0*XI2 + 2.0D0*XI1 )
      QAVG = 3.0D0*XI

      RETURN
      END
*****
      SUBROUTINE LOAD (X,RTERM,N,DTAU,DR,QOLD,QMID,QNNEW, A,B,C,D,DS,
      /
      LAMBDA )

      IMPLICIT DOUBLE PRECISION ( A-H,O-Z)
      DOUBLE PRECISION KF,NF,LAMBDA
      COMMON /INDATA1/EP,QS,DP,KF,CEOCO,RS,NF
      COMMON /INDATA2/RHOP,CO,TEMP
      PARAMETER ( M =100 )
      DIMENSION QOLD(N),QMID(N),A(M),B(M),C(M),D(M),P(M),F(M),
      /
      PO(M),RTERM(N)

      PHI = DTAU/DR**2
      NM1 = N-1
      PSI = EP/RHOP

      DO 10 I = 1, N

      IF ( QMID(I) .GT. 1.0 ) THEN
      QMID(I) = 0.999999990D0
      ELSE
      ENDIF
      CK = 1.0 - QL
      IF ( ( QL .LT. 0.0 ) .OR. (CK .LT. 0.0 ) ) THEN
      DCDQ = 0.0
      ELSE
      QL = LAMBDA*QMID(I)
      DCDQ =(NF/(KF**NF)/QS)*(QL**(NF-1.0))/((1.0-QL)**(NF+1.0))
      ENDIF

      * FOR PSD CONSTANT DS MODEL
      * PO(I) = PSI*DCDQ*X + 1.0
      * FOR PSD WITH VARIABLE DS MODEL
      * PO(I) = PSI*DCDQ*X + NF/(1.0D0 - LAMBDA*QMID(I) )
      * FOR HSSD WITH VARIABLE DS MODEL
      * PO(I) = NF/(1.0D0 - LAMEDA*QMID(I) )

      10 CONTINUE

      DO 20 I = 2, NM1

```

FILE: A4 FORTRAN A1 KING FAHD UNIVERSITY OF PETROLEUM AND MINERALS, DHAHRAN

```

      F(I) = (PHI/4.0D0)*(2.0D0*PO(I)/DBLE(I-1)+(PO(I+1)-PO(I-1))/2.0D0 )A4 02760
20 CONTINUEA4 02770
*
* BOUNDARY NODE 1 .A4 02780
*A4 02790
*
      A(1) = 0.0A4 02800
      B(1) = 1.0D0 + 3.0D0*PHI*PO(1)A4 02810
      C(1) = - 3.0D0*PHI*PO(1)A4 02820
      D(1) = ( 2.0D0 - B(1))*QOLD(1) - C(1)*QOLD(2)-RTERM(1)A4 02830
*
* INTERIOR NODES 2 TO NM1A4 02840
*
      DO 30 I = 2, NM1A4 02850
      A(I) = -PHI*PO(I)/2.0D0 + F(I)A4 02860
      B(I) = 1.0D0 + PHI*PO(I)A4 02870
      C(I) = -PHI*PO(I)/2.0D0 - F(I)A4 02880
      D(I) = -A(I)*QOLD(I-1)+(2.0-B(I))*QOLD(I)-C(I)*QOLD(I+1)-RTERM(I)A4 02890
30 CONTINUEA4 02900
*
* BOUNDARY NODE NA4 02910
*
      A(N) = 0.0A4 02920
      B(N) = 1.0D0A4 02930
      C(N) = 0.0A4 02940
      D(N) = QNNEW - RTERM(N)A4 02950
*
      RETURNA4 02960
      ENDA4 02970
*****A4 02980
      SUBROUTINE RXN (N,TAUJ, DTAU, RS,DS,RCONC,ORDER1,ORDER2,A4 02990
      /CONST,QOLD,RTERM)A4 03000
      IMPLICIT DOUBLE PRECISION ( A-H, O-Z)A4 03010
      DIMENSION QOLD(N),RTERM(N)A4 03020
      TAUJO = 0.0A4 03030
*
      SIGMA = RCONC*((RS**2/DS)**ORDER1)A4 03040
      T2 = TAUJ + DTAU/2.0A4 03050
      TM = (T2**ORDER1)*SIGMAA4 03060
*
      DO 20 I = 1, NA4 03070
      IF ( QOLD(I) .LT. 0.0 ) THENA4 03080
      RTERM(I) = DTAU*CONST*TM A4 03090
      ELSEA4 03100
      RTERM(I) = DTAU*CONST*TM*(QOLD(I)**ORDER2)A4 03110
      ENDIFA4 03120
20 CONTINUEA4 03130
*
      RETURNA4 03140
      ENDA4 03150
*****A4 03160
      SUBROUTINE INTER ( M,NEXP,RS,X,CEOCO,CBAR,TAU,TEXP,A4 03170
      /CEXP,CTAU,DSCAL)A4 03180
*****A4 03190
      A4 03200
      A4 03210
      A4 03220
      A4 03230
      A4 03240
      A4 03250
      A4 03260
      A4 03270
      A4 03280
      A4 03290
      A4 03300

```

FILE: A4 FORTRAN A1 KING FAHD UNIVERSITY OF PETROLEUM AND MINERALS, DHAHRAN

```

* THIS SUBROUTINE INTERPOLATES A SET OF DATA LINEARLY.
* THE DIFFUSIVITY COEFFICIENT IS CALCULATED FROM THE
* RELATION : DSCAL = TAU*RS*RS/TIME
*
*****
*
      IMPLICIT DOUBLE PRECISION ( A-H, O-Z)
      DIMENSION CBAR(M),TAU(M),TEXP(NEXP),CEXP(NEXP),CTAU(NEXP),
      /          DSCAL(NEXP)

      DO 100 IEXP = 2, NEXP
*
* SCAN THROUGH THE DATA
*
      ISCAN = 0
10  CONTINUE
      ISCAN = ISCAN + 1
      IF ( CEXP(IEXP) .LT. CBAR(ISCAN) ) GOTO 10
*
* INTERPOLATE USING LINEAR INTERPOLATION SCHEME :
*
      CTAU(IEXP) = ( TAU(ISCAN) - TAU(ISCAN+1) )
      /              *( ( CEXP(IEXP) - CBAR(ISCAN+1)) /
      /              (CBAR(ISCAN)-CBAR(ISCAN+1))) + TAU(ISCAN+1)
      DPCAL = CTAU(IEXP)*RS*RS/( TEXP(IEXP)*60.0**2)
      DSCAL(IEXP) = DPCAL*X
*
100  CONTINUE

      RETURN
      END
*****
      SUBROUTINE POLATE (M,NEXP,RS,CEOCO,X,CBAR,TAU,TEXP,DP,CEXP,
      /                  CCAL,DSFIT,SQTAU,UPCAL,UPEXP,RMS,RMS2)
*****
* THIS SUBROUTINE INTERPOLATES A SET OF DATA LINEARLY AND
* CALCULATES THE ROOT MEAN SQUARE OF THE DEVIATIONS OF
* PREDICTED CONCENTRATION VALUES FROM EXPERIMENTAL VALUES
*****
*
      IMPLICIT DOUBLE PRECISION ( A-H, O-Z)
      PARAMETER ( N = 20 )
      DIMENSION CBAR(M),TAU(M),TEXP(NEXP),CEXP(NEXP),SQTAU(N),
      /          ETAU(N),CCAL(N),UPCAL(N),UPEXP(N)

      DO 10 I = 1, NEXP
      ETAU(I) = (DP/X)*TEXP(I)*60.0**2/RS**2
10  CONTINUE

      RMS = 0.0
      RMS2 = 0.0

```

A4 03310
A4 03320
A4 03330
A4 03340
A4 03350
A4 03360
A4 03370
A4 03380
A4 03390
A4 03400
A4 03410
A4 03420
A4 03430
A4 03440
A4 03450
A4 03460
A4 03470
A4 03480
A4 03490
A4 03500
A4 03510
A4 03520
A4 03530
A4 03540
A4 03550
A4 03560
A4 03570
A4 03580
A4 03590
A4 03600
A4 03610
A4 03620
A4 03630
A4 03640
A4 03650
A4 03660
A4 03670
A4 03680
A4 03690
A4 03700
A4 03710
A4 03720
A4 03730
A4 03740
A4 03750
A4 03760
A4 03770
A4 03780
A4 03790
A4 03800
A4 03810
A4 03820
A4 03830
A4 03840
A4 03850

FILE: A4 FORTRAN A1 KING FAHD UNIVERSITY OF PETROLEUM AND MINERALS, DHAHRAN 178

```

      DO 100 I = 2, NEXP
      ISCAN = 0
20    CONTINUE
      ISCAN = ISCAN + 1
      IF ( ETAU(I) .GT. TAU(ISCAN) ) GOTO 20
*
* INTERPOLATE USING LINEAR INTERPOLATION SCHEME
*
      CCAL(I)=(CBAR(ISCAN)-CBAR(ISCAN+1))*((ETAU(IEXP)-TAU(ISCAN))/
      /      (TAU(ISCAN) - TAU(ISCAN+1))) + CBAR(ISCAN+1)

      IF ( I .NE. 1 ) THEN
      RMS2 = ( (CEXP(I)-CCAL(I))/CEXP(I) )**2 + RMS2
      ELSE
      ENDIF
      RMS = ( (CEXP(I)-CCAL(I))/CEXP(I) )**2 + RMS

      SQTAU(I) = SQRT( ETAU(I) )
      UPCAL(I) = ABS(1.0 - CCAL(I) )/( 1.0 - CEOCO )
      UPEXP(I) = ABS(1.0 - CEXP(I) )/( 1.0 - CEOCO )

      PRINT*, CCAL(I), UPCAL(I)

100  CONTINUE

      RMS = 100.0*SQRT(RMS/REAL(NEXP))
      RMS2 = 100.0*SQRT(RMS2/REAL(NEXP-1))
      DSFIT = DP/X

      RETURN
      END

*****
      BLOCK DATA
      IMPLICIT DOUBLE PRECISION (A-H, O-Z)
      DOUBLE PRECISION KF,NF
      PARAMETER ( N =20 )
      DIMENSION TEXP(N), CEXP(N)
      COMMON /INDATA1/EP, QS, DP, KF, CEOCO, RS, NF
      COMMON /INDATA2/RHOP, CO, TEMP
      COMMON /INEXP/TEXP, CEXP
      COMMON /EPSI/ EPSI1, EPSI2, ERROR
C    COMMON /RRX/ CONST, ORDER1, ORDER2, RCONC
      COMMON /RRX/ CONST

C    DATA CONST, ORDER1, ORDER2, RCONC /200.0,-0.6,1.0,240.0/
      DATA CONST /200.0/

      DATA EPSI1, EPSI2, ERROR / 1.0D-8,1.0D-9,1.0D-13/

      DATA EP, RHOP, QS, DP, KF, CEOCO, TEMP, RS, NF, CO /0.63,0.67E6,0.25,
      / 1.3957E-6,0.1873,0.021,8.0,0.078,3.125,1000.0/

CCCCCCCCCCCC PH 7,TEMP 8 C: OXYGEN PURGED = 31.1 MG/L,C MASS = 28.6

```


DATA TEXP /0.0,0.16,0.50,1.0,1.5,2.0,3.0,5.0,7.0,9.5,12.0,24.0.	A4 04410
/ 36.0,48.0,72.0,96.0,120.0,144.0,180.0,264.0/	A4 04420
DATA CEXP / 1.0,0.747,0.567,0.467,0.376,0.351,0.322,0.291,	A4 04430
/ 0.279,0.267,0.244,0.197,0.179,0.151,0.110,0.084,	A4 04440
/ 0.059,0.042,0.029,0.021/	A4 04450
END	A4 04460
*****	A4 04470
SUBROUTINE INITIA (N,M,PSI,CEQUIL,DTAU,DR,LAMBDA,QINFQO,ALPHA,	A4 04490
/ Q,QMID, QAVG,CBAR)	A4 04500
IMPLICIT DOUBLE PRECISION (A-H, O-Z)	A4 04520
DOUBLE PRECISION KF,NF,LAMBDA	A4 04530
PARAMETER (NN = 100)	A4 04540
DIMENSION Q(NN,0:1),QMID(NN), QAVG(0:1),CBAR(0:1)	A4 04550
COMMON /INDATA1/EP,QS,DP,KF,CEOCO,RS,NF	A4 04560
COMMON /INDATA2/RHOP,CO,TEMP	A4 04570
COMMON /EPSI/ EPSI1, EPSI2, ERROR	A4 04580
PSI = EP/RHOP	A4 04590
CEQUIL = CO*CEOCO	A4 04600
UPTAKE = 1.0D0 - CEOCO	A4 04610
DTAU = 2.1D0/DBLE(M)	A4 04620
DR = 1.0D0/DBLE(N-1)	A4 04630
LAMBDA = KF*CO**((1.0/NF))/(1.0D0 + KF*CO**((1.0/NF))	A4 04640
QINFQO = KF*(CEQUIL)**((1.0D0/NF)/LAMBDA/	A4 04650
& (1.0D0+KF*(CEQUIL)**((1.0D0/NF))	A4 04660
ALPHA = (1.0D0 - CEOCO)/QINFQO	A4 04670
*** INITIALIZATION : AT TAU = 0	A4 04680
DO 10 I = 1,N	A4 04690
Q(I,0) = 0.0D0	A4 04700
QMID(I) = EPSI2*DBLE(I)	A4 04710
10 CONTINUE	A4 04720
QAVG(0) = 0.0D0	A4 04730
CBAR(0) = 1.0D0	A4 04740
WRITE(7,*) NF,KF,CO,CEOCO	A4 04750
PRINT20, NF,KF,CO,CEOCO	A4 04760
20 FORMAT(7X,' ADSORPTION OF PHENOL ON GAC ',	A4 04770
/ ,7X, 30('-'), /,	A4 04780
/ ,3X,'LANGMUIR FREUNDLICH ISOTHERM CONSTANT = ',F9.3,	A4 04790
/ ,3X,'LANGMUIR FREUNDLICH EQUILIBRIUM PARAMETER = ',F9.3,	A4 04800
/ ,3X,'INITIAL CONCENTRATION = ',F9.3,	A4 04810
/ ,3X,'CBAR AT INFINITY = ',F9.3)	A4 04820
PRINT30, LAMBDA, UPTAKE, QINFQO,ALPHA	A4 04830
30 FORMAT(1X, ' LAMBDA = ',F6.3,	A4 04840
/ ,1X, ' UPTAKE = ',F6.3,	A4 04850
/ ,1X, ' QBAR AT INFINITY(QINFQO) = ',F6.3,	A4 04860
/ ,1X, ' ALPHA = ',F6.3)	A4 04870
C PRINT40, TEMP,OXY,CMASS	A4 04880
	A4 04890
	A4 04900
	A4 04910
	A4 04920
	A4 04930
	A4 04940
	A4 04950

```

RETURN
END
*****
SUBROUTINE OUTPUT(N,CTAU,DSCAL,DSFIT,SQTAU,UPCAL,UPEXP,RMS,RMS2)
IMPLICIT DOUBLE PRECISION ( A-H, O-Z)
DIMENSION SQTAU(N),CTAU(N),DSCAL(N),UPCAL(N),UPEXP(N)

PRINT5
5  FORMAT(/,4X,'I',11X,'SQTAU(I)',9X,'UPEXP(I)',9X,'UPEXP(I)',/,
/    65('='))
DO 10 I = 1, N
10  PRINT20,I, SQTAU(I), UPEXP(I), UPCAL(I)
20  FORMAT( 3X,I2, 5X,F12.6, 5X, F12.6,5X,F12.6,/)

PRINT30
30  FORMAT(/,4X,'I',11X,'CTAU(I)',9X,'DSCAL(I)',/,
/    45('='))
DO 40 I = 1, N
40  PRINT50,I, CTAU(I), DSCAL(I)
50  FORMAT( 3X,I2, 5X,F12.6, 5X, F12.6,/)
PRINT*, 'BEST FIT DS VALUE IS =', DSFIT
PRINT*, 'RMS VALUE IS =', RMS2

RETURN
END

```

Appendix A5

Program to Calculate Breakthrough Curves for Pore and Surface Diffusion
Controlled Systems.

FILE: A5 FORTRAN A1 KING FAHD UNIVERSITY OF PETROLEUM AND MINERALS, DHAHRAN

```

***** A5 *****
C
  IMPLICIT DOUBLE PRECISION (A-H, O-Z)
  PARAMETER (MXPARM=50,NT=112,MC=14,NC=7,MSTEP=300)
  PARAMETER (MABSE=1, MBDF=2, MSOLVE=2)
  DIMENSION Y(NT),CP(NT),YPRIME(NT),PARAM(MXPARM),TP(NT),CBAR(NT)
  DIMENSION Q(NT)
  DOUBLE PRECISION KLF, NLF,L,KF,LAMBDA
  COMMON /INPUT1/ V,L,KF,EPSI,EPSIP,R,RHOP,DP,DSO
  COMMON /INPUT2/ KLF, NLF, CO, QE,DL
  COMMON /BLOCKA/ PE,ST,DGP,DGS,EDP,EDSO,LAMBDA,PHI
  COMMON/BLOCKB/ WZ(14),AZ(14,14),BZ(14,14),WR(7),BR(7,7),AR(7,7)
  EXTERNAL DIVPAG, SSET, UMACH, FCN, FCNJ,INPUT,ORTHOG
  CALL UMACH (2, NOUT)

  CALL INPUT (TMAX)

  CALL ORTHOG (WZ,AZ,BZ,WR,AR,BR)

  TPMAX = TMAX*V/( L*(1.0+DG) )
  DTP = TMAX/MSTEP

  N = MC*NC + MC
  MNC = MC*NC
  T = 0.0
  TP(1) = 0.0
  CBAR(1) = 0.0
  DO 10 I = 1, N
    CP(I) = 0.0
    Y(I) = 0.0
10  CONTINUE
  TOL = 1.E-3
  CALL SSET (MXPARM, 0.0, PARAM, 1)
  PARAM(10) = MABSE
  PARAM(12) = MBDF
  PARAM(13) = MSOLVE

  IDO = 1

  DO 100 I = 2, MSTEP
    TP(I) = TP(I-1) + DPT
    TEND = TP(I)

    CALL DIVPAG (IDO, N, FCN, FCNJ, A, T, TEND, TOL, PARAM, Y)

    CBAR(I) = Y(N)

    IF (I .EQ. MSTEP) IDO = 3

100  CONTINUE

  CALL POLATE(MSTEP, CBAR, TP)

  END

```

FILE: A5 FORTRAN A1 KING FAHD UNIVERSITY OF PETROLEUM AND MINERALS. DHAHRAN

```

*****
SUBROUTINE FCN ( N, T, Y, YPRIME )
IMPLICIT DOUBLE PRECISION ( A-H, O-Z)
DOUBLE PRECISION L,KF,KLF, NLF, LAMBDA
COMMON /INPUT1/ V,L,KF,EPSI,EPSIP,R,RHOP,DP,DSO
COMMON /INPUT2/ KLF, NLF, CO, QE, DL
COMMON /BLOCKA/ PE,ST,DGP,DGS,EDP,EDSO,LAMBDA,PHI
COMMON/BLOCKB/ WZ(14),AZ(14,14),BZ(14,14),WR(7),BR(7,7),AR(7,7)
PARAMETER ( NC = 7, MC = 14, NN = 112 )
DIMENSION Y(N),CP(NN), YPRIME(N),EDS(NN),Q(NN)
EXTERNAL ORTHOG

ND = NC - 1
MD = MC - 1
MND = MC*ND
MNC = MC + MC*ND
N = MNC + MC

CIBAR = 1.0

DGPS = 1.0 + DGP/DGS
DG = DGP + DGS
A = DGP/DG
B = DGS/DG/LAMBDA

DO 9 I = 1, MNC
Q(I) = Y(I)
THETA = LAMBDA*Q(I)
IF( ( THETA .GT. 0.) .AND. (THETA .LT. 1.) ) THEN
CP(I) = ( THETA/(1.0 - THETA)/KLF)**NLF
EDS(I) = EDSO*NLF/(1. - THETA )
ELSE
CP(I) = 0.0
EDS(I) = EDSO
ENDIF
9 CONTINUE

EVALUATING DX/DT(J,K,T)

KK = 0
SUMWW = 0.0
SUMWX = 0.0
SUMDX = 0.0

DO 40 K = 1, MC
SUMDX = 0.0
DO 30 J = 1, NC - 1
SUMAX = AR(NC,J)*Y(MND+K)
SUMAC = AR(NC,J)*CP(MND+K)
SUMBC = (EDP - DGP*EDS(KK+J)/DGS)*BR(NC,J)*CP(MND+K) +
/ (EDS(KK+J) + DGP*EDS(KK+J)/DGS)*BR(NC,J)*Y(MND+K)
DO 20 I = 1, NC-1
SUMAX = SUMAX + AR(I,J)*Y(KK+I)

```

FILE: A5 FORTRAN A1 KING FAHD UNIVERSITY OF PETROLEUM AND MINERALS, DHAHRAN

```

SUMAC = SUMAC + AR(I,J)*CP(KK+I)
SUMBC = SUMBC + (EDP - DGP*EDS(KK+J)/DGS)*BR(I,J)*CP(KK+I) +
/      (EDS(KK+J) + DGP*EDS(KK+J)/DGS)*BR(I,J)*Y(KK+I)
20  CONTINUE
AXAC = (- DGP/DGS)*EDSO*NLF*LAMBDA/((1.-LAMBDA*Y(KK+J))*2)
/      *SUMAX*SUMAC
AXSQ = ( (1.+DGP/DGS)*EDSO*NLF*LAMBDA/((1.-LAMBDA*Y(KK+J))*2) ) *
/      SUMAX**2
YPRIME(KK+J) = ( (DG + 1.0)/DG ) * ( SUMBC - AXAC + AXSQ )
SUMDX = SUMDX + ( WR(J)/WR(NC) ) * YPRIME(KK+J)
SUMWX = SUMWX + WR(J)*YPRIME(KK+J)
30  CONTINUE
SUMDX = SUMDX + ( WR(NC)/WR(NC) ) * YPRIME(MND+K)
SUMWX = SUMWX + WR(NC)*YPRIME(MND+K)

YPRIME(MND+K) = ((DG+1.0)/(DG*WR(NC))) * ST*(Y(MNC+K)-CP(MND+K))
/      -SUMDX
SUMWW = SUMWW + WZ(K)*SUMWX
KK = KK + NC - 1
40  CONTINUE

* EVALUATING DC8/DT(K,T)

AAC = 0.0
WAC = 0.0
DO 60 K = 2, MC-1
PC = 0.0
DO 50 I = 1, MC
PC = PC + (1.+DG)*( BZ(I,K)/PE - AZ(I,K) ) * Y(MNC+I)
50  CONTINUE
PC = PC - 3.0*(DG+1.0)*ST*( Y(MNC+K) - CP(MND+K) )
YPRIME(MNC+K) = PC
AAC = AAC + PC*AZ(MC,K)/AZ(MC,MC)
WAC = WAC + ( WZ(K)-WZ(MC)*AZ(MC,K)/AZ(MC,MC) ) * PC
60  CONTINUE

* AT THE ENTRNACE :
WWA = WZ(1) - WZ(MC)*AZ(MC,1)/AZ(MC,MC)
YPRIME(MNC+1) = ( ((DG+1.0)*(CIBAR-Y(N))-WAC)-3*DG*SUMWW ) / WWA
* AT EXIT
YPRIME(N) = -AAC - (AZ(MC,1)/AZ(MC,MC))*YPRIME(MNC+1)

RETURN
END

*****

SUBROUTINE FCNJ (N, T, Y, DYPDY)
C SPECIFICATIONS FOR ARGUMENTS
INTEGER N
REAL T, Y(N), DYPDY(N,*)
C
RETURN
END

```

FILE: A5 FORTRAN A1 KING FAHD UNIVERSITY OF PETROLEUM AND MINERALS. DHAHRAN

```

*****
SUBROUTINE INPUT (TMAX)
IMPLICIT DOUBLE PRECISION (A-H, O-Z)
PARAMETER (NEXP = 49)
DOUBLE PRECISION L, KLF, NLF, KF, LAMBDA
DIMENSION TAU(NEXP), CEXP(NEXP)
COMMON /INPUT1/ V,L,KF,EPSI,EPSIP,R,RHOP,DP,DSO
COMMON /INPUT2/ KLF, NLF, CO, QE,DL
COMMON /BLOCKA/ PE,ST,DGP,DGS,EDP,EDSO,LAMBDA,PHI
COMMON/EXP/TAU,CEXP

READ*, KLF,NLF,CO,QE,DL
READ*, V,L,KF,EPSI,EPSIP,R,RHOP,DP,DSO
READ*, ( TAU(I), I = 1, NEXP)
READ*, ( CEXP(I), I = 1, NEXP)
TMAX = TAU(NEXP)

PE = V*L/DL
ST = KF*L*(1.-EPSI)/(R*EPSI*V)
DGP = (1.-EPSI)*EPSIP/EPSI
DGS = (1.-EPSI)*RHOP*QE/(EPSI*CO)
DG = DGS + DGP
EDP = L*DP*DGP/(R**2*V)
EDSO = L*DSO*DGS/(R**2*V)
PHI = KLF*CO*(1./NLF)
LAMBDA = PHI/(1.+PHI)

C   PRINT1, V,L,KF,EPSI,EPSIP,R,RHOP,DP,DSO
C 1  FORMAT( 4(E12.6,2X ) )

PRINT2, DGS,EDSO
PRINT2, PE,ST,DGP,DGP/DGS,DGS,EDP,EDSO,LAMBDA,PHI
2  FORMAT( 4(E12.6,2X ) )
END

*****

SUBROUTINE ORTHOG (WZ,AZ,BZ,WR,AR,BR)
IMPLICIT DOUBLE PRECISION(A-H, O-Z)
DIMENSION WZ(14),AZ(14,14),BZ(14,14),WR(7),BR(7,7),AR(7,7)

*THE NUMBER OF RADIAL COLLOC PTS. THE WR VECTOR, AND THE AR,BR
* MATRICES ARE READ IN :
*
READ*, NC
PRINT*, NC
READ*, ( WR(I), I=1, NC )
PRINT*, ( WR(I), I=1, NC )

DO 5 I =1, NC
READ*, ( AR(I,J), J=1, NC )
PRINT*,( AR(I,J), J=1, NC )
5  CONTINUE

DO 10 I =1, NC

```

FILE: A5 FORTRAN A1 KING FAHD UNIVERSITY OF PETROLEUM AND MINERALS. DHAHRAN

```

      READ*, ( BR(I,J), J=1, NC )
      PRINT*,( BR(I,J), J=1, NC )
10    CONTINUE

*THE NUMBER OF AXIAL COLLOC PTS, THE WZ VECTOR, AND THE AZ AND BZ
*MATRICES ARE READ IN :
*
      READ*, MC
      PRINT*, MC
      READ*,( WZ(I), I=1, MC )
      PRINT100,( WZ(I), I=1, MC )

      DO 20 I =1, MC
      READ*, ( AZ(I,J), J=1, MC )
      PRINT100,( AZ(I,J), J=1, MC )
20    CONTINUE

      DO 30 I =1, MC
      READ*, ( BZ(I,J), J=1, MC )
      PRINT100,( BZ(I,J), J=1, MC )
30    CONTINUE

      RETURN
100  FORMAT( 4F20.12 )

      END

*****

      SUBROUTINE POLATE (N, CBAR, TP)
      IMPLICIT DOUBLE PRECISION (A-H, O-Z)
      PARAMETER (NEXP = 49)
      DOUBLE PRECISION L, KLF, NLF, KF, LAMBDA
      DIMENSION TAU(NEXP), CEXP(NEXP), TPE(NEXP), TAU(NEXP), CEXP(NEXP),
      /      CCAL(NEXP), CBAR(N), TP(N)
      COMMON /INPUT1/ V,L,KF,EPSI, EPSIP,R,RHOF,DP,DSO
      COMMON /INPUT2/ KLF, NLF, CO, QE,DL
      COMMON /BLOCKA/ PE,ST,DGP,DGS,EDP,EDSO,LAMBDA,PHI
      COMMON/EXP/TAU,CEXP

      DO 10 I = 1, NEXP
10    TPE(I) = TAU(I)*V/L/(1+DG)

      RMS = 0.0
      DO 100 I = 2, NEXP
      ISCAN = 0
20    CONTINUE
      ISCAN = ISCAN +1
      IF( TPE(I) .GT. TP(ISCAN) ) GOTO 20

      CCAL(I) = (CAR(ISCAN)-CBAR(ISCAN+1))*((TPE(I)-TPE(ISCAN))/
      /      (TPE(ISCAN)-TPE(ISCAN+1))) + CBAR(ISCAN+1)

      RMS = RMS + ((CEXP(I)-CCAL(I))/CEXP(I))*2

```


FILE: A5 FORTRAN A1 KING FAHD UNIVERSITY OF PETROLEUM AND MINERALS, DHAHRAN

100	CONTINUE	A5 02760
		A5 02770
		A5 02780
*	PRINT OUT	A5 02790
	DO 30 I = 2, NEXP	A5 02800
30	PRINT200, TPE(I), CCAL(I), CEXP(I)	A5 02810
200	FORMAT (2X, 4(E22.14, 2X))	A5 02820
		A5 02830
	RETURN	A5 02840
	END	A5 02850

Appendix A6

**Program to Calculate Breakthrough Curves for Pore and Surface Diffusion
Controlled Systems involving Reaction.**

FILE: A6 FORTRAN A1 KING FAHD UNIVERSITY OF PETROLEUM AND MINERALS, DHAHRAN

```

***** A6 *****
C
  IMPLICIT DOUBLE PRECISION (A-H, O-Z)
  PARAMETER (MXPARM=50,NT=112,MC=14,NC=7,MSTEP=300)
  PARAMETER (MABSE=1, MBDF=2, MSOLVE=2)
  DIMENSION Y(NT),CP(NT),YPRIME(NT),PARAM(MXPARM),TP(NT),CBAR(NT)
  DIMENSION Q(NT)
  DOUBLE PRECISION KLF, NLF,L,KF,LAMBDA
  COMMON /INPUT1/ V,L,KF,EPSI,EPSIP,R,RHOP,DP,DSO
  COMMON /INPUT2/ KLF, NLF, CO, QE,DL,RK
  COMMON /BLOCKA/ PE,ST,DGP,DGS,EDP,EDSO,LAMBDA,PHI
  COMMON/BLOCKB/ WZ(14),AZ(14,14),BZ(14,14),WR(7),BR(7,7),AR(7,7)
  EXTERNAL DIVPAG, SSET, UMACH, FCN, FCNJ, INPUT, ORTHOG
  CALL UMACH (2, NOUT)

  CALL INPUT (TMAX)

  CALL ORTHOG (WZ,AZ,BZ,WR,AR,BR)

  TPMAX = TMAX*V/( L*(1.0+DG) )
  DTP = TMAX/MSTEP

  N = MC*NC + MC
  MNC = MC*NC
  I = 0.0
  TP(1) = 0.0
  CBAR(1) = 0.0
  DO 10 I = 1, N
    CP(I) = 0.0
    Y(I) = 0.0
10  CONTINUE
    TOL = 1.E-3
    CALL SSET (MXPARM, 0.0, PARAM, 1)
    PARAM(10) = MABSE
    PARAM(12) = MBDF
    PARAM(13) = MSOLVE

    IDO = 1

    DO 100 I = 2, MSTEP
      TP(I) = TP(I-1) + DPT
      TEND = TP(I)

      CALL DIVPAG (IDO, N, FCN, FCNJ, A, T, TEND, TOL, PARAM, Y)

      CBAR(I) = Y(N)

      IF (I .EQ. MSTEP) IDO = 3

100  CONTINUE

      CALL POLATE(MSTEP, CBAR, TP)

  END

```

A6 00010
 A6 00020
 A6 00030
 A6 00040
 A6 00050
 A6 00060
 A6 00070
 A6 00080
 A6 00090
 A6 00100
 A6 00110
 A6 00120
 A6 00130
 A6 00140
 A6 00150
 A6 00160
 A6 00170
 A6 00180
 A6 00190
 A6 00200
 A6 00210
 A6 00220
 A6 00230
 A6 00240
 A6 00250
 A6 00260
 A6 00270
 A6 00280
 A6 00290
 A6 00300
 A6 00310
 A6 00320
 A6 00330
 A6 00340
 A6 00350
 A6 00360
 A6 00370
 A6 00380
 A6 00390
 A6 00400
 A6 00410
 A6 00420
 A6 00430
 A6 00440
 A6 00450
 A6 00460
 A6 00470
 A6 00480
 A6 00490
 A6 00500
 A6 00510
 A6 00520
 A6 00530
 A6 00540
 A6 00550

FILE: A6 FORTRAN A1 KING FAHD UNIVERSITY OF PETROLEUM AND MINERALS. DHAHRAN

```

*****
SUBROUTINE FCN ( N, T, Y, YPRIME )
IMPLICIT DOUBLE PRECISION ( A-H, O-Z)
DOUBLE PRECISION L,KF,KLF, NLF, LAMBDA
COMMON /INPUT1/ V,L,KF,EPSI,EPSIP,R,RHOP,DP,DSO
COMMON /INPUT2/ KLF, NLF, CO, QE, DL,RK
COMMON /BLOCKA/ PE,ST,DGP,DGS,EDP,EDSO,LAMBDA,PHI
COMMON/BLOCKB/ WZ(14),AZ(14,14),BZ(14,14),WR(7),BR(7,7),AR(7,7)
PARAMETER ( NC = 7, MC = 14, NN = 112 )
DIMENSION Y(N),CP(NN), YPRIME(N),EDS(NN),Q(NN)
EXTERNAL ORTHOG

ND = NC - 1
MD = MC - 1
MND = MC*ND
MNC = MC + MC*ND
N = MNC + MC

*
CIBAR = 1.0

DGPS = 1.0 + DGP/DGS
DG = DGP + DGS
A = DGP/DG
B = DGS/DG/LAMBDA
G = EPSIP*V*CO*RK/DGP/L
M = 1

DO 9 I = 1, MNC
Q(I) = Y(I)
THETA = LAMBDA*Q(I)
IF( ( THETA .GT. 0.) .AND. (THETA .LT. 1.) ) THEN
CP(I) = ( THETA/(1.0 - THETA)/KLF)**NLF
EDS(I) = EDSO*NLF/(1. - THETA )
ELSE
CP(I) = 0.0
EDS(I) = EDSO
ENDIF
9 CONTINUE

*
* EVALUATING DX/DI(J,K,T)
*
KK = 0
SUMWW = 0.0
SUMWX = 0.0
SUMDX = 0.0

DO 40 K = 1, MC
SUMDX = 0.0
DO 30 J = 1, NC - 1

IF(Q(MND+K) .LT. 0) .OR. (T .EQ. 0) ) THEN
RR = 0.0
ELSEIF (Q(MND+K) .EQ. 0) THEN
RR = RK*T*(-0.6)

```

FILE: A6 FORTRAN A1 KING FAHD UNIVERSITY OF PETROLEUM AND MINERALS. DHAHRAN

```

ELSE
RR = RK*T*(-0.6)*Q(MND+K)**M
ENDIF

SUMAX = AR(NC,J)*Y(MND+K)
SUMAC = AR(NC,J)*CP(MND+K)
SUMBC = (EDP - DGP*EDS(KK+J)/DGS)*BR(NC,J)*CP(MND+K) +
/ (EDS(KK+J) + DGP*EDS(KK+J)/DGS)*BR(NC,J)*Y(MND+K) - G*RR
DO 20 I = 1, NC-1

IF(Q(KK+I) .LT. 0) .OR. (T .EQ. 0) THEN
RR = 0.0
ELSEIF (Q(KK+I) .EQ. 0) THEN
RR = RK*T*(-0.6)
ELSE
RR = RK*T*(-0.6)*Q(KK+I)**M
ENDIF

SUMAX = SUMAX + AR(I,J)*Y(KK+I)
SUMAC = SUMAC + AR(I,J)*CP(KK+I)
SUMBC = SUMBC + (EDP - DGP*EDS(KK+J)/DGS)*BR(I,J)*CP(KK+I) +
/ (EDS(KK+J) + DGP*EDS(KK+J)/DGS)*BR(I,J)*Y(KK+I) - G*RR
20 CONTINUE
AXAC = (- DGP/DGS)*EDSO*NLF*LAMBDA/((1.-LAMBDA*Y(KK+J))**2)
/ *SUMAX*SUMAC
AXSQ = ( (1.+DGP/DGS)*EDSO*NLF*LAMBDA/((1.-LAMBDA*Y(KK+J))**2))*
/ SUMAX**2
YPRIME(KK+J) = ( (DG + 1.0)/DG )*( SUMBC - AXAC + AXSQ )
SUMDX = SUMDX + ( WR(J)/WR(NC) )*YPRIME(KK+J)
SUMWX = SUMWX + WR(J)*YPRIME(KK+J)
30 CONTINUE
SUMDX = SUMDX + ( WR(NC)/WR(NC) )*YPRIME(MND+K)
SUMWX = SUMWX + WR(NC)*YPRIME(MND+K)

YPRIME(MND+K) = ((DG+1.0)/(DG*WR(NC)))*ST*(Y(MNC+K)-CP(MND+K))
/ -SUMDX
SUMWW = SUMWW + WZ(K)*SUMWX
KK = KK + NC - 1
40 CONTINUE

* EVALUATING DCB/DT(K,T)

AAC = 0.0
WAC = 0.0
DO 60 K = 2, MC-1
PC = 0.0
DO 50 I = 1, MC
PC = PC + (1.+DG)*( BZ(I,K)/PE - AZ(I,K) )*Y(MNC+I)
50 CONTINUE
PC = PC - 3.0*(DG+1.0)*ST*( Y(MNC+K) - CP(MND+K) )
YPRIME(MNC+K) = PC
AAC = AAC + PC*AZ(MC,K)/AZ(MC,MC)
WAC = WAC + ( WZ(K)-WZ(MC)*AZ(MC,K)/AZ(MC,MC) )*PC
60 CONTINUE

```

FILE: A6 FORTRAN A1 KING FAHD UNIVERSITY OF PETROLEUM AND MINERALS. DHAIRAN

```

* AT THE ENTRANCE :
  WWA = WZ(1) - WZ(MC)*AZ(MC,1)/AZ(MC,MC)
  YPRIME(MNC+1) = ( ((DG+1.0)*(CIBAR-Y(N))-WAC)-3*DGS*SUMW )/WWA
* AT EXIT
  YPRIME(N) = -AAC - (AZ(MC,1)/AZ(MC,MC))*YPRIME(MNC+1)

  RETURN
  END

*****

      SUBROUTINE FCNJ (N, T, Y, DYFDY)
C   SPECIFICATIONS FOR ARGUMENTS
      INTEGER    N
      REAL       T, Y(N), DYFDY(N,*)
C
      RETURN
      END

*****

      SUBROUTINE INPUT (TMAX)
      IMPLICIT DOUBLE PRECISION (A-H, O-Z)
      PARAMETER (NEXP = 49)
      DOUBLE PRECISION L, KLF, NLF, KF, LAMBDA
      DIMENSION TAU(NEXP), CEXP(NEXP)
      COMMON /INPUT1/ V,L,KF,EPSI,EPSIP,R,RHOP,DP,DSO
      COMMON /INPUT2/ KLF, NLF, CO, QE,DL,RK
      COMMON /BLOCKA/ PE,ST,DGF,DGS,EDP,EDSO,LAMBDA,PHI
      COMMON/EXP/TAU,CEXP

      READ*, KLF,NLF,CO,QE,DL,RK
      READ*, V,L,KF,EPSI,EPSIP,R,RHOP,DP,DSO
      READ*, ( TAU(I), I = 1, NEXP)
      READ*, ( CEXP(I), I = 1, NEXP)
      TMAX = T * NEXP

      PE = V*L/DL
      ST = KF*L*(1.-EPSI)/(R*EPSI*V)
      DGP = (1.-EPSI)*EPSIP/EPSI
      DGS = (1.-EPSI)*RHOP*QE/(EPSI*CO)
      DG = DGS + DGF
      EDP = L*DP*DGP/(R**2*V)
      EDSO = L*DSO*DGS/(R**2*V)
      PHI = KLF*CO*(1./NLF)
      LAMBDA = PHI/(1.+PHI)

      END

*****

      SUBROUTINE ORTHOG (WZ,AZ,SZ,WR,AR,BR)
      IMPLICIT DOUBLE PRECISION(A-H, O-Z)
      DIMENSION WZ(14),AZ(14,14),BZ(14,14),WR(7),BR(7,7),AR(7,7)

*THE NUMBER OF RADIAL COLLOC PTS. THE WR VECTOR, AND THE AR,BR

```

FILE: A6 FORTRAN A1 KING FAHD UNIVERSITY OF PETROLEUM AND MINERALS. DIAHRAN

```

* MATRICES ARE READ IN :
*
  READ*, NC
  PRINT*, NC
  READ*, ( WR(I), I=1, NC )
  PRINT*, ( WR(I), I=1, NC )

  DO 5 I =1, NC
  READ*, ( AR(I,J), J=1, NC )
  PRINT*, ( AR(I,J), J=1, NC )
5  CONTINUE

  DO 10 I =1, NC
  READ*, ( BR(I,J), J=1, NC )
  PRINT*, ( BR(I,J), J=1, NC )
10 CONTINUE

*THE NUMBER OF AXIAL COLLOC PTS. THE WZ VECTOR. AND THE AZ AND BZ
*MATRICES ARE READ IN :
*
  READ*, MC
  PRINT*, MC
  READ*, ( WZ(I), I=1, MC )
  PRINT100, ( WZ(I), I=1, MC )

  DO 20 I =1, MC
  READ*, ( AZ(I,J), J=1, MC )
  PRINT100, ( AZ(I,J), J=1, MC )
20 CONTINUE

  DO 30 I =1, MC
  READ*, ( BZ(I,J), J=1, MC )
  PRINT100, ( BZ(I,J), J=1, MC )
30 CONTINUE

  RETURN
100 FORMAT( 4F20.12 )

  END

*****

SUBROUTINE POLATE (N, CBAR, TP)
IMPLICIT DOUBLE PRECISION (A-H, O-Z)
PARAMETER (NEXP = 49)
DOUBLE PRECISION L, KLF, NLF, KF, LAMBDA
DIMENSION TAU(NEXP), CEXP(NEXP), TPE(NEXP), TAU(NEXP), CEXP(NEXP),
/ CCAL(NEXP), CBAR(N), TP(N)
COMMON /INPUT1/ V, L, KF, EPSI, EPSIP, R, RHOP, DP, DSO
COMMON /INPUT2/ KLF, NLF, CO, QE, DL, RK
COMMON /BLOCKA/ PE, ST, DGP, DGS, EDP, EDSP, LAMBDA, PHI
COMMON /EXP/ TAU, CEXP

DO 10 I = 1, NEXP
10 TPE(I) = TAU(I)*V/L/(1+DG)

```

A6 02210
A6 02220
A6 02230
A6 02240
A6 02250
A6 02260
A6 02270
A6 02280
A6 02290
A6 02300
A6 02310
A6 02320
A6 02330
A6 02340
A6 02350
A6 02360
A6 02370
A6 02380
A6 02390
A6 02400
A6 02410
A6 02420
A6 02430
A6 02440
A6 02450
A6 02460
A6 02470
A6 02480
A6 02490
A6 02500
A6 02510
A6 02520
A6 02530
A6 02540
A6 02550
A6 02560
A6 02570
A6 02580
A6 02590
A6 02600
A6 02610
A6 02620
A6 02630
A6 02640
A6 02650
A6 02660
A6 02670
A6 02680
A6 02690
A6 02700
A6 02710
A6 02720
A6 02730
A6 02740
A6 02750

FILE: A6 FORTRAN A1 KING FAHD UNIVERSITY OF PETROLEUM AND MINERALS. DHAIRAN

RMS = 0.0	A6 02760
DO 100 I = 2, NEXP	A6 02770
ISCAN = 0	A6 02780
20 CONTINUE	A6 02790
ISCAN = ISCAN +1	A6 02800
IF(TPE(I) .GT. TP(ISCAN)) GOTO 20	A6 02810
	A6 02820
CCAL(I) = (CAR(ISCAN)-CBAR(ISCAN+1))*((TPE(I)-TPE(ISCAN))/	A6 02830
/ (TPE(ISCAN)-TPE(ISCAN+1))) + CBAR(ISCAN+1)	A6 02840
	A6 02850
RMS = RMS + ((CEXP(I)-CCAL(I))/CEXP(I))*2	A6 02860
	A6 02870
	A6 02880
100 CONTINUE	A6 02890
	A6 02900
* PRINT OUT	A6 02910
DO 30 I = 2, NEXP	A6 02920
30 PRINT200, TPE(I), CCAL(I), CEXP(I)	A6 02930
200 FORMAT (2X, 4(E22.14, 2X))	A6 02940
	A6 02950
RETURN	A6 02960
END	A6 02970

VITA

Name : Ekhaton Emmanuel Osagie

Personal Address : 15 Ogunbor Street, Upper Lawani, Benin, Nigeria.

Personal Data : Born on December 7, 1968; single.

Education : B.Eng. in Chemical Engineering, 1991.

Publication : “The Adsorption of Phenol and its Reaction in the Presence of Oxygen on Granular Activated Carbon” presented at the Fifth Fundamentals of Adsorption Conference at Asilomar, San Francisco California. 13-18 May, 1995